SLOVAK MAGAZINE
GEOLOGICAL

SLOVAK GEOLOGICAL MAGAZINE

Periodical journal of Geological Survey of Slovak Republic is a quarterly presenting the results of investigation and researches in a wide range of topics:

- regional geology and geological maps
- lithology and stratigraphy
- petrology and mineralogy
- paleontology
- geochemistry and isotope geology
- geophysics and deep structure
- geology of deposits and metallogeny

- tectonics and structural geology
- hydrogeology and geothermal energy
- environmental geochemistry
- engineering geology and geotechnology
- geological factors of the environment
- petroarcheology

The journal is focused on problems of the Alpine-Carpathian region.

3902001018472

SLOVAK GEOLOGICAL MAGAZINE

VOLUME 12   NO 2

2/2006

Bacterial leaching of ore minerals from waste at the Pezinok deposit (Western Slovakia)

[1,2]Peter Andráš, [3]Mária Kušnierová, [1]Marcel Adam, [4]Martin Chovan
and [3]Andrea Šlesárová

[1] Geological Institute of the Slovak Academy of Sciences, Severná 5, 974 01 Banská Bystrica, Slovakia
[2] Department of Ecology and Environmental Education, Matej Bel University, Tajovského 40,
974 01 Banská Bystrica, Slovakia
[3] Institute of Geotechnics of the Slovak Academy of Sciences, Watsonova 45, 043 53 Košice, Slovakia
[4] Department of Mineralogy and Petrology, Faculty of Natural Sciences, Comenius University, Mlynská dolina,
842 15 Bratislava, Slovakia

Abstract The paper reports the chemical characteristic of acid mining drainage waters as well as the results of leaching experiments conducted with *Thiobacillus ferrooxidans* and *Thiobacillus thiooxidans* at the same conditions in the solution. The experiments were realized using tailing impoundment sediments and ore minerals from the Sb-(Au-) base metal deposit Pezinok (Malé Karpaty Mts., Western Carpathians, Slovakia). The research results show the oxidation sequence and the leaching progression on the surface of the following ore minerals: löllingite, arsenopyrite, stibnite, native Sb, gudmundite, berthierite, pyrite, sphalerite and chalcopyrite. The differences between chemical and biological-chemical leaching activity of various ore minerals on the polished sections surface are discussed. The extent and the kinetics of the biological-chemical leaching of ore minerals are significantly higher than the chemical leaching of ore minerals without bacteria.

Key words: acid mine drainage water, ore minerals, biological-chemical oxidation, chemical oxidation, *Thiobacillus ferrooxidans*, *Thiobacillus thiooxidans*, etching-patterns.

Introduction

More than 100 years of mining activity in the Pezinok deposit caused changes of the land relief. The ore material was displaced from the original environment of the mountain massif, in which it was in the relatively equilibrium state to the environment exposed to the combined action of atmosphere and water saturated with atmospheric gases and to the biological effects. The fine grinding of ores and application of chemical reagents in the technological process of sulphide concentrates production increased the reactive surface of the relict ore minerals in the deposited waste.

Sludge lagoons and setting-pits contain a lot of waste ore minerals which represent the main substrate necessary for the metabolic activity of autochthonous, acidophilous and thionic bacteria *Acidithiobacillus ferrooxidans* (*ATF*), *Acidithiobacillus thiooxidans* (*ATT*) and *Leptospirillum ferrooxidans* (*LF*) catalyzing the ore minerals oxidation processes. The high residual concentrations of metals Sb, Fe, As in the deposited solid wastes and contaminated soils are currently the permanent source of in-situ pollution and due to the activity of autochthonous microflora the source of acid mine drainage (AMD) generation. Surface and underground waters are also polluted with elements from the flotation agents used in the ore processing. The released metals and other chemical agents may enter to the food chain of animals and humans through plants and water.

Characteristic of the Pezinok deposit

The Pezinok – Kolársky vrch (Fig. 1) deposit is situated in a 1200 m long tectonic fault of NW-SE direction. The mineralized structure is 25-70 m thick at the surface and about 430 m long (Chovan et al., 1992).

In the Pezinok deposit two types of ore mineralization were described: (1) metamorphosed, primarily exhalation-sedimentary pyrite mineralization genetically related to Devonian basic volcano-sedimentary cycle which was subsequently metamorphosed and (2) hydrothermal Sb-Au-As mineralization of epigenetic character which is most frequently localized in beds of tectonically deformed black schists (Chovan et al., 1992).

About 20 000 tons of antimony was exploited from this deposit. The reported content of Sb ranges from 1 % to 4 %, of As from 0.5 % to 1.5 % and the average content of Au is 3.60 ppm (Uher et al., 2000). The exploitation of Sb-Au ores in the Pezinok deposit terminated in 1991. The mine was closed in 1992.

Characterization of the deposited waste

The mining-waste is deposited in several tailings impoundments and two sludge lagoons containing 380 000 m³ of material (Trtíková, 1999). As- and Fe-minerals (predominantly arsenopyrite and pyrite) were during the ore dressing process suppressed and moved to the waste.

80
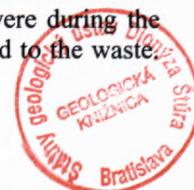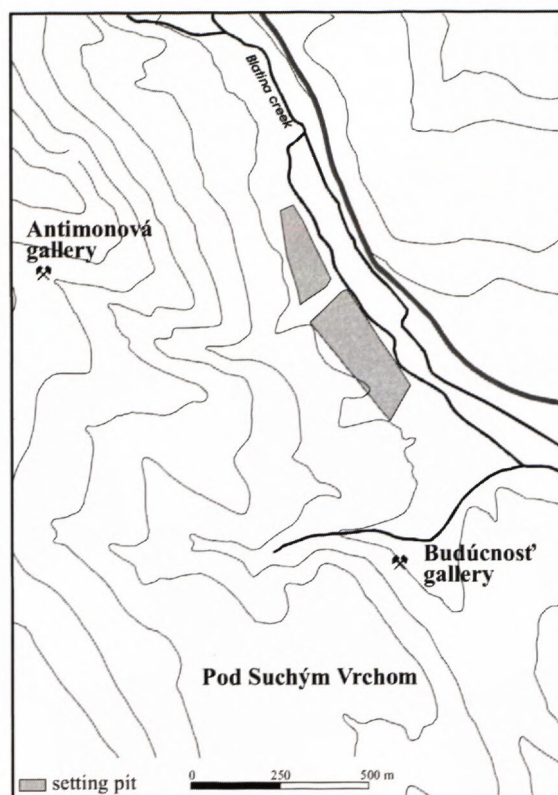
Fig. 1. Sketch of the studied area of the setting pits at the Pezinok deposit.

The content of these minerals in the sludge lagoons is considerably higher than that of Sb-minerals. The most frequent sulphide minerals in the sludge lagoons are arsenopyrite and pyrite. Gudmundite and stibnite occur rarely, pyrrhotine sporadically. In some samples Sb- and Fe-oxides, tetrahedrite, löllingite and chalcopyrite were determined (Chovan et al., 1994).

The gangue minerals are represented mainly by carbonates and quartz. The schist fragments occur only rarely. The dominant clay mineral is illite. Chlorite is abundant but kaolinite is very rare (Chovan et al., 1994). Also Fe-oxyhydroxides and Sb-oxides are formed in the oxidation zone of the sludge lagoons (Trtíková, 1999; Trtíková et al., 1999).

Biological–chemical oxidation

The principle of biogenic catalysis of sulphide oxidation consists in the activity of acidophilous, thionic, sulphur and iron oxidizing bacteria having a transporting function in the oxidation process, i.e. in the transfer of released electrons from the donor - sulphide to acceptor – oxygen (Mustin et al., 1992). Such activity of specific species of acidophilous bacteria results in the 2.10^5 multiple acceleration of Fe^{2+} oxidation (Bennett and Tributsch, 1978; Martyčák et al., 1994; Dopson and Borje, 1999).

As for sulphide minerals the autochthonous, acidophilous, chemolithotrophic bacteria of *Pseudomonales* family and *Thiobacillus* genus represent one of the basic components of the biogenic catalysis. A large number of

species of these bacteria was discovered and at least 14 species fall into the *Acidithiobacillus* genus. Mesophilic *ATF* species are of the highest value, sometimes *ATT*, but also the *Spirillaceae* tribe *LF* bacteria oxidizing Fe^{2+} in the ultra acidic environment. *Acidithiobacillus ferrooxidans* species are gram-negative nonsporeforming rods, 0.5–0.8 µm in diameter and 0.9–1.5 µm in length with one spiral flagellum (Spirito et al., 1982). Bacteria obtain the energy by oxidizing of Fe^{2+}-ore minerals. All bacteria of *Acidithiobacillus* genus also oxidize the elementary sulphur formed during the sulphides decomposition.

Sulphide minerals can be oxidized by indirect biological-chemical process (metabolic catalysis), i.e. by products of *ATF* bacteria metabolism formed in the presence of sulphides. In most cases both processes occur simultaneously. In addition to the oxidation of sulphides, there are reactions with CO_2 observed in the system.

Activity of ATF is usually associated with the aerobic environment. In the anaerobic conditions ATF bacteria oxidize sulphur indirectly by the biological-chemical oxidized Fe^{3+} cations (Pronk et al., 1994).

The marked alternation of surface morphology and consequently the structure uniformity of oxidized minerals represent the direct effect of biological-chemical oxidation processes. The changes are of individual character and related to the energetic state of individual parts and the whole crystalline structure of attacked sulphide mineral (Kušnierová and Štyriaková, 1994; Gueremont et al., 1998).

Morion et al. (1991) reported that there is a galvanic interaction between sulphide minerals and the transport of electrons from the sulphide mineral forming anode to the electrochemically less electro-active mineral occurs. According to Crundwell (1989) and Silva (2003) this effect can be interpreted as the modification of the semiconductive properties of sulphide minerals accompanied with the tiny changes in the structure and physical properties such as reflection, microhardness, conductivity, etc.

Materials and methods

The AMD waters were analysed by atomic absorption analysis for Fe, Mn, As, Cu, Ni, Pb, Sb and Zn. Two types of leaching experiments were realized to study the mobility of previously mentioned metals from the tailings impoundment sediments as well as the oxidation of ore minerals.

During the first experiment the tailings impoundment sediment and the polished sections of ore minerals were immersed to solution containing *ATF* bacteria isolated from the mine waters from Pezinok deposit (biological-chemical process) at pH 1.57. Biogenic catalysis of the selected sulphides oxidation was studied using the leaching nutrient medium 9K, part A according to Silverman and Lundgren (1959) with the content of nutrients for *ATF* cells growth.

The second experiment was the abiotic control carried out with the chemically identical leaching agent without bacteria *ATF* (chemical process).

The selected sample of the sediment X-1, the ochre sample X-2 from the tailings impoundments and the AMD of various pH and origin were analysed by atomic absorption analysis.

Polished sections of natural arsenopyrite, löllingite, native Sb, stibnite, gudmundite, berthierite, sphalerite, pyrite and chalcopyrite were studied under conditions of two parallel experiments (biological-chemical and chemical processes):

The polished sections of the ore samples were within the both experiments leached in Petri's dishes. Experiments took place at the room temperature. The changes on the ore minerals surface were evaluated optically at set time intervals using electron microprobe JEOL JXA – 840 in CLEOM laboratories at the Faculty of Natural Sciences of the Comenius University in Bratislava. Analytical conditions were as follows: accelerating voltage 10–20 kV, distance of sample from the secondary electrons detector 39 mm.

Results

Characterization of AMD waters

The investigated sample of sediment from tailing impoundments X-1 used for the next experiments was analysed by atomic absorption analysis (Tab. 1). The X-1 sediment sample from the tailing impoundments was employed in experimental works for the investigation of the leaching process by using of both types of drainage waters: acidic and neutral.

The AMD waters contain relatively high contents of Sb, As, Fe, Cu, Cd, Ni, Zn and other metals. The set of the drainage waters from Pezinok was completed with one sample of water from the wider mining ore field (P 1; Tab. 2).

The leaching activity in dependence to the leaching medium is presented in Tab. 3. For this experiment the drainage water P 2 from Pezinok with autochthonous ATF and ATT bacteria was used. The pH of the water was 4.5. The second sample of drainage water used for experiments was drainage water from Pezinok P 4 without bacteria (pH = 6.45). During the study of catalytic influences the parallel experiments were realized with rainwater for comparison.

The results show negligible differences of leaching activity between the medium containing bacteria species and those without bacteria but there was a great difference between two AMD samples and rainwater. We suppose that when pH of drainage water containing bacteria was >4, the activity of bacteria was very low (the highest activity of bacteria is in medium with pH <3) and caused the comparable results with the results of drainage water without bacteria.

The next experiment was realized using nutrient medium 9KA according to Silverman and Lundgren (1959) with bacteria and without bacteria (abiotic control). For the study of the biogenic catalytic influence in oxidation processes of weathering at the tailings impoundments was used pure culture of autochthonous ATF and ATT bacteria isolated from the drainage water P 1 at the deposit

Pernek. Bacteria were dispersed into nutrient medium WHH pH 1.57 at following conditions: P : K=1 : 3, temperature 30 °C, agitation at laboratory shaker during 4 weeks (Tab. 4).

The leaching of the X-1 sediment sample and heavy fraction of this sample by nutrient medium containing bacteria was compared with the results of X-1 sample leaching by nutrient medium without bacteria. The leaching continuance was studied by monitoring of selected elements (As, Cu, Co, Fe, Ni and Sb) and the experiment was interrupted after 4 weeks to segregate the product of precipitation: secondary salts and Fe ochres created by biological-chemical transformation.

From the Tab. 4 there follows, that in strongly acidic medium (pH = 1.57) ATF and ATT are active, and vigorously assist to the oxidation of ore minerals. Extraction rate of Fe, As and Sb is highest in the first week of leaching. As it could be expected, concentration of metal cations in the leaching product is highest in the run, where the heavy fraction of the sediment sample was employed.

In the second period of leaching we can observe the gradual decrease of Fe concentration in liquid phase in consequence of precipitation of Fe-oxyhydroxides. After leaching, the solid fraction was examined by means of XRD. Besides the detritic minerals (quartz, muscovite, phlogopite, chlorite and clinochlore) the secondary minerals, such as jarosite, hydrojarosite and gypsum were detected.

The activity of ATF bacteria considerable accelerated predominantly the extraction process of Fe, As and Sb both from the sample of the sediment (X-1) as well as from the sample of the heavy fraction.

Biological-chemical oxidation of As-minerals (löllingite and arsenopyrite)

The experimental study of biogenic catalysis of As-minerals showed that löllingite (mineral with the highest As content) is the first which is intensively attacked by biological-chemical oxidation. Already after 5 days of leaching its surface was markedly etched. After 14 days of leaching the minerals were entirely dissolved to the depth of about 100 μm (Fig. 2).

After 2 days of biological-chemical oxidation of arsenopyrite there was possible to observe the creation of dissolving channels at the cracks and at the contact of individual grains. The first pearl-string-like-chains began appear after 10 days of oxidation. The chains followed along the structural macro-defects of grain (Fig. 3) are probably formed due to the accumulation of metals at the surface of ATF cells. The heterogeneous distribution of As within the arsenopyrite grains is a characteristic feature, along with well developed zonal microstructures, which may be interpreted as growth-banding in the oscillatory hydrothermal fluid system. The origin of caves and preferential dissolution of As-abundant growth zones (Fig. 4) suggest the positive impact of galvanic effect of contact zones with the different As content. This galvanic dissolution allows to explain a complete dissolution of arsenopyrite on the contact with pyrite already after 18

Tab. 1. AAS analysis of the chemical composition of sediment sample from tailings impoundments

Sample	pH	ppm							
		Fe	Mn	As	Cu	Ni	Pb	Sb	Zn
X – 1	1.67	1 071	3.45	0.104	0.69	1.34	0.05	220.7	0.76
X – 1	1.67	1 014	2.57	0.090	0.48	0.02	0.05	196.1	0.52

Tab. 2. Composition of AMD water from Pezinok mining area including pH, content of investigated elements and presence of acidophilous bacteria.

Sample	pH	g/l						mg/l		Bacteria	
		As	Cu	Fe	Pb	Sb	Zn	Ag	Au	ATF	ATT
P 1	5.54	<5	<0.02	24.50	<2	<2	0.16	1.3	<2	+	+
P 2	4.50	<5	0.03	0.12	3.1	<2	0.11	0.9	<2	+	+
P 3	6.63	<5	<0.02	8.36	<2	3.4	0.12	0.8	<2	-	+
P 4	6.64	5.1	<0.02	31.20	<2	6.6	0.12	0.9	<2	-	-

Explanatory notes: P 1 – drainage water from Pernek locality, P 2 – drainage water from measuring-point 8, P 3 – drainage water from the creek near adit Michal, P 4 – Pezinok, drainage water from adit Budúcnosť, ATF, ATT – presence of the bacteria

Tab. 3. AAS analysis of various liquid media of different pH and rainwater used for leaching of the sediments from the tailings impoundments.

Medium	Time of leaching (weeks)	mg/l					
		As	Co	Cu	Fe	Ni	Sb
Drainage water P 2 ATF+ATT pH = 4.5	I	17.8	<0.06	0	213.7	2.7	8.0
	II	16.5	<0.06	0	253.4	5.3	8.8
	III	<2.0	0	6.3	195.7	5.2	<0.4
	IV	<2.0	0	5.2	126.5	4.4	<0.4
Drainage water P 4 pH = 6.45 no bacteria	I	16.8	<0.06	0	225.2	3.0	9.4
	II	12.1	<0.06	0	157.0	3.9	7.0
	III	<2.0	0	5.9	156.0	5.4	<0.04
	IV	<2.0	0	5.2	84.2	4.4	<0.04
Rainwater pH = 5.6 no bacteria	I	13.3	<0.06	0	188.9	2.9	8.8
	II	9.6	<0.06	0	142.1	3.5	7.4
	III	<2.0	0	4.1	115.3	3.2	<0.4
	IV	<2.0	0	5.1	95.6	4.1	<0.4

Tab. 4. Leaching of the sediment sample (A) and of its heavy fraction (B) from the tailings impoundments by *A. ferrooxidans* (ATF). a) nutrient medium; b) abiotic control without bacteria

Medium	Time of leaching (weeks)	mg/l					
		As	Co	Cu	Fe	Ni	Sb
(A) 9K-A ATF pH = 1.57	I	23.9	<0.06	0	4259.0	<0.1	9.0
	II	123.2	<0.06	0	2100.0	1.2	12.3
	III	72.0	0	3.3	167.4	1.5	7.5
	IV	58.6	0	3.6	135.6	1.7	9.2
(B) 9K-A ATF pH = 1.57	I	72.1	<0.06	0	4576.0	0	12.6
	II	317.3	<0.06	0	3183.0	0	21.6
	III	288.0	0	8.0	280.2	7.2	19.7
	IV	208.1	0	7.5	249.4	6.5	13.0
(A) 9K-A no bacteria pH = 1.57	I	32.6	<0.06	0	167.0	1.2	1.2
	II	36.8	<0.06	0	578.4	4.5	10.1
	III	22.6	0	8.8	378.0	7.1	<0.04
	IV	<2.0	0	7.4	271.1	5.9	<0.04

days of leaching (Fig. 5). Kinetics of chemical corrosion of pyrite was slower and was indicated by the formation of linear depressions (Fig. 6). In comparison with the biological-chemical oxidation the less intensive decomposition of the crystal surface was observed after 18 days of chemical leaching.

Biological-chemical oxidation of Sb-minerals (native Sb, stibnite, gudmundite and berthierite)

The first signs of dissolution and subsequent degradation of native antimony surface as a result of *ATF* bacteria activity was possible to observe already after 2 days of oxidation. Etching-patterns reminding the colomorphous structure were formed gradually with the period of leaching (Fig. 7), as well as the dissolving cracks at the points of bacteria attachment. The advancing etching gradually denuded the trigonal structure of the mineral (Fig. 8). The interesting concentrically lined spherical shapes were formed as the consequence of surface dissolution after 10 days of biological-chemical oxidation (Fig. 9). Chemical oxidation of native antimony is not so intensive. After 18 days of oxidation its surface is only planary etched (Fig. 10).

The first indications of dissolution by *ATF* bacteria medium were on the stibnite - Sb_2S_3 surface observed after 7 days of oxidation (Fig. 11). The etching-patterns and triangular-shaped caves appeared after 10 days of leaching (Fig. 12) arranged along lines parallel with axis c of the stibnite needle. Such progress of leaching reflected the stibnite crystallographic structure. At the contact of stibnite with sphalerite there was observed an intensive dissolution and hollows forming process after 10 days of leaching.

Etching-patterns highlighting the crystal structure were observed after 15 days of chemical leaching of stibnite (Fig. 13). The gypsum crystals formation along the carbonate veins and the intensive mineral dissolution was observed on the stibnite surface after 18 days.

Biological-chemical dissolution of gudmundite is relatively fast. The attachment of bacteria on the surface of crystal (Fig. 14) and the formation of dissolving rims round the mineral circuit and along the mineral cracks were possible to observe after 7 days of oxidation. The linear depressions following the gudmundite crystal structure were formed after 18 days of leaching (Fig. 15). The gudmundite surface chemical etching was ascertained only after 15 days (Fig. 16).

Berthierite is more resistant to biological-chemical and chemical oxidation in comparison with gudmundite (Fig. 17). The first signs of etching appeared on the crystals after 18 days of oxidation process. The intensive biological-chemical degradation started after 21 days. The significant chemical dissolution began markedly after 30 days (Fig. 18).

Biological-chemical oxidation of sphalerite

The selected sphalerite polished crystal pieces were kept in *ATF* cultures containing solution for a period of 50 days. The first signs of dissolution along the inclusions of individual grains (Fig. 19a) of mineral aggregate were observed after 18 days of leaching but the crystal surface was channelled markedly only after 25 days of leaching (Fig. 19b). However, no significant signs of biodegradation were observed on the euhedral inclusions of pyrite crystals (except for the flat etching-patterns). The final phase of biological-chemical oxidation of sphalerite is the intensive crystal etching after 40 days uncovering the tetrahedral structure of the lattice (Figs. 20 and 21).

The chemical leaching had minor kinetics. Only moderate etching patterns and channels were described after 20 days of leaching. The surface of crystals was evenly etched after 25 days. After 10 days of leaching the intensive dissolution of sphalerite was observed only along the contact of sphalerite, pyrite and chalcopyrite (Fig. 22), probably as a result of galvanic effect.

Biological-chemical oxidation of pyrite

After 10 days of biological-chemical leaching the morphological changes at the pyrite surface were observable only along the cracks: cells of bacteria formed chains or aggregates. After 25 days of leaching the surface of pyrite grains was covered with the rough crust of secondary minerals. The microprobe examination of pyrites revealed that the dissolution developed preferentially along pre-existing cracks and veinlets, as well as along grain contacts. The point dissolution and the formation of caves in the size of several μm were seen on the edges and in the centre of grain. The porous parts of the crystal were biodegraded faster than the compact growth zones (Fig. 23).

The shape of caves depended on the orientation of individual crystallographic faces. The caves of hexagonal cross-section (Fig. 24) are developed on screw dislocations of the cubic lattice, the triangular caves on (111) faces (Fig. 25a), while the square holes on (001) faces of the pyrite cubes (Fig. 25b).

After 30 days of chemical oxidation of pyrite the grains surface seemed to be intacted. Only euhedral gypsum crystals were found along the calcite veins (Fig. 26). The linear depressions and oriented tunnels were formed gradually after about 2 months of leaching. They were developed, similarly as in the case of arsenopyrite, preferentially in As-rich zones. The pyrite firstly dissolved around the inclusions of other sulphide minerals as a result of galvanic effect. Inclusions of euhedral pyrite in carbonates dissolved slower than those in quartz.

Biological-chemical leaching of chalcopyrite

The product of the chalcopyrite chemical oxidation is the elementary sulphur inhibiting the surface of chalcopyrite grains and is responsible for the process deceleration. Already Baláž et al. (1994) showed that the biological-chemical oxidation with *ATF* bacteria enables partial eliminating of this deceleration. Even the leaching in the *ATF* bacteria containing medium showed that the kinetics of oxidation processes is the slowest for chalcopyrite.
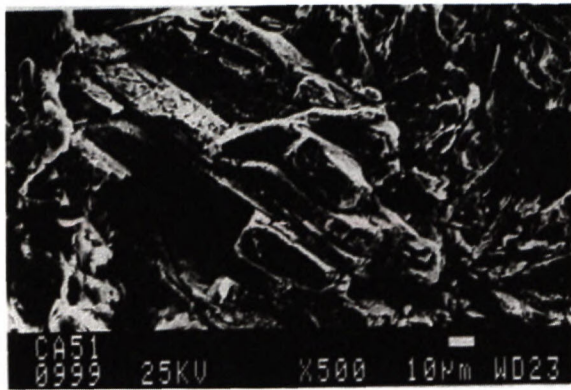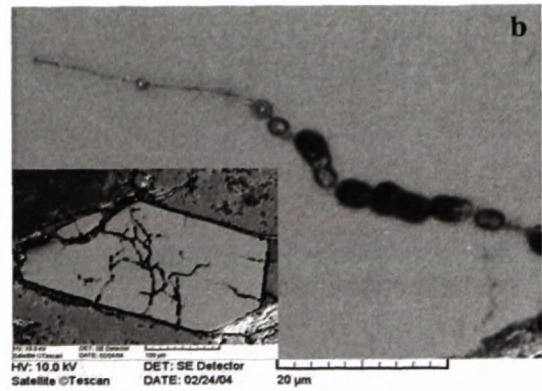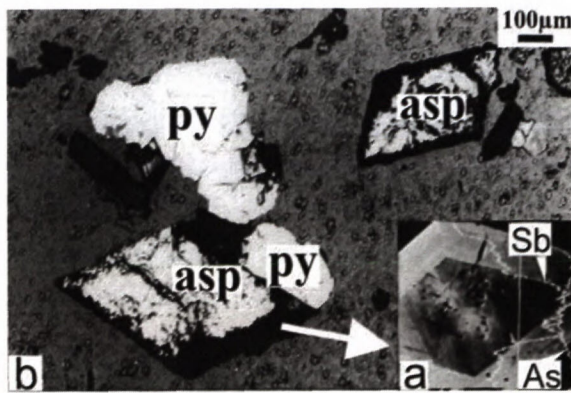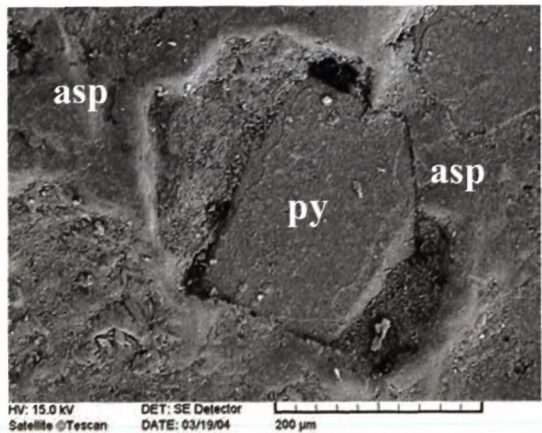
Fig. 2

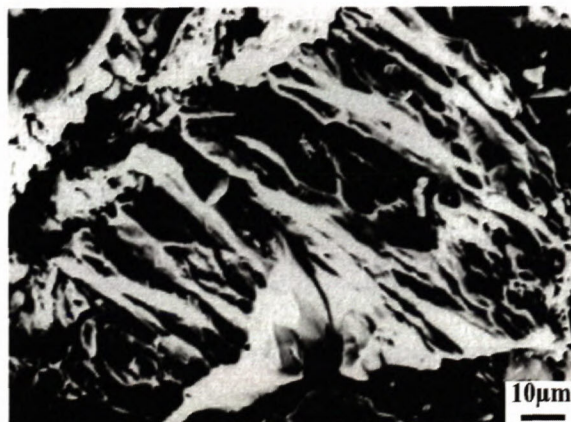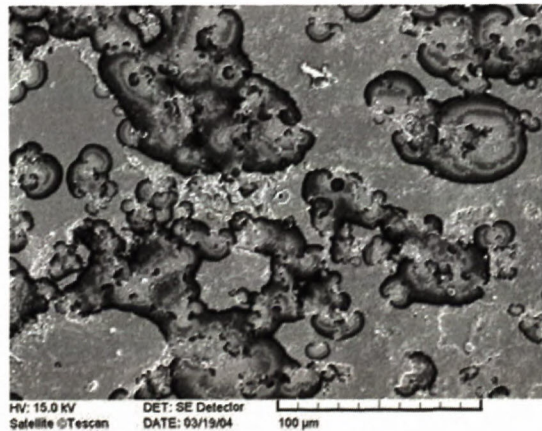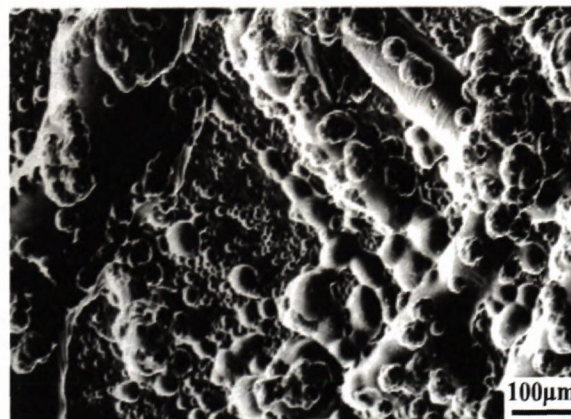
Fig. 3

Fig. 4

Fig. 5

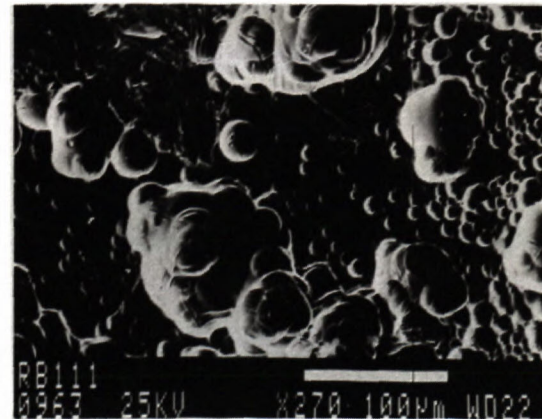
Fig. 6

Fig. 7

Fig. 8

Fig. 9

Fig. 2. Aggregate of euhedral löllingite crystals after 14 days of biological-chemical leaching (SEM secondary electron image).

Fig. 3. a – Demonstration of the pearl-string-like chains at the arsenopyrite surface after 10 days of biological-chemical leaching, b - detail of patterns after attachment of ATF bacteria (SEM secondary electron image).

Fig. 4. Preferential dissolution of arsenopyrite (asp) compared with pyrite during biological-chemical oxidation of sulphide ores (As-abundant arsenopyrite zones show intensive corrosion). After 18 days of biological-chemical leaching the surface of pyrite (py) remains intacted. a) Arsenopyrite crystal with line diagram of As and Sb contents (SEM secondary electron image).

Fig. 5. Preferential dissolution of arsenopyrite (asp) on the contact with pyrite (py) as a result of galvanic effect after 18 days of leaching.

Fig. 6. Linear depressions on the pyrite surface after chemical leaching (SEM secondary electron image).

Fig. 7. SEM secondary electron image of the colomorphous–like etching patterns at the native Sb surface after 6 days of biological-chemical leaching.

Fig. 8. Etching-patterns reflecting the trigonal mineral structure of native Sb after 10 days of biological-chemical leaching.

Fig. 9. Concentrically lined globular shapes at the surface of native Sb after 18 days of biological-chemical leaching (SEM secondary electron image).

After 30 days of chemical and biological-chemical oxidation there was only a weak etching of the surface observed (Fig. 27).

Discussion

Research studies of Trtíková et al. (1999), Trtíková (1999) and Andráš et al. (2004) demonstrated that there are two types of acid mine drainages in the area of the Pezinok deposit:

– First type → extremely acid (pH < 3) mine water associated with synsedimentary massive pyrite-pyrrhotine ores,

– Second type → neutral mine water (pH 5.5–7) associated with Sb-carbonate mineralization.

The activity of *ATT* and *ATF* bacteria in the first type of acid mine drainage is much higher. It is the neutral water that percolates through the sludge lagoons of Sb-ores in the Kolársky hill area and that is why the leaching intensity is much lower than in the area of pyrite-mineralized parts (Augustin adit and the like). A considerable amount of Fe precipitates in the form of ochres during the neutralization of solutions. Ochres form the geochemical barrier and their surface serves as a sorbent of a considerable amount of metals. It is impossible to exclude that during torrential rains and under other influences the ochres may overcome the barriers of the tailing dams and reach the water flows. According to Luptáková (2001) concentration of heavy metals in the water of sludge lagoons may be influenced also by anaerobic sulphate reducing bacteria producing hydrogen sulphide reacting with ions of heavy metals producing the secondary minerals. Luptáková realized the isolation of those bacteria from the solid samples of the reducing zone of the sludge lagoon. The undercritical content of metals in waters, if flowing through the country for a long time, intoxicates river-sediments and gradually increases the metal concentrations as well.

Experimental studies of biogenic catalysis from the point of view of changes in the ore mineral surfaces in the sludge lagoons confirmed considerable differences in the kinetics and decomposition of studied minerals. The reaction ability of minerals reflects the distribution of the reactive planes and points at the crystal surfaces and the relation of these points to the energy of mineral crystalline lattice. During the biological-chemical oxidation processes it was possible to observe various signs of dissolution at the mineral surfaces that related to the metabolic processes of bacteria. For instance, the biological-chemical oxidation of pyrite is marked by the formation of characteristic etching-holes described by Morion et al. (1991). Morion described the galvanic interaction between different sulphide minerals during which the electrons are transferred from one sulphide mineral (anode) to less electroactive sulphide mineral. According to Crundwell (1989) this effect can be interpreted as the modification of sulphide semiconductive properties accompanied with the tiny changes in the structure and physical properties (reflection, microhardness, conductivity, etc.) of sulphide minerals. The galvanic effect accelerates the dissolution of minerals. Such an effect was also observed during experiments carried out with the selected sulphide minerals from the Pezinok deposit. The preferential dissolution of contact grains was observed at the interface of different sulphide minerals or around the inclusions of sulphide minerals. On the other hand, a considerable deceleration of chemical and biological-chemical oxidation (with the formation of gypsum as an associated phenomenon) was observed as a result of neutralization effect of inherent carbonate component for sulphide inclusions in carbonates.

The presented results of native Sb biological–chemical leaching suggest also the possible role of Sb in metabolism of *ATF* bacteria.

Conclusion

The control of acidity is of utmost importance in leaching, because of acidic environment must be maintained in order to keep ferric iron and other metals in solution. Acidity is controlled by the oxidation of iron, sulphur (and also antimony?), by the dissolution of carbonate ions and by the decomposition of ferric iron through reaction with water.

The process of studied ore minerals degradation during biological-chemical oxidation in the presence of autochthonous, acidophilous, sulphur and iron oxidizing *ATF* and *ATT* bacteria and during chemical oxidation is
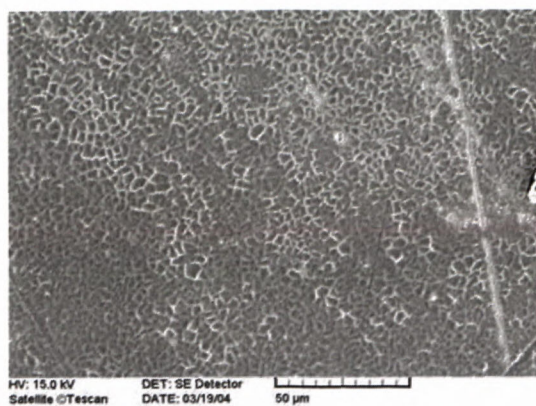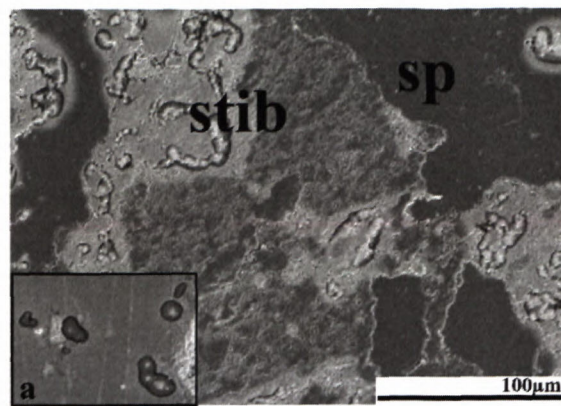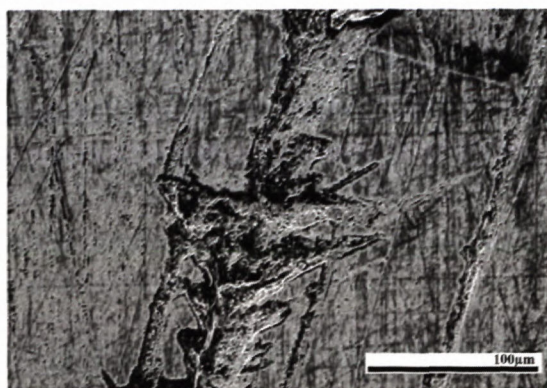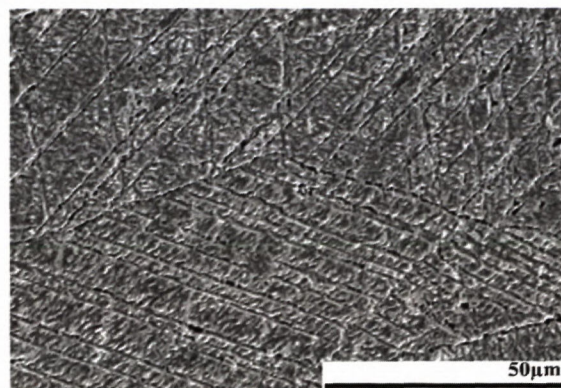
Fig. 10

Fig. 11
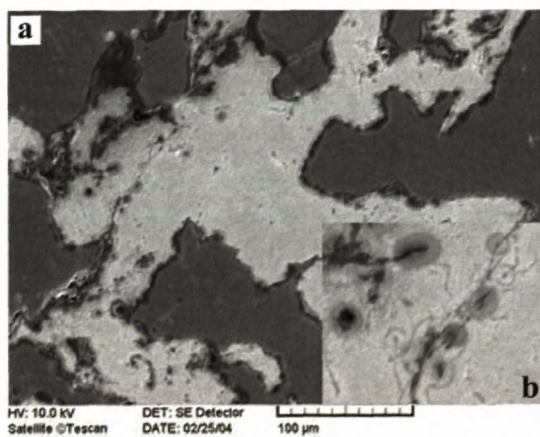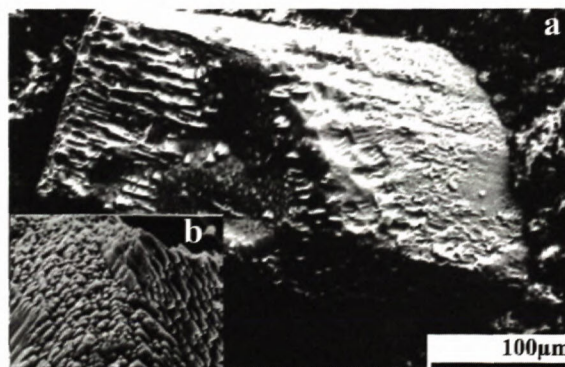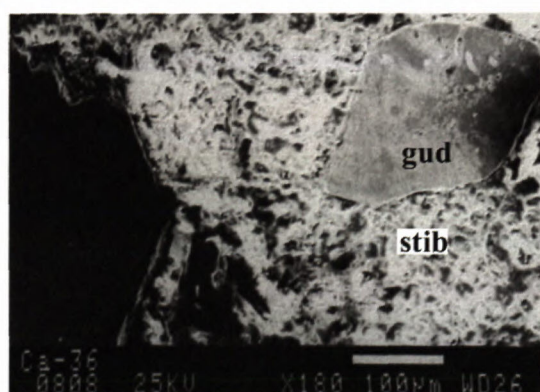

Fig. 12

Fig. 13

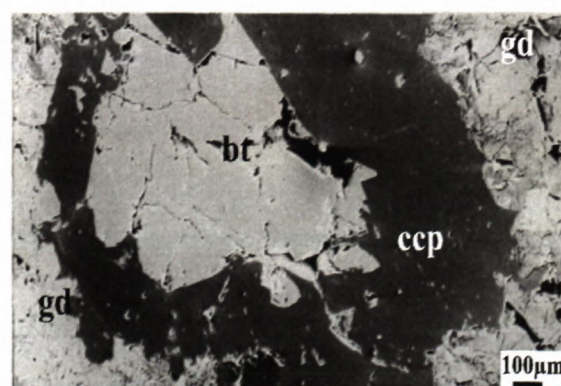Fig. 14

Fig. 15

Fig. 16

Fig. 17

Fig. 10. Biodegradation of native Sb after 18 days of chemical leaching (SEM secondary electron image).
Fig. 11. First etching patterns (a) on the stibnite (stib) after 7 days of biological–chemical leaching (sp - sphalerite).
Fig. 12. Triangular-shaped etching-patterns at the stibnite surface after 10 days of biological-chemical oxidation. a) Attachment of ATF bacteria on the stibnite surface after 7 days of biological-chemical leaching.
Fig. 13. SEM secondary electron image of the etching-patterns (reflecting the lattice structure) on the stibnite surface after 10 days of chemical leaching.
Fig. 14. a - Attachment of ATF bacteria on the gudmundite surface after 10 days of biological-chemical leaching (b – detail).
Fig. 15. a - SEM secondary electron image of the etched gudmundite surface after 18 days of biological-chemical degradation; (b – detail).
Fig. 16. Chemically etched gudmundite (gud) surface after 18 days of chemical leaching (stib - stibnite).
Fig. 17. Non-interfered chalcopyrite surface (ccp), weakly etched berthierite surface (bt) and markedly corroded gudmundite surface (gd) after 18 days of biological-chemical leaching.

principally similar, but the kinetics of both processes is different. Higher kinetics of biological-chemical oxidation processes of studied minerals confirms the bio-catalytic influence of autochthonous bacteria.

The result of experiments confirmed that the biogenic catalysis is the most intensive in löllingite. The other studied minerals can be arranged according to the decreasing oxidation kinetics as follows: arsenopyrite, native Sb, stibnite, gudmundite, berthierite, and sphalerite. Pyrite and chalcopyrite seem to be the most resistant to the biological-chemical as well as chemical oxidation.

The positive correlation between the oxidation rate and As contents was ascertained for löllingite, arsenopyrite and pyrite. At the contact of two different minerals or two mineral growth zones with the different content of isomorphic components (in arsenopyrite, pyrite and gudmundite) the galvanic effect was ascertained. Pyrite crystals in carbonates are degraded slower than those in quartz. In some minerals (mainly pyrite) the shape of dissolving caves and tunnels depend on the crystallographic orientation of individual crystal faces.

The comparison of biological-chemical oxidation with chemical oxidation enabled to find the differences in the leaching mechanism. The structures formed during the biological-chemical oxidation in *ATF* containing medium are characterized as follows:

- The bacterial leaching causes the origin of caves and point etching-patterns probably due to the direct mechanism of biological-chemical oxidation of the contact dissolution by microorganisms. They relate to the metabolic processes of applied bacteria.

– The shape of formed caves depends on the crystallographic orientation of etched faces.

– The formation of various oriented tunnels, lines and dissolving planes is the implication of the chemical corrosion.

After a certain time the crusts of the secondary minerals appears at the mineral surfaces for both types of oxidation mechanisms.

Acknowledgements

References

Andráš, P., Milovská, S., Kušnierová, M., Chovan, M., Adam, M., Šlesarová, A., Hajdučková, Ľ. & Lalinská, B., 2004: Environmental hazards at the Sb- (Au-) deposit Pezinok (Slovakia) in relation to the chemical and biological-chemical oxidation processes. 7th International symposium on environmental geotechnology and global sustainable development introduction (International Society of Environmental Technology), Helsinki 2004, 8-20.

Baláž, P., Kušnierová, M., Varencova, V. I. & Mišura, B., 1994: Mineral properties and bacterial leaching of intensively ground sphalerite and sphalerite-pyrite mixture. Int. J. Mineral Processing, 40, 273-285.

Bennett, J. C. & Tributsch, H., 1978: Bacterial leaching patterns on pyrite crystal surfaces. Journal of Bacteriology, 134, 1, 310316.

Chovan, M., Rojkovič, I., Andráš, P. & Hanas, P., 1992: Ore mineralization of the Malé Karpaty Mts. (Western Carpathians). Geologica Carpathica, 43, 5, 275-286.

Chovan, M., Khun, M., Vilinovič, V., Šucha, V. & Trtíková, S., 1994: Mineralogy, petrography and geochemistry of Au-As-Sb mineralization in Tojárová adit. Univerzita Komenského, Bratislava – Geologický prieskum, Spišská Nový Ves, Manuscript, 83 p.

Crundwel, F. K., 1989: The influence of the electronic structure of solids on the anodic dissolution and leaching of semiconducting sulphide minerals. Hydrometallurgy, 22, 141-157.

Dopson, M. & Borje, L. E., 1999: Potential role of Thiobacillus caldus in arsenopyrite. Applied and Environmental Microbiology, 65, 1, 36-43.

Gueremont, J. M., Elsetinow, A. R., Strongin, D. R., Bebie, J. & Schoonen, M. A. A., 1998: Structure sensitivity of pyrite oxidation. Comparison of the (100) and (111) planes. American Mineralogist, 83, 1353-1356.

Kušnierová, M. & Štyriaková, I., 1994: Biotransformtion of sulphides. In: Biohydrometalurgy - III., ÚGt SAV Košice, 19-25.

Luptáková, A., 2001: Bioaccmulation of heavy metals from acid mine water. Acta Avionica, 4, 104-107.

Martyčák, K., Zeman, J. & Vacek-Veselý, M., 1994: Supergene processes on ore deposits: A source of heavy metals. Environmental Geology, 23, 156-165

Morion, P., Monroy, M., Mustin, C. & Berthelin, J., 1991: Effect of auriferous sulphide minerals structure and composition on their bacterial weathering. Source, transport and deposition of metals, Balkema, Rotterdam, 561-564.

Mustin, C., Berthelin, J., Marion, P. & Donato, P., 1992: Corrosion and electrochemical oxidation of a pyrite by Thiobacillus ferrooxidans. Applied and Environmental Microbiology, 58, 4, 1175-1182.
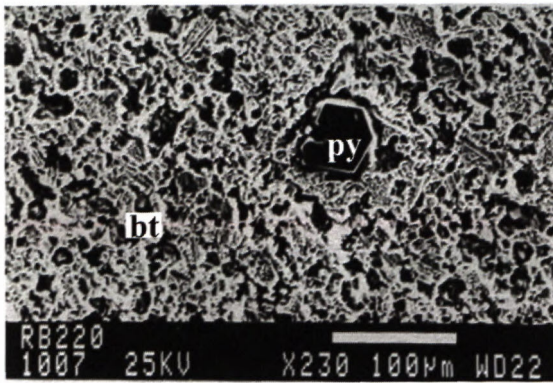
Fig. 18
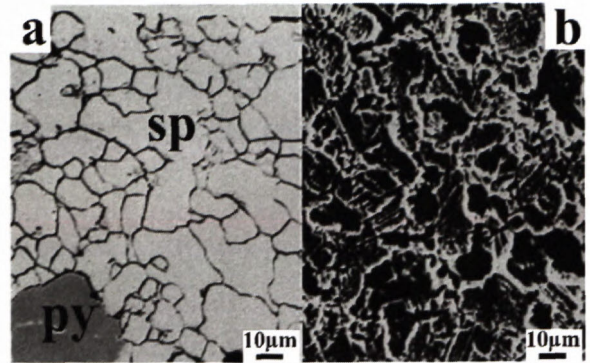
Fig. 19
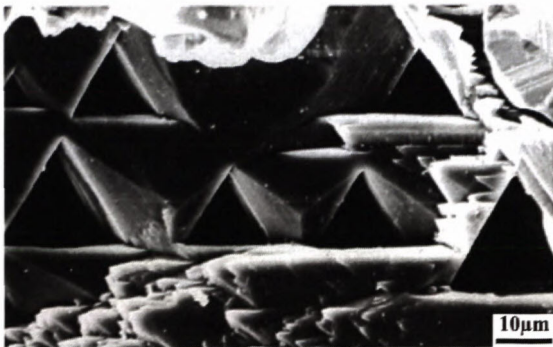
Fig. 20
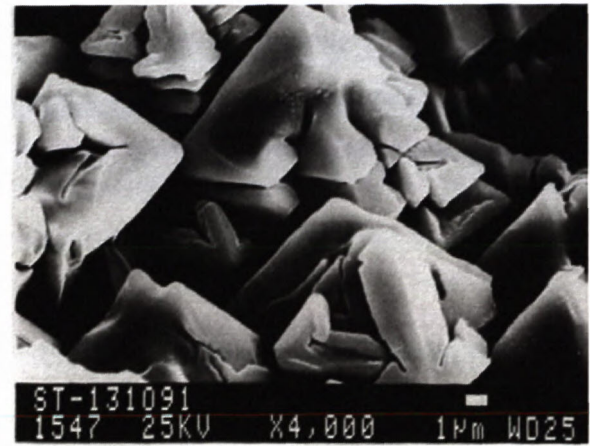
Fig. 21
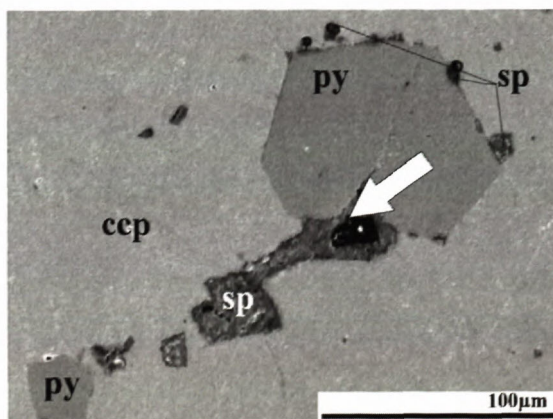
Fig. 22
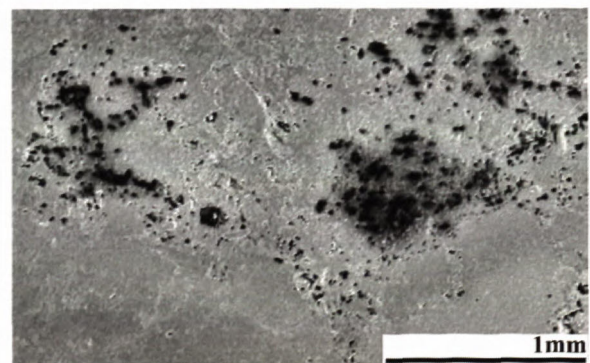
Fig. 23
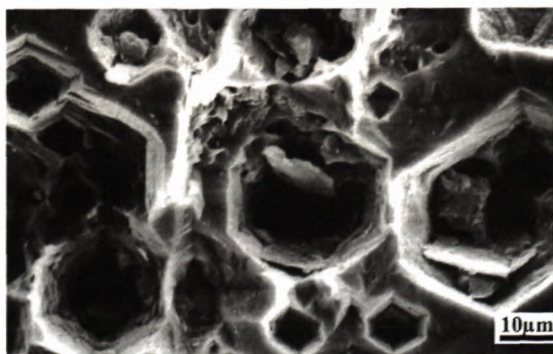
Fig. 24
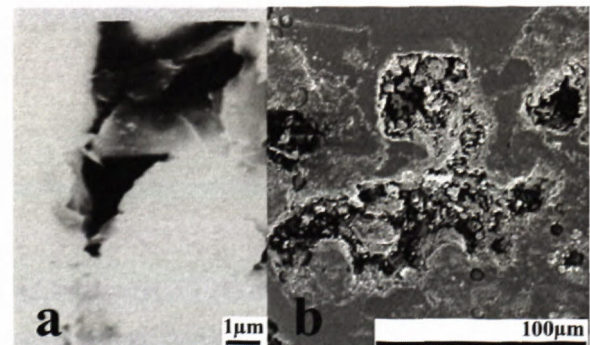
Fig. 25

Fig. 18. Significant chemical dissolution of berthierite (bt) after 30 days (py – pyrite) SEM secondary electron image.

Fig. 19. a - Sphalerite (sp) dissolution along the inclusions after 20 days of chemical leaching. There are no signs of etching or dissolution at the pyrite (py) surface; b - channelled surface of the sphalerite aggregate after 25 days of biological-chemical leaching in ATF containing medium.

Fig. 20. Etched sphalerite crystal structure after 40 days of biological-chemical leaching in ATF containing medium. SEM secondary electron image.

Fig. 21. Etched sphalerite crystal structure after 40 days of biological-chemical leaching in ATF containing medium.

Fig. 22. Preferential sphalerite (sp) dissolution along the contact with pyrite (py) as a result of galvanic effect (ccp – chalcopyrite).

Fig. 23. Formation of small caves within the porous parts of pyrite grains after 25 days of biological-chemical leaching.

Fig. 24. Caves of hexagonal cross-section in the points of lattice loop-deformations of pyrite octahedrons after 40 days of biological-chemical leaching.

Fig. 25. SEM secondary electron image of oxidation progress at the surface of pyrite crystals. a) Formation of triangle-shaped caves on (111) faces. b) Formation of square-cross-section holes on (001) faces of pyrite cubes.
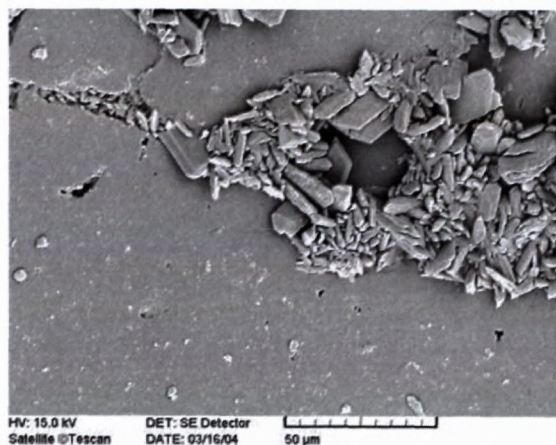
Fig. 26
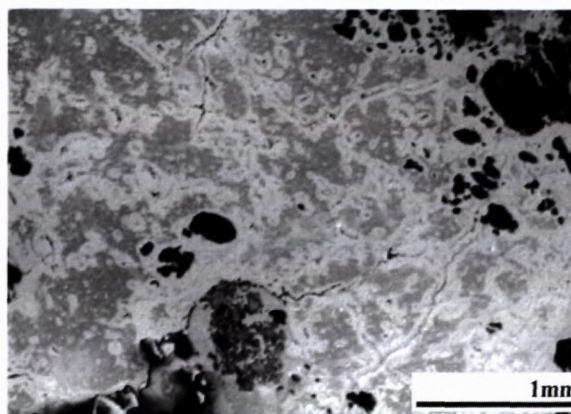
Fig. 27

Fig. 26. Formation of euhedral gypsum crystals (gy) along the carbonate cement within chalcopyrite grains (ccp) after 10 days of biological-chemical leaching.

Fig. 27. First etching patterns of chalcopyrite surface after 30 days of biological-chemical leaching

Pronk, T. T., de Bruyn, J. C., Bos, P. & Kuenen, J. G., 1994: Anaerobic growth of Thiobacillus ferrooxidans. *Appl. Environ. Microbiol.*, 58., 2227-2230.

Silva, G., Lastra, M. R. & Budden, J. R., 2003: Electrochemical passivation of sphalerite during bacterial oxidation in the presence of galena. *Minerals Engineering*, 16, 199-203.

Silverman, M. P. & Lundgren, D. G., 1959: Studies on the chemoautotrophic iron bacterium Ferrobacillus Ferrooxidans II. Manometric Studies, Bacteriol; 78(3), 326–331.

Spirito, Di, A. A., Silver, M., Voss, L. & Tuovinen, O. H., 1982: Flagella and Pili of iron-oxidizing Thiobacilli isolated from a uranium mine in Northern Ontario, Canada. *Appl Environ Microbiol.* 43, 5, 1196–1200.

Trtíková, S., 1999: Iron ochres: Products o weathering process in Fe and Sb-Au-As deposits in the Malé Karpaty Mts. *PhD Thesis. Faculty of Natural Sciences, Comenius University*, Bratislava, 102 p.

Trtíková, S., Chovan, M. & Kušnierová, M., 1999: Oxidation of pyrite and arsenopyrite in the mining wastes (Pezinok – Malé Karpaty Mts.). *Folia Fac. Sci. Nat., Univ. Mas. Brun. Geologia*, 39, 225-231.

Uher, P., Michal, S. & Vitáloš, J., 2000: The Pezinok antimony mine, Malé Karpaty Mts., Slovakia. *The Mineralogical Record*, 31, 153-162.

Decompression cooling of the basement garnet-sillimanite paragneisses from Palmas (Tocantins, Brazil)

[1]MARIAN DYDA, [2]GERVALINO ALMEIDA JUNIOR, [3]FRANTISEK MARKO and [4]MÁRCIO REIS DE OLIVEIRA

[1]Department of Mineralogy and Petrology, Comenius University, Bratislava, Slovakia; dyda@fns.uniba.sk
[2]Governo do Estado do Tocantins, Agencia de Desenvolvimento, Tocantins, Brasil
[3]Department of Geology and Paleontology, Comenius University, Bratislava, Slovakia
[4]Governo do Estado do Tocantins, Agencia de Desenvolvimento, Tocantins, Brasil

Abstract: Protolithic rocks of the paragneisses were well sorted high aluminous pelitic sediments. Medium pressure regional metamorphism of slow heating, indicated by slow garnet nucleation rate (3.8×10^{-10} N/cm^{3}s), attained the culmination conditions at 604 ± 30 °C and pressure of 3.4 ± 0.4 Kbar at the depth of ca. 12-14 km. Garnet-sillimanite assemblage without foliation had been formed, representing one dominant Precambrian metamorphic event. The rock cooling from the peak conditions was slow (1.2-3.3 °C/Ma), as calculated from garnet concentration profile and might have lasted ca. 30-80 Ma. However, the final process of the cooling and uplift was more rapid when closing P-T conditions (515 ± 15 °C and 2.5 ± 0.3 Kbar) were established. No retrograde fluid infiltration that could have changed the peak assemblage has been observed. Paragneisses are considered to represent a low pressure portion of the cratonic crystalline complex.

Key words: Precambrian metamorphism, thermobarometry, cooling, metapelites, Palmas, Brazil.

Introduction

Many uncertainties surround the metamorphic processes in the crust, their later cooling and uplift from the depth to the positions where they are currently exposed. Paragneisses are particularly frequent in Precambrian terranes and are generally thought to represent the exhumed roots of the old mountain belts complexes and the associated metamorphism is considered to be the result of burial during crustal thickening.

Detailed studies however point at more complex development of paragneisses than the simplified crustal thickening and exhumation. Many paragneisses develop under significant perturbation of "normal" continental geotherm with different intensity and extent. Lower pressure paragneisses may also be formed, in some cases, with andalusite and cordierite occurrence in rocks. Some Precambrian metamorphites show high pressure isobaric cooling generally accepted as the evidence of prolonged residence in the lower crust after the peak temperature mineral assemblage had been formed and deformation later followed. But many data suggest that in some Precambrian terranes deformation continued during cooling at constant or slightly increasing crustal thickness (Phillips & Wall, 1981; Waren, 1983; Clarke et al., 1987). The crustal stability that apparently postdates metamorphic processes in many metamorphic terranes contrasts with the isothermal, rapid uplift of metamorphic rocks from the roots of many Phanerozoic orogenic belts (see e. g. Selverstone et al., 1984), where the effects of extension, erosion, or both seem to terminate the metamorphic process (England & Richardson, 1977; England, 1987). The crustal stability after metamorphism and deformation is that the synmetamorphic deformation did not result in the

overthickened crust and the rocks in these terranes were probably uplifted to the Earth's surface by later events which were casually unrelated to thermal metamorphism. The general cause of high grade metamorphism in many terranes must be external to the rocks we observe, and most probably external to the crust (Vernon et al., 1990). Thermal perturbations required for the high grade facies formation are established with difficulty by just an overthickening of the crust (Thompson & England, 1984). In many events they would occur late in the evolution of a mountain belt during the isothermal decompression of deeply buried rocks. Although the remnants of an eroded mountain chain may cool isobarically from a late thermal peak of metamorphism (Thompson & England, 1984; Ellis, 1987). The thinning, deformation and peak metamorphism in many terranes preclude such a tectonic setting. The heat contribution to a terranes by magmas is often presented as a direct cause of some high grade metamorphism. However, the magmas commonly do not appear to be abundant enough or they are not synchronous with the metamorphic peaks (Wells, 1980).

Field occurrence

Metapelitic garnet gneisses occur near capital of Tocantins, Palmas, along the banks of the creek Corrente Mirindiba. Measured dip direction and dip was 156/45°. Rock occurred also as isolated blocks of different sizes, maximum 3-5 m in diameter, within the field area given by the coordinates: W-47°50' S-10°10'; W-48°00', S-09°50'; W-48°20', S-10°20' (see Fig. 1a,b.).

Studied gneisses occurrence is located in the Proterozoic crystalline basement near the western edge of post orogenic Paleozoic-Mesozoic Parnaiba (Maranhao) sedi-
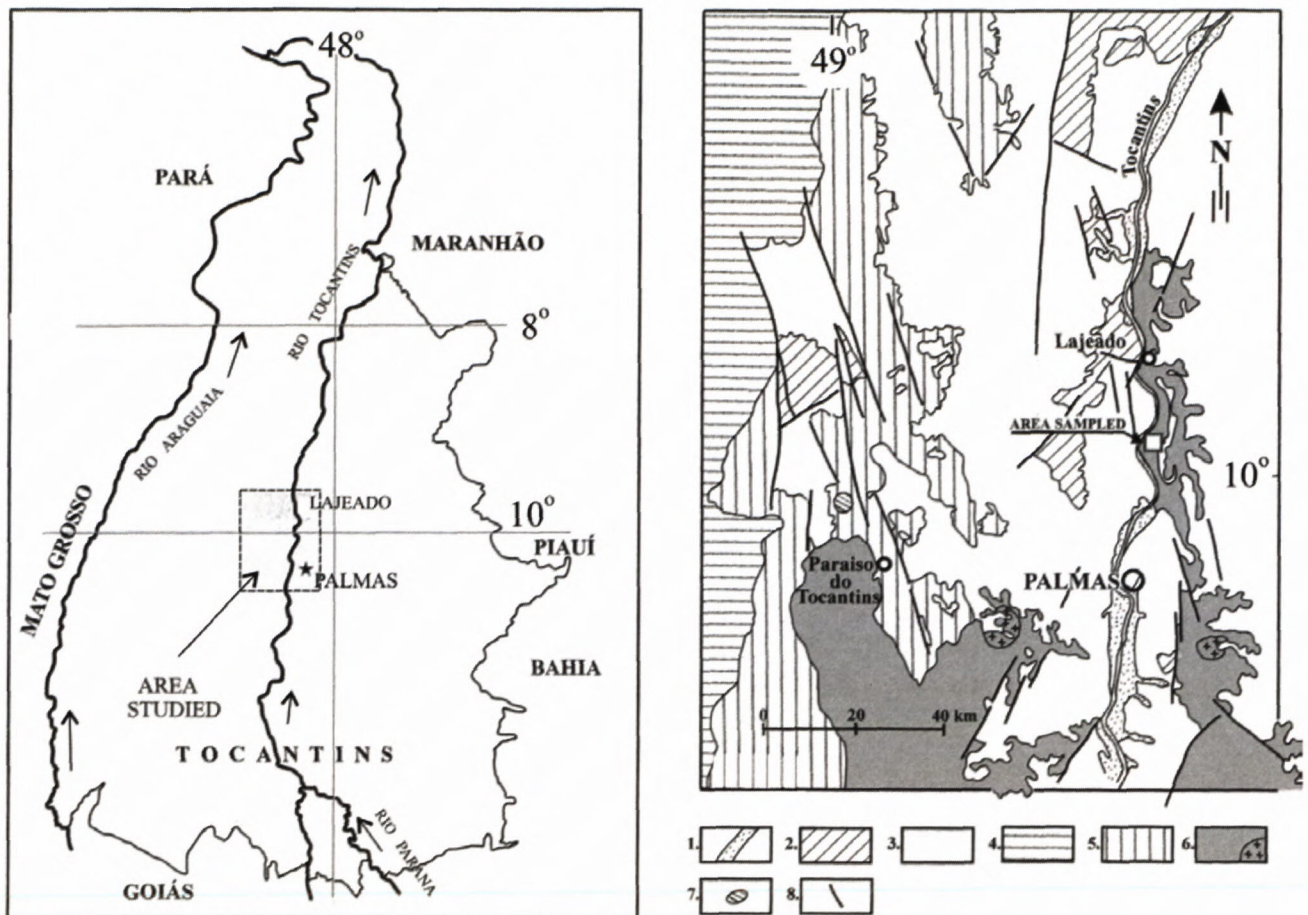
Fig. 1a,b. Schematic geological map of the studied area compiled from geological map Projeto Radambrasil, 1981. 1 - alluvial sediments of the Tocantins river (Quaternary), 2 - arenites, silts, locally conglomerates (Carboniferous), 3 - arenites, silts, conglomerates (Silurian-Devonian), 4 - metasediments of the Tocantins Group (Middle Precambrian), 5 - metamorphic rocks of the Araxa Group (Middle Precambrian), 6 - gneisses and granites of the Gioano Complex (Lower Precambrian), 7 - igneous alkaline rocks, 8 - airborne faults. Sampled area locations - banks of the Corrente Mirindiba.

mentary basin. Sediments of the inverted Parnaiba basin currently forming elevated plateau overlie Sao-Francisco crystalline shield, which is from the western border rimmed by the Neoproterozoic Tocantins mobile belt. The crystalline Goiania Complex (Projeto Radambrasil, 1981), is composed of metapelitic garnet gneisses, migmatites, amphibolites, quartzites, granites, pegmatites, granulites, marls, sporadically basic and ultrabasic intrusive bodies

Garnet gneisses are mostly massive with no distinct foliation and some isolated blocks have a lensoid appearance. Some may be characterized by an inhomogeneous structure, reflecting probably the protolithic compositional changes.

Petrography and structure of the garnet-sillimanite paragneisses

The outcropping rocks show small differences in mineral modes. They are medium to coarse grained with semipelitic composition and exhibit granoblastic to lepidoblastic texture. No banded structures composed of leucocratic and melanocratic parallel bands are present.

The main minerals of the studied gneisses are: sillimanite (Sil, ~18 mod.%), garnet (Grt, ~ 8 mod.%), biotite (Bt, ~ 40 mod.%), plagioclase (Pl, ~ 10 mod.%) and quartz (Qtz, ~ 22 mod.%). Sil and Bt are dominant mineral phases. Rare postculmination minerals with quantitative amount less than 1 mod.% are andalusite (And) and cordierite (Crd). In accessory amount there are present: ilmenite (Ilm), zircon (Zrn), apatite (Ap) and chlorite (Chl).

Garnet porphyroblasts up to ~1 cm in diameter are regularly scattered in the rock matrix and are microscopically homogeneous with occasional poikilitic minute inclusions of Bt, Pl and Qtz. No significant inclusions were observed within garnet, that may serve as a strong reminiscence of prograde breakdown of e.g. chloritoid, staurolite, deciphering thus the progressive pre-culmination metamorphic stages with the Grt+Sil equilibrium assemblage. Garnet rims are in few cases slightly chloritized as the consequence of the restricted post-culmination retrograde reactions. At the edges and interstitions no signs of development of the symplectite textures have been observed.

On the basis of the mode of appearance, only one type of biotite is distinguishable forming the equilibrium cul-

M. Dyda et al.: Decompression cooling of the basement garnet-sillimanite...

93

mination matrix with the other felsic minerals. Biotite as a dominant phyllosilicate shows no sub-parallel alignment, flakes' orientation and do not represents distinctive rock schistosity. As the biotite is abundant and pyroxene is still missing, the transition of rocks from upper amphibolite to granulite facies conditions has not been attained.

The presence of Al_2SiO_5 minerals in rocks is important as their stabilities are controlled by temperatures and solid pressures (see e.g. Richardson et al., 1969; Holdaway, 1971). The presence of metastable Al_2SiO_5 relics is particularly important for inferring earlier metamorphic P-T conditions and assessing the metamorphic trajectory. No pseudomorphs after andalusite, staurolite or chloritoid reaction rests have been found, indicating the progressive passing into the sillimanite stability field.

The coexistence of Grt and Sil is important in order to estimate the peak metamorphic condition on the basis of their structural appearance. This assemblage is commonly observed in the region, without primary or secondary muscovite, except some vanishing retrograde modal amount. If K-feldspars would have been present that might have formed an argument that muscovite was not more stable in the presence of quartz. A few fine muscovite and chlorite grain flakes seldom develop at matrix mineral contacts and are considered to be produced during the retrogression with restricted hydratation.

The rock structure, common occurrence of Grt+Sil+Qtz assemblage and decompression reaction Grt + Sil + Qtz = Crd would be responsible for rare cordierite presence. Microscopic reaction domains, restricted garnet and sillimanite decomposition reaction features support this presumption. Some matrix domains favour tiny cordierite development at the grain contacts of Bt+Qtz and Bt+Sil.

Consequently, this cordierite microscopic appearance and its crossing of the biotite culmination grains forms an argument for its post-peak development during decompression processes. In few cases, minute chlorite grains

participate on the Grt decomposition. Only some muscovite flakes are associated with plagioclase at their grains interstitions. At some garnet edges, tiny aggregates of muscovite and chlorite indicate the restricted complex retrograde reactions with a minimum extent. Thus, the thermal culmination mineral assemblage was almost untouched by the later retrograde reactions.

The garnet grains have no significant mineral relics useful for reasonably interpretation of early stages of recrystallization, what makes difficult to infer the preculmination metamorphic trajectory of these rocks on the basis of microscopic mineral appearance. The post-culmination retrograde processes producing tiny amounts of andalusite, cordierite, chlorite and muscovite have left the peak mineral assemblage unhydrated.

The paragenetic and structural relationships among garnet, biotite and sillimanite in the studied rock domains suggest, that the peak temperature and pressure formed the well equilibrated mineral assemblage.

Geothermobarometry, diffusion and garnet crystal size data

Chemical analyses of minerals were carried out on CAMECA SX 100 electron microprobe analyser with an accelerating voltage of 15 kV, 20 nA beam at GÚDŠ (Dr. P. Konečný, Bratislava, Slovakia). The analyses of garnets, biotites and plagioclases are given in Tab.1.

Chemical composition of the garnet porphyroblasts (Tab.1) was determined in five rock samples, where mineral equilibrium domains were confirmed. The garnet grains are unzoned, almost homogeneous and the compositional uniformity suggests that diffusion homogenization was realized during metamorphic thermal culmination of this terrane. The compositional changes at the garnet edges and mineral grain contacts in the analysed domains are ascribed to the post-culmination processes

Tab. 1. Chemical analyses of coexisting garnets, biotites and plagioclases from Palmas paragneisses.

GARNET ANALYSES

N°	1.	2.	3.	4.	5.	6.	7.	8.	9.	10.	11.	12.
Sample	I.1c	I.1r	I.3c	I.3c'	I.3r	II.2c	II.2r	II.3c	II.3r	II.4c	II.4c'	II.4r
SiO_2	36.66	37.52	37.18	37.14	36.56	35.65	36.71	36.91	36.78	36.78	36.71	36.67
TiO_2	0.00	0.02	0.00	0.01	0.03	0.00	0.03	0.01	0.05	0.08	0.07	0.00
Al_2O_3	20.66	20.88	20.32	20.31	20.18	19.85	20.19	20.41	20.23	20.35	20.38	20.38
Cr_2O_3	0.00	0.00	0.00	0.03	0.02	0.04	0.07	0.01	0.00	0.05	0.03	0.00
FeO	37.60	37.67	37.39	37.57	37.55	37.24	37.54	38.08	37.30	37.00	37.76	38.09
MnO	1.65	1.35	1.45	1.49	1.56	1.70	1.99	1.56	1.65	2.30	1.22	2.08
MgO	2.26	2.04	2.11	2.32	1.91	2.27	1.61	2.58	1.90	1.45	2.63	1.57
CaO	1.12	1.57	1.74	1.25	1.71	1.15	1.62	0.92	1.68	1.25	0.89	1.61
Total	99.95	101.05	100.19	100.12	99.52	97.90	99.76	100.48	99.59	99.66	99.73	100.40
Cations on 12 oxygen basis												
Si	2.986	3.014	3.018	3.016	2.998	2.977	3.007	2.993	3.009	3.020	2.994	2.991
Ti	0.000	0.001	0.000	0.000	0.002	0.000	0.002	0.001	0.003	0.004	0.004	0.000
Al	1.984	1.977	1.944	1.944	1.951	1.954	1.949	1.951	1.951	1.969	1.959	1.960
Cr	0.000	0.000	0.000	0.002	0.001	0.002	0.004	0.001	0.000	0.003	0.002	0.000
Fe	2.562	2.530	2.538	2.551	2.575	2.601	2.572	2.582	2.551	2.541	2.576	2.599
Mn	0.114	0.092	0.099	0.103	0.109	0.120	0.138	0.107	0.115	0.159	0.084	0.144
Mg	0.275	0.244	0.256	0.281	0.233	0.283	0.197	0.312	0.232	0.177	0.320	0.191
Ca	0.098	0.135	0.151	0.109	0.150	0.103	0.142	0.080	0.147	0.109	0.077	0.141

94

Slovak Geol. Mag., 12, 2 (2006), 91 – 101

Tab. 1 (continued)

PLAGIOCLASE ANALYSES

N°	1.	2.	3.	4.	5.	6.	7.	8.	9.	10.
Sample	I.1m	I.1r	I.3m	I.3r	II.2m	II.2r	II.3m	II.3r	II.4m	II4r
SiO_2	61.25	60.37	61.20	60.50	60.44	59.08	60.40	59.63	59.71	59.81
Al_2O_3	24.32	25.04	24.31	25.00	24.89	25.71	25.60	25.33	25.36	25.35
FeO	0.59	0.02	0.59	0.02	0.03	0.42	0.05	0.03	0.03	0.05
CaO	5.36	6.36	5.32	6.36	6.48	7.37	4.48	6.82	6.77	6.81
Na_2O	8.30	8.00	8.32	8.00	7.86	7.44	8.91	7.79	7.84	7.86
K_2O	0.12	0.05	0.03	0.03	0.04	0.03	0.04	0.04	0.03	0.04
Total	99.94	99.86	99.77	99.91	99.74	100.05	99.44	99.67	99.74	99.92
Cations on 8 oxygen basis										
Si	2.724	2.688	2.725	2.691	2.693	2.638	2.666	2.665	2.666	2.666
Al	1.274	1.314	1.276	1.311	1.307	1.353	1.332	1.334	1.334	1.332
Fe	0.022	0.000	0.021	0.000	0.001	0.015	0.002	0.001	0.001	0.002
Ca	0.255	0.303	0.253	0.303	0.309	0.353	0.212	0.326	0.323	0.325
Na	0.716	0.690	0.719	0.690	0.679	0.644	0.763	0.675	0.678	0.679
K	0.007	0.002	0.001	0.002	0.002	0.002	0.002	0.002	0.0011	0.002

BIOTITE ANALYSES

N°	1.	2.	3.	4.	5.	6.	7.	8.	9.	10.
Sample	**I.1m**	**I.1r**	**I.3m**	**I.3r**	**II.2m**	**II2r**	**II.3m**	**II.3r**	**II.4m**	**II.4r**
SiO_2	33.63	35.08	34.18	34.69	33.21	33.72	33.86	34.67	33.70	33.85
TiO_2	2.98	1.92	2.49	2.50	2.22	2.92	1.92	2.39	2.82	2.08
Al_2O_3	18.13	20.04	19.23	19.36	19.13	18.59	19.19	18.87	19.32	19.26`
Cr_2O_3	0.09	0.05	0.12	0.14	0.13	0.24	0.08	0.09	0.09	0.18
FeO	23.02	21.31	21.62	21.14	22.53	22.75	22.30	21.55	21.90	23.85
MnO	0.08	0.05	0.02	0.00	0.02	0.06	0.04	0.05	0.01	0.07
MgO	7.92	8.27	7.63	7.65	7.00	7.19	7.26	7.78	6.93	7.03
CaO	0.01	0.03	0.00	0.01	0.03	0.03	0.01	0.03	0.05	0.01
Na_2O	0.19	0.33	0.37	0.36	0.36	0.34	0.34	0.33	0.29	0.28
K_2O	9.01	8.61	8.63	8.57	8.63	8.42	8.42	8.43	8.52	7.99
F	0.00	0.04	0.13	0.13	0.15	0.25	0.18	0.00	0.00	0.65
Cl	0.11	0.10	0.11	0.13	0.10	0.09	0.09	0.11	0.10	0.09
Total	95.21	95.83	94.53	94.31	93.34	94.81	93.69	94.30	93.73	95.34
Cations on anhydrous 22 oxygen basis										
Si	5.240	5.334	5.297	5.319	5.251	5.254	5.310	5.352	5.279	5.240
Ti	0.349	0.220	0.291	0.291	0.264	0.342	0.227	0.277	0.332	0.242
Al	3.330	3.591	3.512	3.532	3.564	3.415	3.548	3.433	3.566	3.513
Cr	0.011	0.006	0.015	0.018	0.016	0.030	0.010	0.012	0.011	0.022
Fe	3.000	2.710	2.803	2.736	2.979	2.965	2.924	2.912	2.869	3.087
Mn	0.011	0.006	0.003	0.000	0.003	0.008	0.006	0.007	0.002	0.009
Mg	1.840	1.875	1.764	1.765	1.649	1.671	1.698	1.751	1.619	1.622
Ca	0.002	0.005	0.000	0.002	0.005	0.005	0.001	0.005	0.008	0.002
Na	0.059	0.098	0.112	0.110	0.111	0.104	0.105	0.100	0.088	0.085
K	1.792	1.670	1.708	1.692	1.699	1.716	1.684	1.660	1.702	1.579

associated with decompression uplift and cooling of the whole metamorphic complex. The garnet porphyroblasts remained with idioblastic morphology and restricted resorption.

Almandine component in garnets is ranging considerably high for metapelitic paragneisses. Almandine ≈ 83.6-84.5 mol.%, pyrope ≈ 6.0-10.4 mol.%, spessartine 3.0-4.6 mol.% and grossular ≈ 3.2-5.1 mol.%. Postculmination diffusion rims of most garnet grains are also slightly richer in almandine and spessartine component than the cores. The grossular component is almost constant (Fig. 2). At the garnet edges no symplectitic features and garnet overgrowth were developed.

Matrix biotite has a stable chemical composition within the sample and thus documents one dominant equilibrium recrystallization event during culmination of metamorphic process.

Plagioclases appear to be microscopically homogeneous. Lamellar twinning is not frequent. The microprobe analyses of discrete plagioclase grains (Tab. 1) in the rock domains reveal a weak compositional zoning. The composition of matrix plagioclase and at the plagioclase grain edge against garnet has been used for pressure calculations of the culmination and closing retrograde processes.

M. Dyda et al.: Decompression cooling of the basement garnet-sillimanite...

95

Fig. 2. Biotite-garnet grain edge. The composition profile documents the relative homogeneity of the garnet and the continuous slow cooling process. The concentration change of Mg and Fe in garnet when normalized as the function of garnet size depends on type of cooling and time. The schematic approach presupposes that Mg and Fe redistribution process has been formed by effective diffusion in the post-culmination cooling stage and is independent on the given Mg and Fe concentration. Rim diffusion penetration distance is strictly dependent on temperature and time.


In order to calculate the metamorphic culmination recrystallization temperatures, the reaction Almandine + Phlogopite = Pyrope + Annite with calibrations of different authors was applied and the obtained temperature data are listed in Tab. 2. Consequently, the prograde culmination, as well as the closing retrograde temperatures are presented with respect to their scattering. Culmination temperature data are consistent with the mineral assemblages and sillimanite presence in the samples. The P-T calculations used different calibrations and THERMOCALC software of Powell & Holland (1988, 1998) and Powell et al. (1998). See Tabs. 2 and 3 for details.

Since the Grt-Bt geothermometer is based on the Fe-Mg exchange reaction, Ferry & Spear (1978) give the thermometrical limits for additional components as Ca, Mn in garnets $(Ca+Mn)/(Ca+Mn+Mg+Fe)$ up to ≈ 0.2 and coexisting biotites $(Al^{VI}+Ti)/(Al^{VI}+Ti+Mg+Fe)$ up to ≈ 0.15. The studied garnets satisfy well this composition requirements with limiting values of 0.06-0.09. However, the high aluminous biotites with compositional value 0.37-0.41 overstep this limit and affect the calculated temperature values given in Tab. 2.

Differences in calculated P-T data are mainly due to the calibration used and non-ideality of the mineral solid solutions. The high Ti and Al^{VI} contents of biotites may be responsible for the higher calculated temperatures obtained with lnK_D^{MgFe} v. T relation calibrated by Ferry & Spear (1978) and confirms the Thompson's (1976) calibration suitability applied to high grade metamorphic rocks (Essene, 1982; Indares & Martignole, 1985).

For geobarometric purposes the reaction Plagioclase = Grossular + Sillimanite + Quartz has been used and different calibrations adopted. The pressure calculation results are summarized in Tabs. 3 and 4. The peak temperature and the corresponding retrograde closure temperature for particular rocks (Tab. 2) are assumed to be the calculated average temperatures given by used calibrations.

The garnets edges are modified by penetration diffusion and the central parts are almost chemically homogeneous (see Fig. 2). Thus, the calculated pressures at thermal culmination and at retrograde thermal minimum
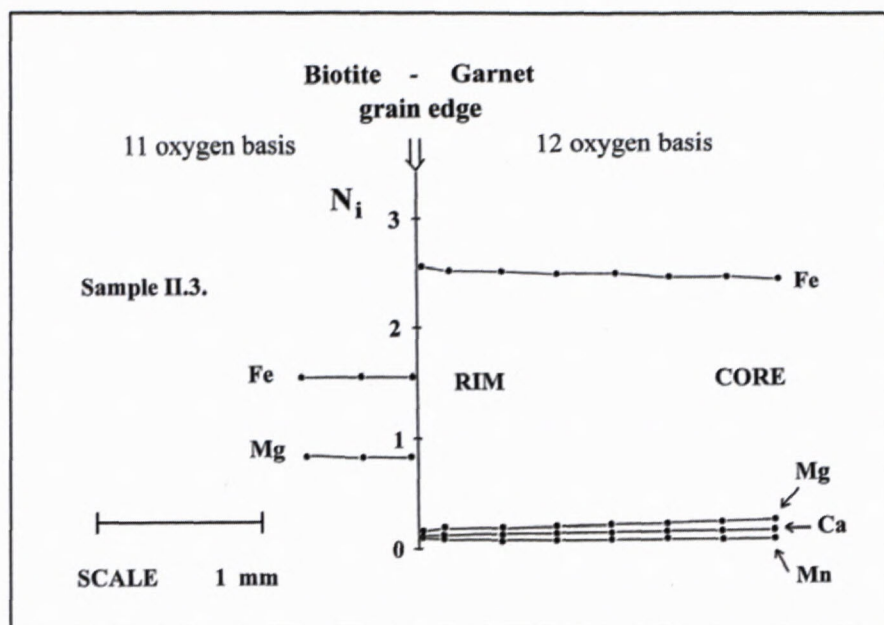
are presumed to be reasonable. The consequent construction of metamorphic post-culmination trajectory, presented graphically in Fig. 4, is based on calculated peak progressive culmination and closing retrograde P-T data.

The garnet post-culmination diffusion penetration rims (see Fig. 2) may serve for calculation of an approximate time span, that was needed for the diffusion penetration at the given retrograde P-T conditions.

Crank (1975) defines the relation among diffusion penetration distance X, diffusion coefficient $D_{(T,P)}$ and time (t) by the expression

$$X = \sqrt{4Dt} \qquad (1)$$

The diffusion coefficient for Fe-Mg interdiffusion in garnet was calculated for specific P and T conditions according to the expression:

$$D_{(T,P)} = D_0 \, e \, [(\Delta E* + (P-1).\Delta V*)/RT] \qquad (2)$$

where D_0 is the preexponential factor, ΔE^* is the activation energy for Fe-Mg interdiffusion and ΔV^* is the activation volume.

Using the retrograde P-T data, 2.5 Kbar at 515-525 °C and measured penetration distance in garnet $\sim 14 \pm 2$ μm, the time required for penetration has been calculated in the considerably wide range ca. 9-70 Ma (see Tab. 5). Maximum diffusion penetration into a garnet will be given by time during which a rock has been exposed to higher temperatures. Speedy cooling of rock complex (say 80-120 °C/Ma) may restrict the diffusion significantly which will be limited by the small penetration distances. Slow cooling of $\sim$ 0.05-1 °C/Ma, from higher culmination temperatures, causes the longer diffusion penetration distance in crystal. Temperature higher than ~750 °C causes rapid garnet homogenization. Thus the development of garnet rim composition is strictly temperature-time controlled phenomena.

The activation energy for diffusion plays the crucial role in penetration distance calculation and in the cooling rate approximate calculation. Using the obtained P-T data, garnet size, normalized concentration profile and

Slovak Geol. Mag., 12, 2 (2006), 91 – 101

96

Tab. 2. Metamorphic recrystallization temperatures of basement paragneisses from Palmas. *

		lnK$_D$	T	F&S	N&H	G&S	H&L	Tn
I. 1.)	c	1.742	560	573	586	590	575	579
	r	1.967	505	497	514	521	520	523
3.)	c	1.732	561	570	585	586	572	579
	r	1.961	506	498	517	528	522	524
2.)	c	1.626	589	608	621	625	597	599
	r	1.995	499	489	507	529	515	517
II. 3.)	c	1.569	605	629	640	635	611	612
	r	1.955	508	500	518	530	523	539
II. 4.)	c	1.511	621	652	662	653	626	622
	r	1.965	505	497	515	540	521	537

*Based on the reaction: Almandine + Phlogopite = Pyrope + Annite
using equilibrium calibrations of: T - Thompson (1976); F&S - Ferry and Spear (1978); N&H - Newton and Haselton (1981); G&S - Ganguly and Saxena (1984); Holdaway and Lee (1977); Thoenen (1989). c - culmination temperatures of metamorphic recrystallization, r - retrograde closure temperatures.

Tab. 3. Metamorphic recrystallization pressures of basement paragneisses from Palmas.*

aAn	aGr	G	N&H	P&H	P&H^P		
I. 1.)	c	0.4440	0.0394	3.67	2.98	3.93	3.52
	r	0.5950	0.0500	2.84	1.96	3.13	2.71
I. 3.)	c	0.4387	0.0396	3.65	3.12	4.05	3.55
	r	0.6021	0.0552	3.09	2.19	3.38	2.87
II. 2.)	c	0.5065	0.0364	3.13	2.64	3.45	3.21
	r	0.6907	0.0494	2.34	1.31	2.49	2.23
II. 3.)	c	0.3334	0.0257	3.46	2.96	3.76	3.44
	r	0.6255	0.0532	2.98	2.09	3.24	2.87
II. 4.)	c	0.5129	0.0391	3.70	3.13	3.87	3.69
	r	0.6222	0.0495	2.75	1.84	2.98	2.66

* Based on the reaction: 3 Anorthite = Grossular + 2 Sillimanite + Quartz
using equilibrium pressure calibrations of: G - Ghent et al. (1979), N&H - Newton & Haselton (1981), P&H - Powell & Holland (1988), P&H^P-THERMOCALC, Powell & Holland (1988, 1998). Activity of anorthite (aAn) and grossular (aGr) is based on formulation of Newton & Haselton (1981). c - pressures of metamorphic recrystallization at thermal maximum. r - pressures at retrograde temperature minimum.

Tab. 4. Composition and pressure characteristics of basement paragneisses from Palmas using the calibration of Hoisch (1990, 991) and Koziol & Newton (1988). *

lnK$_D$R1	lnK$_D$R2	P$_{R1}$	P$_{R2}$	ΔV(J/bar)	K&N*		
I. 1.)	c	6.667	4.965	3.20	3.23	-0.2973	2.91
	r	6.189	4.285	2.61	2.63	-0.2491	2.39
I. 2.)	c	6.065	4.368	3.96	3.84	-0.2866	3.14
	r	6.112	4.219	2.91	2.91	-0.2285	2.73
II. 2.)	c	6.441	4.854	3.12	3.10	-0.2945	2.71
	r	6.891	4.961	2.09	2.15	-0.2439	1.87
II. 3.)	c	5.873	4.333	4.13	4.08	-0.3075	3.78
	r	6.347	4.458	2.69	2.73	-0.2321	2.52
4.)	c	6.658	4.613	2.82	3.81	-0.2883	3.36
	r	6.630	4.727	2.40	2.48	-0.2491	2.26

*R1: 1/3 Pyrope + 2/3 Grossular + Eastonite + 2 Quartz = 2 Anorthite + Phlogopite
R2: 1/3 Almandine + 2/3 Grossular + Siderophyllite + 2 Quartz = 2 Anorthite + Annite
ΔV - partial molar volume change; K&N* -calibration according to Koziol & Newton (1988).

Tab. 5. Diffusion penetration distance calculations for garnets from Palmas paragneisses.

	ΔE*[Kjmol^{-1}]	P[Kbar]	T [°C]	X [μm]	D^{515}[cm²/s]	D^{525}[cm²/s]	t[Ma]	t[Ma]
I*	293.1	2.5	515 - 525	14	1.16×10^{-21}	2.03×10^{-21}	13	9
II*	273.8	2.5	515 - 525	14	2.21×10^{-22}	3.74×10^{-22}	70	41

I* according to activation energy [ΔE*] of Lasaga et al. (1977) and II* of Chakraborty & Ganguly (1992).

M. Dyda et al.: Decompression cooling of the basement garnet-sillimanite...

97

diffusion data, the petrological cooling rate estimates have been assessed (Tab. 6).

Tab. 6. Calculated petrological cooling rate estimates for basement paragneisses from Palmas *.

Sample:	II.3.
T [°C]:	624 ± 15
P [Kbar]:	3.65 ± 0.40
a [mm]:	3.41
	Diffusion coefficient
$D_{[T,P]}$:	7.26×10^{-19}
$D_{[T,P]}$:	2.45×10^{-19}
γ':	170
	Cooling rate estimates [°C / Ma]
S (E):	3.3
S (L):	1.2

* calculated for metamorphic culmination P-T conditions using the activation energy for diffusion (Δ E*) according to E - Elphic et al., (1985) - Δ E* = 224.4 [Kjmol^{-1}] and L - Lasaga et al. (1977) - Δ E* = 293.1 [Kjmol^{-1}]. Cooling rate [S] has been calculated according to formula of Lasaga (1983), $S = RT^2 \gamma' / \Delta E^* a^2$, where γ'- is given by the shape of the normalized measured composition profile and a is the garnet size.

If the calculated cooling rate estimates ($\sim$ 1.2 and 3.3 °C/Ma) have been accepted, then the linear cooling period from culmination to retrograde temperature conditions would have lasted approximately from $\sim$ 27 to 80 Ma. This is relatively slow cooling if considering e.g. Spanish Betic metamorphic terrane with cooling rates of 200 °C/Ma (Zeck et al., 1992) or 150-350 °C (Monié et al., 1994) and corresponding exhumation rate of 5-10 km/Ma. Exhumation and cooling rates of Dora Maira terrane are 22 km/Ma and ca. 90 °C/Ma (Gebauer, 1996). Thermobarometric data and normalized concentration garnet zonality of some Variscan basement paragneisses of the Western Carpathians indicate cooling rate from $\sim$ 4 up to 90 °C/Ma (Dyda, 2002).

Detailed analyses of crystal size distribution (CSD) data in chemical and technological processes (see e.g. Avrami, 1939; Randolph & Larson, 1971) attributed their wide application to different petrological studies of igneous and metamorphic rocks (see e.g. Kretz, 1973, 1974; Baronnet, 1984; Cashman, 1988, 1990; Marsh, 1988, 1998).

The CSD data for garnets in the unretrograded assemblage (Fig. 3) may have an importance for evaluation of the particular garnet growth crystallization process in this assemblage.

Plotting the population density $\ln(n)$ versus garnet crystal size (L) is usually a line with the slope $k/G\tau$ and intercept n_0, where G is the average growth rate of a given mineral, τ is the growth residence time and k is the constant. As the average growth rate is known, the growth residence time may be calculated directly. The average nucleation rate (J) may be calculated from linear equation parameters given by the slope of the line - $\ln(n)$ versus size (L).

Crystal size distribution data of garnets from the assemblage II.3. (Fig. 3), give the calculated line, ln *(n)* versus size (L), determined by the slope: $b = 9.53$ [cm^{-1}] and intercept $ln \ n_0 = 6.65$ [n/cm^4]. Consequently, the calculated average nucleation rate is $\sim 4 \times 10^{-10}$ N/cm^{3}s.

Nucleation rate (J) changes with metamorphic regimes. Contact metamorphism is characterized by the highest nucleation rates (e.g. $J \approx 5 \times 10^{-3}$) and high grade regional metamorphism with lower J values (ca. 3×10^{-8} - 4×10^{-6}). In regional metamorphic rocks of sillimanite zone from Waterville Formation (south-central Maine, USA) Cashman & Ferry (1988) give the average nucleation rate for garnets $J = 1.98 \times 10^{-6}$ and some Variscan regionally metamorphosed basement metapelites from the Western Carpathians have the garnet nucleation rate $J = 3 \times 10^{-8} - 1 \times 10^{-7}$ N/cm^{3}s (Dyda, 1997).

Thus, the obtained garnet crystal size data of the metapelitic gneisses from Palmas form an argument for the slow regional metamorphic pre-culmination heating rate, documented by the slow nucleation rate of the garnet.
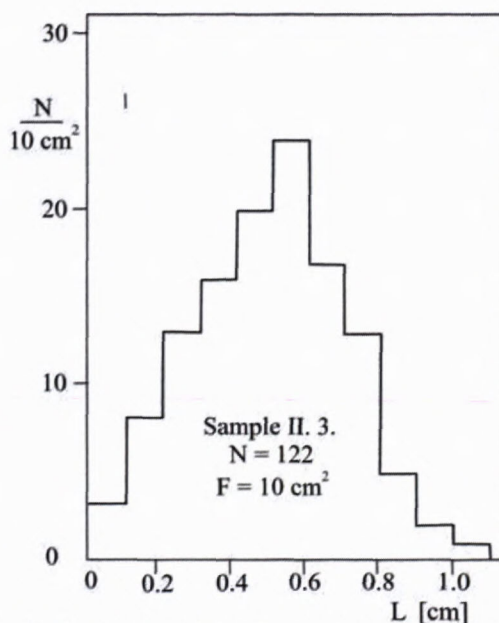
Fig. 3. Garnet crystal size frequency histogram in metapelitic gneisses from the Palmas area. The distribution data are used for garnet nucleation rate and growth estimates.

Results and discussion

The assessment of the thermal and pressure changes may form a basic frame for further collecting of petrological data. More observations of sequence and extent of metamorphic reactions on a larger field scale are needed for a better understanding of metamorphism in the region.

Metamorphic trajectory can be derived using different pieces of petrological evidence mainly based on the sequence of mineral assemblages, as the rock passes through the mineral stability fields during prograde metamorphism to the culmination P-T conditions. Subsequently, retrograde processes may occur, accompanied by

Fig. 4. The calculated metamorphic culmination and closing retrograde P-T characteristics of metamorphic recrystallization calculated from Grt-Bt-Plg-Sil-Qtz mineral equilibria. Temperat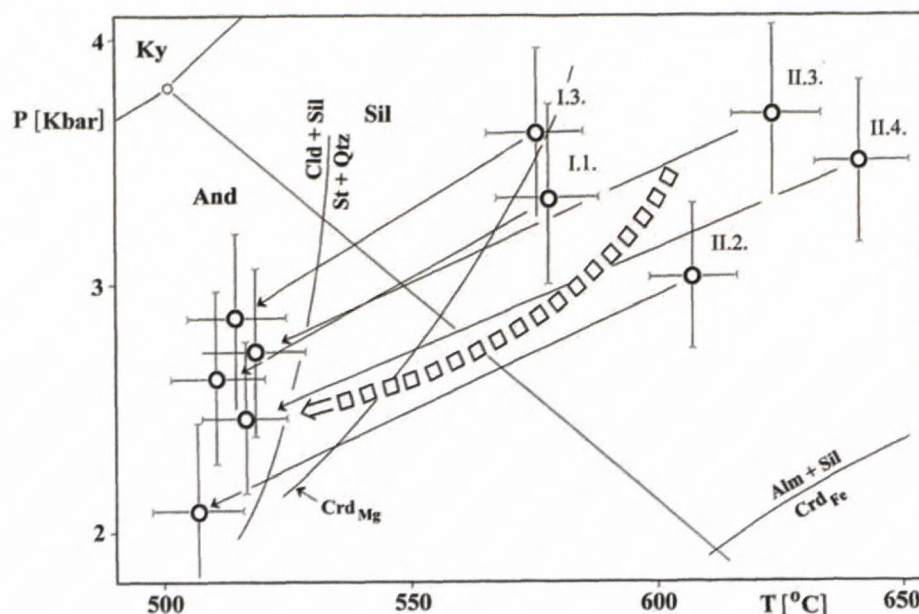ure data were obtained on the basis of Grt-Bt calibrated equilibria (Ferry & Spear, 1978; Thompson, 1976; Newton & Haselton, 1981; Ganguly & Saxena, 1984; Hodges & Crowley, 1985). Pressure was calculated from calibrated equilibria Grt-Plg-Sil-Qtz (Ghent et al., 1979; Powell & Holland, 1988; Newton & Haselton, 1981) and equilibria including Grt-Bt-Ms-Plg-Qtz (Hoisch, 1990). The staurolite (St) and cordierite (Crd_{Mg}, Crd_{Fe}) appearance limits are taken from Bucher & Frey (1994).

changes in mineral assemblage. Heat adding intrusions often form early, followed by uplift that was caused by the rise of the crystalline domes (Schumacher et al., 1990).

The potential complexity of P-T paths makes generalization about their form difficult. Chamberlain & Karabinos (1987) have shown, that in structural terranes dominated by folding and thrusting, details of P-T paths can vary dramatically within a single metamorphic belt. This is due to the heat redistribution caused by folding of the isotherms and by differential cooling rates that are dependent on the rock's position in the structure following deformation. However, many models of geological processes and examples from metamorphic terranes (e.g. England & Thompson, 1984; Thompson & England, 1984) document, that P-T paths can be simplified and broadly classified as curved clockwise or curved counterclockwise trajectories in P-T coordinates.

The field occurrence of garnet-sillimanite paragneisses from Palmas area, their recrystallization history inferred from microscopic studies and the P-T data suggest, that their petrological character can be useful for the tectono-metamorphic reconstruction of this terrane.

The paragneisses represent the culmination temperature of 604 ± 30 °C at pressure of 3.4 ± 0.4 Kbar with ca. 12-14 km of the overlying pile at one dominant metamorphic event. No data have been collected to classify and estimate the metamorphic intensity gradient with respect to the territorial scale.

The prograde P-T data form an important clue to the definition of the culmination of metamorphic conditions. However, the pre-culmination trajectory is not yet well constrained. The absence of inclusions in garnet and the coexistence of matrix phases did not allow to asses the prograde whole rock reactions. Neither muscovite nor

K-feldspars have been revealed as possible dehydration reaction participants and temperature indicators. The post-peak decompression and retrograde closing P-T conditions have been determined in rather narrow temperature range, from 604 ± 30 °C for culmination tempera-

tures, to 515 ± 15 °C for retrograde closing temperatures (Fig. 4). Symplectitic features, simple corona textures, resorbed or embayed garnets are absent. These textural features, together with the garnet rim zonality and limited retrograde hydratation, indicate the slow cooling in depth of the gneissic complex from Palmas. Cooling generally attended decompression on the retrograde path and calculated P-T data involve decrease in pressure from 3.4 ± 0.4 to 2.5 ± 0.3 Kbar, indicating thus slow cooling and uplift. However, typical "isobaric cooling" gradients have rather flat dP/dT slopes ca. 0.3-0.5 Kbar per 100 °C (Harley & Hensen, 1990). The cooling retrograde processes led to the closing temperature and pressure conditions of 515 ± 15 °C and 2.5 ± 0.3 Kbar respectively. The post-peak mineral inter-granular equilibrium adjustation is considered to be a diffusion process of one dominant terminating metamorphic event.

In the studied paragneisses, sillimanite is the common Al-silicate mineral. Andalusite, or pseudomorphs after andalusite have not been found. Thus, it is presumed, that these paragneisses passed first through the kyanite stability field during the prograde metamorphism. Subsequent increasing temperature drove these rocks into sillimanite stability field. Avoiding probably the andalusite field, they are indicated by the clockwise curved P-T trajectory. The geothermobarometrical data also support a clockwise trajectory and imply terms of crustal thickening, compression prior to the reaching of the thermal and pressure maximum and subsequent slow cooling and decompression.

On the other hand, some cratonic metamorphic terranes characterized by isobaric cooling (e.g. Adirondacs, Namaqualand, Broken Hill) have demonstrated that evolved their thermal maximum along a counter-clockwise P-T path (see e.g. Bohlen, 1987; Waters, 1986). Such counter-clockwise P-T-t paths would be consistent with magmatic and/or extensional settings (Sandiform & Powell, 1986).

The studied garnet-sillimanite gneisses are located at the westernmost margin of the Sâo Francisco craton, rimmed by the Neo-Proterozoic mobile belt.

M. Dyda et al.: Decompression cooling of the basement garnet-sillimanite...

99

Mobile belts of Brazil evolved during juxtaposition and amalgamation of single continental fragments of Gondwana supercontinent in Brasiliano tectonic cycle 950-600 Ma ago (Brito-Neves & Cordani, 1991; Brito-Neves et al., 1999). Tectonic style of mobile belts is typical for accretionary wedge structure developing due to closing of Goias ocean (Pimentel & Fuck, 1992). Tocantins fold and thrust belt comprise strongly folded and sheared 1 200–600 Ma old rocks. Ensimatic units, relics of oceanic crust (Pimentel & Fuck, 1992; Viana & Pimentel, 1994, ex Strieder & Suita, 1999) and granulite metamorphism of the mafic-ultramafic complexes (Suita et al., 1994) are related to this event. After final closing of Goias ocean, the continental collision of Sao Francisco and Amazonian shield started, probably 800 Ma ago (Strieder & Suita, 1999). CC collision 650–550 Ma ago imprinted to Tocantins mobile belt tectonic style of accretionary wedge. Contemporaneously, I-type to A-type granitoids intruded into the Neo-Proterozoic gneisses (Almeida et al., 1973, ex Nairn & Stehli, 1973). The Proterozoic Goiania Complex, where metapelitic garnet-sillimanite gneisses come from, tectonically belongs to the Goias Median massif (sensu Strieder & Suita, 1999), triangular zone resulting from CC collision of Amazonian with São Francisco plate during Brasiliano orogeny. The last tectonic deformation phases took place 500 Ma ago (Strieder & Suita, 1999). The Pre-Cambrian crystalline complex has not been significantly disturbed since Silurian, but it is affected by younger deep seated warping and faulting (Fairbridge, 1975). During the Lower Tertiary, important block faulting in many areas took place, influencing thus geomorphology of the recent surface.

The gneissic complex from Palmas was isostatically and thermally well equilibrated. These results imply, that the paragneisses, presently outcropped, were buried at ca. 12-14 km depth throughout the long Precambrian time interval. Thus the presumed crustal residence is inferred for this gneissic terrane as a "true craton", at least until its local and marginal remobilization and partial exhumation in late Proterozoic and younger tectonic events. The petrological features and P-T data may lead us to the conclusion that the metapelitic gneisses from Palmas are a low pressure portion of the cratonic crystalline complex. This is consistent with the data of DaCruz & Kuyumjian (1998) who consider this terrane to be subjected to medium pressure and variable temperatures up to amphibolite facies.

The rocks do not possess the synkinematic crystal growth (e.g. rotational garnets, etc.) or deformation features. They represent one dominant regional pre-Cambrian metamorphic thermal event. They cooled slowly isostatically in depth and in the final stages they were, presumably, rapidly uplifted. They represent the fragmented rigid rests of the western marginal part of the São Francisco craton.

The uplift movements were associated with the activity of the Late-Proterozoic mobile belt and fault tectonic activities between Amazonian and São Francisco cratons.

There is an absence of the deformational and/or further metamorphic events related to any tectonic activities within the studied rocks. Thus we presume, that reactivation connected with uplift of the Goias Median complex was not significantly affected by the dynamo-metamorphic events, at least in the studied region.

Thus the gneissic complex remained unaffected by the post-metamorphic geological activities since Precambrian. This mechanism of stability should be one of the basic geological problems for the future studies as well as for geochronological investigation when considering the tectonic and metamorphic history of the gneissic complex from Palmas.

Acknowledgments

Literature

Almeida, F. F. M., Amaral, G., Cordani, U. G. & Kawashita, K. (eds.)., 1973: The Pre-Cambrian evolution of the South America cratonic margin south of Amazon river. In: Nairn, A. E. M. & Stehli, F. G. (eds): The ocean basins and margins. Vol. 1, The South Atlantic. Plenum Press, London, 411-443

Avrami, M., 1939: Kinetics of phase change. J. Chem. Phys., 7, 1103-1112.

Baronnet, A., 1984: Growth kinetics of the silicates. Fortschr. Mineral., 62, 187-232.

Brito-Neves, B. B., Campos-Neto, M. C., & Fuck, R. A. 1999: From Rodinia to Western Gondwana: An approach to the Brasiliano-Pan African cycle and orogenic collage. Episodes, 22, 155-168.

Brito-Neves, B. B. & Cordani, U. G., 1991: Tectonic evolution of South America during Late Proterozoic. Precambrian Res. 53, 23-40

Bohlen, S. R., 1987: Pressure-temperature-time paths and tectonic model for the evolution of granulites. J. Geology, 95, 617-632.

Bucher, K. & Frey, M., 1994: Petrogenesis of Metamorphic Rocks. 6th edition. Springer Verlag, 318p.

Cashman, K. V., 1988: Crystallization of Mount St. Helens dacite: A quantitative textural approach. Bull. Volcanol., 50, 194-209.

Cashman, K. V., 1998: Textural constraints on the kinetics of crystallization of igneous rocks. In: Nicholls, J. & Rusell, J. K. (eds.): Modern Methods in Igneous Petrology: Understanding Magmatic Processes. Mieral. Soc. Amer., Rew. Mineral., 24, 259-314.

Cashman, K. V. & Ferry, J. M., 1998: Crystal size distribution (CSD) in rocks and kinetics and dynamics of recrystallisation. Amer. J. Sci., 99, 401-415.

Chakraborty, S. & Ganguly, J., 1992: Cation diffusion in aluminosilicate garnets: Experimental determination in spessartine-almandine diffusion couples, evaluation of effective binary diffusion coefficients and applications. Contrib. Mineral. Petrol., 111, 74-86.

Chamberlain, C. P. & Karabinos, P., 1987: Influence of deformation on pressure: Temperature paths of metamorphism. Geology, 15, 42 - 4.

Slovak Geol. Mag., 12, 2 (2006), 91 – 101

100

Clarke, G. I., Guiraud, R., Powell, R. & Burg, G. P., 1987: Metamorphism in the Olary Block, South Australia: Compression with cooling in a Proterozoic fold belt. J. Metamorph. Geol., 5, 294 - 306.

Crank, J., 1975 : *The Mathematics of Diffusion*. Oxford University Press, 456 s.

DaCruz, E. L. C. C. & Kuyumjian, R. M., 1998: The geology and tectonic evolution of the Tocantins granite-greenston terrane: Almas-Dianopolis region, Tocantins State, Central Brazil. Rev. Brasil. Geocienc., 28, 2, 173-182.

Dyda, M., 1997: Disturbance of the Variscan metamorphic complex indicated by mineral reactions, P-T data and crystal size of garnets (Malé Karpaty Mts.). In: Grecula, P., Hovorka, D. & Putiš, M. (eds.): *Geological Evolution of the Western Carpathians*. Geocomplex, Bratislava 1997, 333-342.

Dyda, M., 2002: Cooling and uplift trajectories of the Malé Karpaty Mts. Variscan Basement (West Carpathians), Slovak Geol. Mag., 8, 49-63.

Ellis, D. J., 1987: Origin and evolution of granulites in normal and thickened crust. Geology, 15, 167-170.

Elphic, S. C., Ganguly, J. & Loomis, T. P., 1985: Experimental determination of cation diffusivities in aluminosilicate garnets. I. Experimental methods and interdiffusion data. Contrib. Miner. Petrol., 90, 36-44.

England, P. C., 1987: Diffuse continental deformation: Length scales, rates and metamorphic evolution. Phil. Trans. Royal Soc. London, A 321, 3-22.

England, P. C. & Thompson, A. B., 1984: Pressure-temperature-time paths of regional metamorphism. I. Heat transfer during the evolution of regions of thickened continental crust. J. Petrology, 25, 894-928.

England, P. C. & Richardson, S. W., 1977: The influence of erosion upon the mineral facies of the rocks from different metamorphic environment. J. Geol. Soc. London, 134, 210-213.

Essene, E. J., 1982: Geologic thermometry and barometry. In: Ferry, J. M. (ed.): Characterization of metamorphism through mineral equilibria. Mineral. Soc. Amer., 10, 153-206.

Fairbridge, R. W. (edit.), 1975: The encyclopedia of World regional geology, part 1: Western hemisphere (including Antarktica and Australia). Halsted press, 127-138.

Ferry, J. M. & Spear, F. S., 1978: Experimental calibration of the partitioning of Mg and Fe between biotite and garnet. Contrib. Mineral. Petrology, 66, 113-117.

Ganguly, J. & Saxena, S. K., 1984: Mixing properties of aluminosilicate garnets: Constrains from natural and experimental data and applications to geothermobarometry. Amer. Mineralogist, 69, 88-97.

Gebauer, D., 1996: A P-T-t path for (ultra?-) high-pressure ultramafic/mafic rock associations and their felsic country rocks based on SHRIMP dating of magmatic and metamorphic zircon domains: Example: Alpe Arami (Central Swiss Alps). In: Basu, A., Hart, S., (eds.): *Earth Processes: Reading the isotopic code*. Geophys Monograph Series, 95, 307-329.

Ghent, E. D., Robbins, D. B. & Stout, Z. M., 1979: Geothermometry, geobarometry and fluid composition of metamorphosed calc-silicates and pelites, Mica Creek, British Columbia. Amer. Mineralogist, 64, 874-885.

Harley, S. L. & Hensen, B. J., 1990: Archean and Proterozoic high-grade terranes of East Antarctica (40-80 °E): A case study of diversity in granulite facies metamorphism. 320-370. In: Ashworth, J. R. & Brown, M.: *High-temperature Metamorphism and Crustal Anatexis*. Unwin Hyman, London, UK, 407 p.

Hodges, K. V. & Crowley, P. D., 1985: Error estimation in empirical geothermobarometry for pelitic systems. Amer. Mineralogist, 70, 702-709.

Hoisch, T. D., 1990: Empirical calibration of six geobarometers for the mineral assemblage quartz + biotite + plagioclase + garnet. Contrib. Mineral. Petrology, 104, 225-234.

Hoisch, T. D., 1991: Equilibria within the mineral assemblage quartz + muscovite + biotite + garnet + plagioclase, and implications for the mixing properties of octahedrally coordinated cations in muscovite and biotite. Contrib. Mineral. Petrology, 108, 43-54.

Holdaway, M. J., 1971: Stability of andalusite and the aluminum silicate phase diagram. Amer. J. Sci., 271, 97-131.

Holdaway, M. J. & Lee, S. M., 1977: Fe-Mg cordierite in high grade pelitic rocks based on experimental and natural observations. Contrib. Mineral. Petrol., 63, 175-198.

Holland, T. J. B. & Powell, R., 1990: An enlarged and updated internally consistent thermodynamic dataset with uncertainties and correlations: The system $K_2O-Na_2O-CaO-MgO-MnO-FeO-Fe_2O_3-Al_2O_3-TiO_2-SiO_2-C-H_2-O_2$. J. Metamorphic Geol., 8, 89-124.

Indares, A. & Martignole, J., 1985: Biotite-garnet geothermometry in the granulite facies: The influence of Ti and Al in biotite. Amer. Mineralogist, 70, 272-278.

Koziol, A. M. & Newton, R. C., 1988: Redetermination of the anorthite breakdown reaction and improvement of the plagioclase-garnet-Al_2SiO_5-quartz geobarometer. Amer. Mineralogist, 73, 216-223.

Kretz, R., 1973: Kinetics of the crystallization of garnet at two localities near Yellowknife. Can. Mineralogist, 12, 1-20.

Kretz, R., 1974: Some models for the rate of crystallization of garnet in metamorphic rocks. Lithos, 7, 123-131.

Kretz, R., 1983: Symbols for rock-forming minerals. Amer. Mineralogist, 68, 277-279.

Lasaga, A. C., 1983: Geospeedometry: An extension of geothermobarometry. In: Saxena, S. K., (ed.): *Kinetics and Equilibrium in Mineral Reactions*. Advances in Physical Geochemistry 3., 81-114.

Lasaga, A. C., Richardson, S. M. & Holland, H. D., 1977: The mathematics of cation diffusion and exchange between silicate minerals during retrograde metamorphism. In: Saxena, S. K. & Battachanji, S. (eds.): *Energetics of Geological Processes*. Springer Verlag, New York, 353-388.

Mapa geológico 1 : 1 000 000 (1981), Projeto Radambrasil, Tocantis folha SC 22, Ministério das minas e energia, 1981.

Marsh, B. D., 1988: Crystal size distribution (CSD) in rocks and the kinetics and dynamics of crystallization. I. Theory. Contrib. Miner. Petrol., 99, 277-291.

Marsh, B. D., 1998: On the interpretation of the crystal size distribution in magmatic systems. J. Petrology, 39, 553-599.

Monié, P., Torres-Roldan, R. L. & Garcia-Casco, A., 1994: Cooling and exhumation of the Western Betic Cordilleras, $^{40}Ar/^{39}Ar$ thermochronological constraints on a collapsed terrane. Tectonophysics, 238, 353-379.

Newton, R. C. & Haselton, H. T., 1981: Thermodynamics of the garnet-plagioclase-Al_2SiO_5 - quartz geobarometer. In: Newton, R. C., Navrotsky, A., & Wood, B. J. (Eds.): *Thermodynamics of minerals and melts*. Springer Verlag, New York, 131-147.

Phillips, G. N. & Wall, V. J., 1981: Evaluation of prograde metamorphic conditions: Their implications for the heat source and water activity during metamorphism in the Willyama Complex, Brolen Hill, Australia. Bull. Mineralog., 104, 801-810.

Pimentel, M. M. & Fuck, R. A., 1992: Neoproterozoic crustal accretion in Central Brazil. Geology, 20, 375-379.

Powell, R. & Holland, T. J. B., 1988: An internally consistent dataset with uncertainties and correlations: 3. Application to geobarometry, worked examples and computer program. J. Metamorphic Geol., 6, 173-204.

M. Dyda et al.: Decompression cooling of the basement garnet-sillimanite...

101

Powell, R., Holland, T. & Worley, B., 1998: Calculating phase diagrams involving solid solutions via non-linear equations, with examples using THERMOCALC. J. Metamorphic Geol., 16, 577-588.

Randolph, A. D. & Larson, M. A., 1971: *Theory of Particulate Processes,* Academic Press, New York, 251 p.

Richardson, S. W., Gilbert, M. C. & Bell, P. M., 1969: Experimental determination of kyanite-andalusite and andalusite-sillimanite equilibria: The aluminum silicate triple point. Amer. J. Sci., 267, 259-272.

Sandiform, M. A. & Powell, R., 1986: Deep crustal metamorphism during continental extension, modern and ancient examples. Earth Planet. Sci. Lett., 79, 151-158.

Selverstone, J., Spear, F. S., Franz, G. & Morteani, G., 1984: High-pressure metamorphism in the SW Tauern Window, Austria: P-T paths from hornblende-kyanite-staurolite schists. J. Petrol., 25, 501-531.

Schumacher, J. C., Hollocher, K. T., Robinson, P. & Tracy, R. J., 1990: Progressive reactions and melting in the Acadian metamorphic high of central Massachusetts and southwestern New Hampshire, USA. 198-234. In: Ashworth, J. R. & Brown, M. *High-temperature Metamorphism and Crustal Anatexis.* Unwin Hyman, London, UK, 407 p.

Strieder, A. J. & Suita, M. T., 1999: Neoproterozoic geotectonic evolution of the Tocantins Structural Province, Central Brazil. Geodynamics, 28, 267-289.

Thoenen, T., 1989: A comparative study of garnet-biotite geothermometers, PhD Thesis, University of Basel, 118 p.

Thompson, A. B., 1976: Mineral reactions in pelitic rocks: I. Prediction of P-T-X (Fe-Mg) phase relations. Amer. J. Sci., 276, 401-424.

Thompson, A. B. & England, P. C., 1984: Pressure-temperature-time paths of regional metamorphism II: Their inference and interpretation using mineral assemblages in metamorphic rocks. J. Petrology, 25, 894-928.

Vernon, R. H., Clarke, G. L. & Collins, W. J., 1990: Local, mid-crustal granulite facies metamorphism and melting: An example in the Mount Stafford area, central Australia. 272-319. In: Ashworth, J. R. & Brown, M.: *High-temperature Metamorphism and Crustal Anatexis.* Unwin Hyman, London, UK, 407 p.

Waters, D. J., 1986: Metamorphic zonation and thermal history of pelitic gneisses from Western Namaqualand, South Africa. Trans. Geol. Soc. South Africa, 89, 97-102.

Waren, R. G., 1983: Metamorphic and tectonic evolution of granulites. Aruna Block, central Australia. Nature, 305, 300-303.

Wells, P. R. A., 1980: Thermal model for the magmatic accreation and subsequent metamorphism of continental crust. Earth Planet. Sci. Letters, 46, 253-265.

Zeck, H. P., Monié, P., Villa, I. M. & Hansen, B. T., 1992: High rates of cooling and uplift in the Betic Cordilleras, S. Spain. Alpine lithospheric slab detachment, mantle diapirism and extensional tectonics. Geology, 20, 79-82.

Modelling of oil substances migration in river Danube

[1]KATARÍNA KMINIAKOVÁ and [2]MIROSLAV LUKÁČ

[1]AQUIFER s.r.o., Dúbravská cesta 9, 845 20 Bratislava 45, Slovakia
[2]Výskumný ústav vodného hospodárstva, Nábr. Ľ. Svobodu 5, 812 49 Bratislava, Slovakia

Abstract. Migration of contaminants in the river Danube was in the focus of study aimed at the risk assessment of industrial plant, which manipulates with hazardous substances. Modelling techniques were applied for the evaluation of impacts of possible serious industrial accidents at the Danube water quality.

Two basic concepts of contaminant migration in the surface water were considered:

1. Migration of contaminant at the water surface in the form of film, due to difference in densities and depending on the flow velocity.

2. Partial dissolution of contaminant in the water and migration at the water surface in the form of phase.

In the cases *of "major" oil spills* (from mobile tanks – vessels, assumed quantities 80-199 t) harmful effects of contamination with regard to *assumed toxic impacts at water organisms* (concentrations of petroleum hydrocarbons in the range 2-3 mg.l^{-1} and higher) can be expected:

- in 11 km long river section from oil spill site (profile Patince) at the discharge of 1140 m^3.s^{-1} (petroleum hydrocarbons concentrations in the range 2.0-7.8 mg.l^{-1})
- in 3 km long river section from oil spill site (profile Szony) at the flood discharges 5350–9000 m^3.s^{-1} (petroleum hydrocarbons concentrations in the range 2.0-4.6 mg.l^{-1})
- in the close surrounding of oil spill site (around 500 m) even higher concentrations of petroleum hydrocarbons can be expected.

Total frequency of "major" oil spills in the estimated quantity 80–199 t as a consequence of mobile tanks (vessels) failure (collision with other vessel, or leakage) is substantially lower than in the case of "minor" spills. Analysis of "failure tree" (Kminiaková and Jelemenský, 2006) indicates that all possible sources of basic failures are of very low probability (frequency in the order F=n.10^{-7} to n.10^{-8} /year), comparable with meteor impact.

Keywords: modelling, surface water flow, surface water quality, oil pollution, serious industrial accidents

1. Introduction

Several research studies by Klúčovská and Topoľská (1994), Szolgay et al. (1994) and Szolgay et al. (1996), which were solved at the Water Research Institute in Bratislava, dealt with the modelling of the Danube river flow. These works focused at the calculation of surface water levels and discharges, based at the evaluation of roughness coefficients. Surface water quality of Danube was modelled in the frame of the project PHARE EC/WAT/01 "Danubian Lowland – Groundwater Model" (MŽP, 1995). The focus was put at the oxygene regime, BOD, ammonia and nitrates. Modelling was based at the oxygene balance and connected parameters. The parameters of dispersion and advection for the river Danube were estimated.

Our study goal was to investigate migration of possible oil pollution in the Slovak-Hungarian border section of the Danube river. Study was performed in two basic steps. Firstly, water flow velocities and travel time were determined by previous modelling works, which are described in the reports (Szolgay et al., 1994, 1996). These data represented input information for further modelling of oil substances migration in the Danube river.

Theory of water quality modelling is described in Chapra (1997). Determination of transport parameters for substances dissolved in water was the key issue in our case. Detail study of oil pollution migration using the analytical models can be found in Hellweger (2005), together with practical examples of major oil spills in the rivers Missouri (1967), Rhine (1986), Sacramento (1991), as well as Tisza and Danube (2000). This study was based at real field data of pollution concentration and its variation along the investigated river sections. Based at these data, it was possible to determine advection-dispersion parameters in the conditions similar to our area of interest. Danube data from 2000 were taken into account after necessary adjustment, which was based at the actual flow area of river cross-sections in the model area.

2. Input data

Pollution migration in the surface waters was investigated in the frame of risk evaluation of industrial plant, which is involved in the operation of dangerous substances. It is located in Komárno, upstream from the confluence of the Danube and Vah rivers. Its services include

transport, treatment, storage and distribution of fuels (propellants). Two kinds of dangerous substances according to the classification of the Act 261/2002 Dig. are stored and manipulated in this plant – petrol BA95 and fuel oil.

Evaluated division of plant deals with the storage of mentioned substances, as well as their permanent (24 hours a day) distribution between road, railway and waterway transport lines. Fuel entry and outgoing is realized via railway cisterns and cistern trucks. Upon entry fuel is distributed from cisterns through the pipelines to the river vessels – tankers, which are used as storage tanks. Outgoing fuel is pumped to railway cisterns or cistern trucks with pumping plant located at the anchored pontoon vessel. Individual products are pumped using self-priming pumps, hoses and rack (comb).

The layout of the Danube river in the investigated Slovak-Hungarian section is given in the Fig. 1a, b.

Fig. 1a. Layout of investigated Danube river section between the oil spill site and the end of Slovak-Hungarian section – part 1.

Fig. 1b. Layout of investigated Danube river section between the oil spill site and the end of Slovak-Hungarian section – part 2.

K. Kminiakova and M. Lukáč: Modelling of oil substances migration...

105

Oil spill scenarios

In general, spills of oil substances, which can potentially cause contamination of the Danube river water, can be divided into following two groups.

A) minor spills of petrol and fuel oil – from the connecting hose and delivery piping during the tanker filling, or from the suction piping when cisterns are not being filled. In such cases, spill quantities are as follows:

- 98-587 kg of fuel oil, with a total frequency of spill $F = 1.27 \cdot 10^{-3}$ /year – $6.1 \cdot 10^{-4}$ /year
- 35-530 kg of petrol, with a total frequency of spill $F = 1.2 \cdot 10^{-3}$ /year – $3 \cdot 10^{-3}$ /year

B) major spills of petrol and fuel oil – from the mobile tank (vessel)

In these cases, spill quantities are as follows:

- 80-199 t of fuel oil, with a total frequency of spill $F = 4.1 \cdot 10^{-7}$ /year
- 188 t of petrol, with a total frequency of spill $F = 4.1 \cdot 10^{-7}$ /year

3. Evaluation methodology

The impacts of oil spills at the Danube surface water quality in the cases of serious industrial accidents in the given plant were evaluated based on the modelling results.

Two basic concepts of contaminant migration in the surface water were assumed:

1. Film of spilling contaminant will originate at the water surface, as a result of difference in the density of water and contaminant (830/1000 for fuel oil or 750/1000 for petrol). This film will migrate downstream on the Danube water surface. The expected film thickness is less than 1 mm (in the case of minor spills from hoses and pipes) with respect to large surface area of Danube and relatively small spill quantity (approximately 100-600 kg), as well as low viscosity of oil substances and significantly turbulent water flow in the Danube river. Larger thickness of oil substances phase (several mm to several cm) can be expected in the case of spills (approximately 80–200 t).

Resulting effects are influenced with several uncertainties. Seasonal changes of climatic conditions can be considered as the most important. The influence of these conditions was omitted in the model.

2. Partial dissolution of contaminant in the surface water was assumed after the spill, with the rest migrating in the form of phase on the Danube water surface.

Both forms of pollution are transported downstream (advection) and dispersed due to varying flow velocity and diffusion (dispersion).

The estimate of Danube water travel time along the Slovak-Hungarian section represented basic input data for the evaluation of oil substances migration. The end of this section is situated in the river km 1708.5. Travel times were estimated for three selected hydrological situations, which were taken into account in the studies (Szolgay et al., 1994, 1996; Mišík et al., 1994):

- discharge **1140 m³.s⁻¹**, which corresponds to so-called low regulation and navigation water level,
- discharge **5350 m³.s⁻¹**, which approximately corresponds to so-called high navigation water level and
- flood discharge Q100 = 9000 m³.s⁻¹, which corresponds to discharge with a return period of 100 years.

According to the assessment of period 1931-1980, done by the Slovak Hydrometeorological Institute, discharge of 1140 m3.s-1 was exceeded by about 330 days in the average year and discharge of 5350 m³.s⁻¹ by about 3-5 days. Discharge regime of Danube in the Komárno gauging station can be further characterized with the following parameters:

- mean annual discharge in the period 1931-1980: 2290 m³.s⁻¹,
- maximum observed discharge in the period 1931-1980: 8290 m³.s⁻¹ * (17. 6. 1965),
- minimum observed discharge in the period 1931-1980: 660 m³.s⁻¹

Fig. 2 provides information about the occurrence of different discharges in the period 1931-1980 in the average year, up to the value of around 4600 m³.s⁻¹. Site of possible oil spill is located in Komárno, around 200 m upstream from the Váh and Danube rivers confluence (river km 1766.2). Above mentioned studies provided necessary output data in the whole modelled section between Komárno and Szob (river km 1766.2-1708.5). Travel time of water and migrating contaminant (in seconds) in the sub-sections bordered with neighbouring cross-sections of the river, was determined based on the values of average cross-sectional flow velocity for different discharges, according to relation:

$$T = \frac{\Delta L}{0.5(v_1 + v_2)}$$

where:

ΔL – length of partial sub-section, based on the distance of neighbouring cross-sections (m),

v_1, v_2 – average cross-sectional flow velocities in the neighbouring cross-sections (m.s⁻¹).

Resulting travel time between the oil spill site (Komárno) and any site situated downstream, on the Slovak-Hungarian section of Danube river, was determined by summarizing of partial travel times.

Travel times between Komárno and any site (determined with river chainage) for three basic discharge conditions (discharge Q in m³.s⁻¹) are given in the Fig. 3. Numerical values of travel time for selected sites at the Slovak side of Danube river are given in Tab. 1. Fig. 4 provides more details on the estimated travel times for selected sites. Using presented graphs, it is possible to estimate travel time between oil spill site (Komárno) and given site also for different discharges than analysed.

The second concept of pollution transport, i.e. migration of dissolved oil substances in surface water, was simulated by means of 1-dimensional model of advection-dispersion transport (Nordin and Troutman, 1980; Hellweger, 2005). The following assumptions were taken into account:
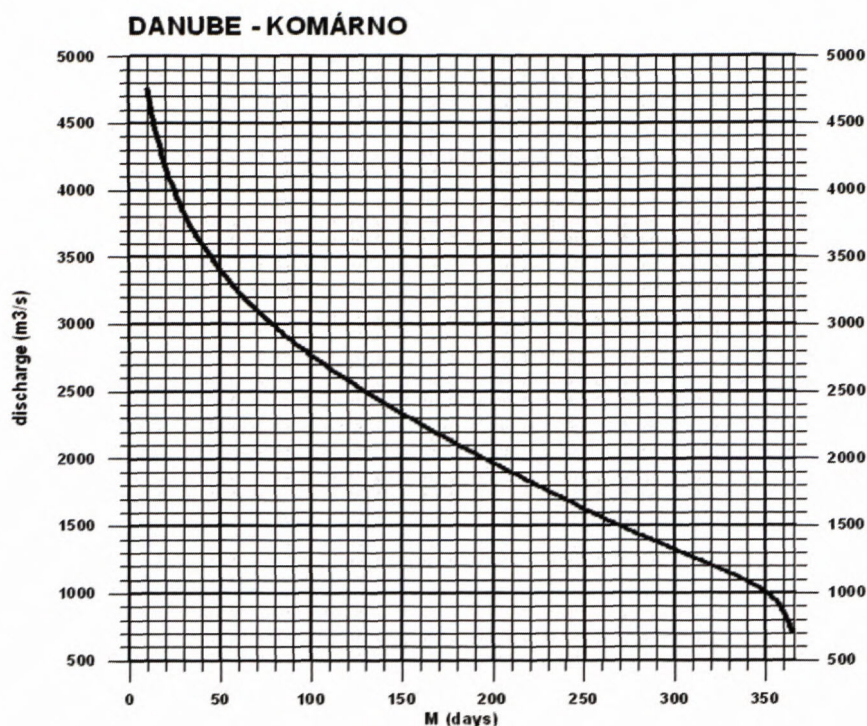
DANUBE - KOMÁRNO

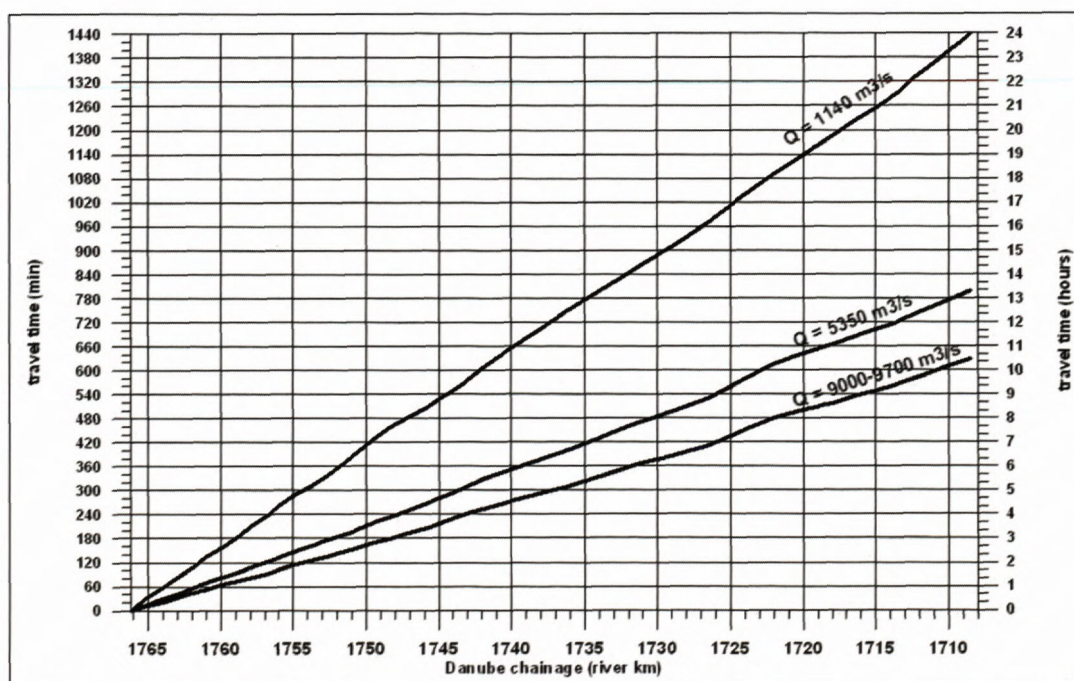*Fig. 2. Occurrence of discharges in the average year – M-days discharges.*

Fig. 3. Travel times of Danube river for different discharges.

- Oil spill site is situated in the active part of river cross-section, not in the so-called dead zone, which does not contribute to flow conveyance (bay, for instance).
- After the spill, petrol or fuel oil will be partially dissolved in the Danube water. Oil pollution will be transported in the form of petroleum hydrocarbons (non-polar extractable substances).
- Pollution will be dispersed gradually in the Danube water as a result of diffusion and flow velocity variability.

No data are available at the Slovak-Hungarian section of the Danube on the experiments to investigate coefficients of both longitudinal and lateral dispersion. Data from real cases of industrial oil spills, which could enable to estimate the coefficients, are not available as well.

In our study, we used published results from the reconstruction of pollution migration at the Somes-Tisza-Danube rivers (Sorentino, 2000; UNEP, 2000; Hellweger, 2005). This accident happened on January 30th, 2000.

K. Kminiakova and M. Lukáč: Modelling of oil substances migration...

107

Tab. 1. Travel times – sites on the Slovak side of Danube

| Site / km from oil spill site	River km	Travel time T (min), Slovak side of Danube		
		Q = 1140	Q = 5350	Q = 9000
Iža, beginning /5.7 km/	1760.5	145	75	60
Iža, end /7.7 km/	1758.5	195	100	75
Patince, beginning /10.2 km/	1756	260	130	100
Patince, end /12.2 km/	1754	310	160	120
Stara Žitava /15.2 km/	1751	385	195	150
Radvaň, beginning /16.2 km/	1750	415	210	160
Radvaň, end /18.7 km/	1747.5	475	245	190
Moča, beginning /20.2 km/	1746	505	265	205
Moča, end /21.7 km/	1744.5	540	290	225
Kravany nad Dunajom, beginning /25.7 km/	1740.5	645	345	270
Kravany nad Dunajom, end /27.2 km/	1739	680	365	285
Štúrovo, beginning /43.7 km/	1722.5	1080	605	470
Štúrovo, end /48.7 km/	1717.5	1200	670	525
Chľaba, beginning /55.2 km/	1711	1365	760	595
Chľaba, end /56.2 km/	1710	1400 23.3 hours	775 12.9 hours	610 10.2 hours
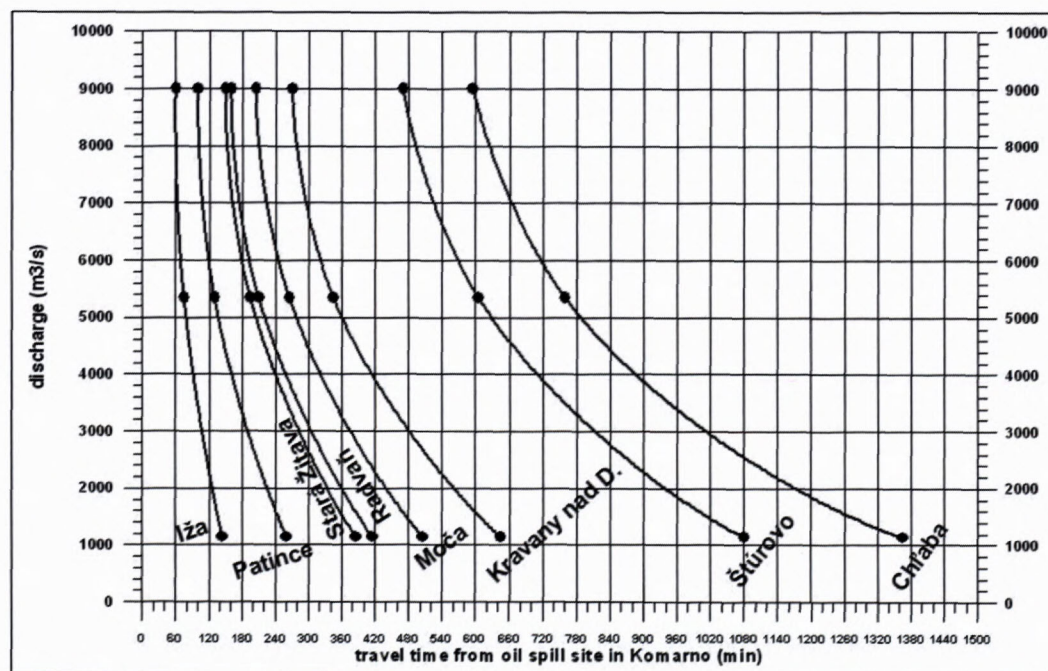
Fig. 4. Travel times for individual sites – Slovak side of Danube river.

The numerical scheme according to Nordin and Troutman (1980) was applied in the calculations, which takes into account influence of river dead zones. Such zones are characteristic with stagnant (or almost stagnant) water and no contribution to flow conveyance – bays, old river branches, meanders, areas behind groynes, etc.:

$$\frac{\partial c_m}{\partial t} = -U \frac{\partial c_m}{\partial x} + E \frac{\partial^2 c_m}{\partial x^2} - K c_m + \frac{\varepsilon}{T}(c_d - c_m)$$

$$\frac{\partial c_d}{\partial t} = -K c_d + \frac{1}{T}(c_m - c_d)$$

c = pollutant concentration [g m^{-3}]
c_m = concentration in the main river channel [g m^{-3}]
c_d = concentration in the dead zone [g m^{-3}]

A_t = area of cross-section which contributes to flow conveyance [m^2] (reach specific)
E = coefficient of longitudinal dispersion [m^2 s^{-1}] (reach specific)
K = pollution decay constant (1st order) [s^{-1}]
T = retention time in dead zone [s]
$\varepsilon = A_d / A_m$ = ratio between dead zones area and cross-section area
$Q = A_t U$ = discharge [m^3 s^{-1}]
M = quantity of spilling pollutant [g]
A_m = cross-section area [m^2]
A_d = dead zones area [m^2]
U = flow velocity [m s^{-1}]

Model HUSKY1, which accounts the influence of dead zones was applied for the numerical solution. Governing equations were solved using the method of finite differences, as published by Hellweger (2005).

Cross-section areas and flow velocities for individual discharges were based at above mentioned hydraulic studies. Dispersion parameters based on river Tisza real case were used in the model of longitudinal migration of pollution - $E=30\ m^2/s$ and $\varepsilon = 0.05$. These values are equal to minimum values recommended by the MIKE 11 software manual (MIKE 11 1-Dimensional Surface water modeling software - Reference manual) for the Danube-type rivers. This model of DHI Water & Environment (Denmark) was applied for the water quality modelling at the Slovak section of Danube in the frame of project Phare EC/WAT/01.

Solubility ratio of oil substances (petroleum, fuel oil) is not known for the Danube river. Available publications indicate only inconsiderable solubility of oil substances in the water. As a consequence, persistence of oil substances in water organisms is not assumed.

Therefore, the following simplified considerations were used in our model:

– for alternatives of minor oil spills (from suction pipings and connecting hoses in the amount of approximately 35-600 kg of oil substances) there was assumed dissolution of 5 % of contaminants in 10 % of surface water volume in the given cross-section,

– for alternatives of major oil spills (from the mobile tankers in the amount of approximately 80-200 t of oil substances) there was assumed dissolution of 5 % of spilling contaminants in the whole water volume (100 %) in the given cross-section.

Tables 8–10 provide overview of the highest assumed concentration for individual alternatives of oil spills (both minor and major) taking into account average concentration of petroleum hydrocarbons 0.05 mg/l in the profile Danube – Komárno as a background value of concentration (determined from the period 2002-2005).

From the viewpoint of environmental impacts (water and biota), the effects of industrial accidents can be divided according two evaluation criteria:

1) Legislation viewpoint – Appendix Nr. 1 of the governmental Decree Nr. 296/2005, which appoints requirements for quality and qualitative goals of surface waters and limit values of pollution parameters for waste waters and special waters. For oil substances (indicator – petroleum hydrocarbons) it is a concentration of 0.1 mg.l^{-1}.

We do not recommend applying this criterion in the given case, as the implementation of the Water Framework Directive 2000/60/ES is currently on the way in the Slovak Republic. Directive will settle new reference limits for physical, chemical and biological quality indicators, separately for individual water bodies (including Danube). The finishing of implementation process is assumed in 2015.

In the frame of WFD implementation in the Slovak Republic the benthic fauna, namely benthic macrovertebrates, benthic diatoms and macrophytes, was used as one of evaluation criterion.

Reference conditions for fishes and phytoplankton had not been settled yet. Until now, ichtyofauna was not a part of the surface waters status evaluation. Comparable data are not available. Therefore, the impact at the water organisms can not be designated clearly.

Tab. 2. Evaluation of surface water quality (Danube) according to petroleum hydrocarbons-UV concentration in 2005 (governmental Decree Nr. 296/2005 and Slovak technical standard STN 75 7221; Mucha et al., 2006)

Micropollutants	OH Decree Nr. 296/2005	STN 75 7221			
		II.	III.	IV.	V.
petroleum hydrocarbons [mg/l]	< 0.1	< 0.05	> 0.05 and < 0.1	>0.1 and < 0.3	> 0.3
petroleum hydro-carbons-UV [mg/l]	1x (3530, 1205, 4016, 111, 311, 3739) 2x (109, 112, 308, 309, 2560) 3x (307)	measured values usually ranged from values below detection limit (corresponding with class II) to values representing class III		1x (1205, 4016, 111, 311, 3739) 2x (109, 112, 308, 309, 2560) 3x (307)	1x (3530)

Explanation: (3530) – ID codes of sampling profiles, where limit values were exceeded

Tab. 3. Maximum values of petroleum hydrocarbons$_{UV}$ at the Danube in mg/l (Mucha et al., 2003-2006)

ID	site	1996-2001	2002	2003	2004	2005
109	Bratislava (New bridge, C)	0.10	0.09	0.10	0.13	**0.17**
112	Medveďov (road bridge, C)	**0.37**	0.11	0.17	0.17	0.14
1205	**Komárno (road bridge, C)**		0.13	0.14	0.12	**0.17**
3376	Dobrohošť (intake structure)	**0.63**	0.13	0.11	0.15	0.09
3530	Sap (tailrace canal, LB)	0.35	0.07	0.09	0.13	**0.56**
4016	Dobrohošť (upstream from weir Dunakiliti, LB)	0.05	0.10	0.10	**0.15**	0.11

Note: C - central part of cross-section, LB – left bank

K. Kminiakova and M. Lukáč: Modelling of oil substances migration...

109

The qualitative data from the summary report of Danube surface waters monitoring from 2005 (Mucha et al., 2006) are summarized in the Tabs. 2-5 for illustration.

The layout of sampling profiles in the frame of Danube water quality monitoring is shown in Fig. 5.

It is evident, that petroleum hydrocarbons concentrations in the range 0.1-0.3 $mg.l^{-1}$ occur 1-3 times a year (from 12 measurements in some profiles). It can be concluded from given facts, that risk of Danube water pollution due to oil spills has to be evaluated keeping in mind existing background values, which are given in Tabs. 3-5.
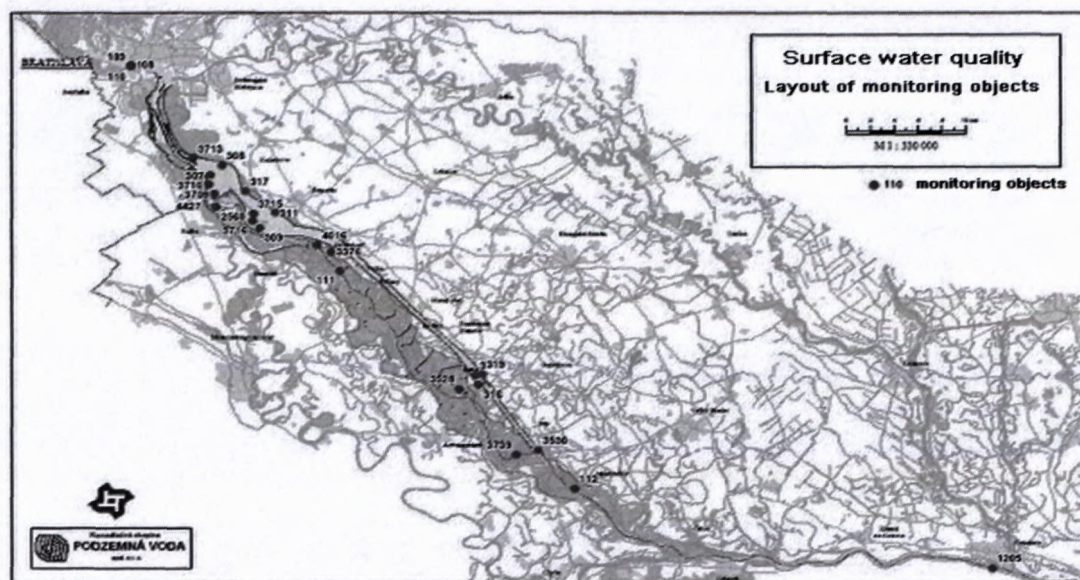

Fig. 5. Layout of monitoring objects.

Tab. 4. Average values of petroleum hydrocarbons$_{UV}$ for Danube in $mg.l^{-1}$ (Mucha et al., 2003-2006)

ID	Site	1996-2001	2002	2003	2004	2005	1996-2005
109	Bratislava (New bridge, C)	0.060	0.040	0.053	0.053	0.075	0.056
112	Medveďov (road bridge, C)	0.055	0.040	0.055	0.062	0.043	0.051
1205	**Komárno (road bridge, C)**		0.042	0.061	0.048	0.050	0.050
3376	Dobrohošť (intake structure)	0.044	0.039	0.042	0.054	0.033	0.043
3530	Sap (tailrace canal, LB)	0.043	0.029	0.039	0.053	0.072	0.045
4016	Dobrohošť (upstream from weir Dunakiliti, LB)	0.032	0.037	0.031	0.048	0.032	0.035

Tab. 5. Occurrence frequency of petroleum hydrocarbons values in the period 1996-2005 (Mucha et al., 2003-2006)

ID	Site	N total	N <0.05 mg/l	N >0.1 mg/l	N >0.3 mg/l
109	Bratislava (New bridge, C)	59	29	8	0
112	Medveďov (road bridge, C)	71	43	10	1
1205	**Komárno (road bridge, C)**	48	28 / 58.3 %	6 / 12.5 %	0
3376	Dobrohošť (intake structure)	120	82	6	1
3530	Sap (tailrace canal, LB)	119	78	5	2
4016	Dobrohošť (upstream from weir Dunakiliti, LB)	77	63	5	0
	Total:	494	323 / 65.4 %	40 / 8.1 %	4 / 0.8 %

Tab. 6. (based on the data of Danube river waterboard)

Control profile	petroleum hydrocarbons UV characteristic value (c_{90}) year 2005 $mg.l^{-1}$	petroleum hydrocarbons UV maximum value (c_{90}) year 2005 $mg.l^{-1}$	petroleum hydrocarbons UV maximum value 01.- 06/2006 $mg.l^{-1}$
Danube **Komárno – bridge C, r. km 1767**	0.11	0.17	0.19
Danube **Radvaň LB, r. km 1748**	0.12	0.21	0.15

110

Monitoring reports provide overview of maximum concentrations of petroleum hydrocarbons$_{UV}$, which are given in Tab. 3 for individual monitoring profiles.

Besides maximum values of petroleum hydrocarbons concentrations, average values for individual profiles (Tab. 4), as well as frequency of significant values occurrence (Tab. 5) are given for the illustration. These data were derived from values published in monitoring reports, taking into account also the values below the detection limit. Detection limit value for petroleum hydrocarbons$_{UV}$ is 0.05 mg.l^{-1}. The concentration values below this limit were considered in the calculation of average as a value of 0.025 mg.l^{-1}

Based on the data given in Tab. 5 and keeping in mind, that sampling is performed once a month, it can be stated that value of petroleum hydrocarbons$_{UV}$>0.3 mg.l^{-1} use to occur once in 10.3 years at the Danube and the values of petroleum hydrocarbons$_{UV}$>0.1 mg.l^{-1} once in 1.03 years. The concentration value of petroleum hydrocarbons$_{UV}$>0.5 mg.l^{-1} occurred once in 20.3 years in the evaluated period of years 1996-2005 (see Tab. 6).

Due to intensive shipment, increased values of petroleum hydrocarbons$_{UV}$ were observed in the period 2005–June 2006 in the monitoring profiles, being situated in our area of interest (Komárno – bridge C, river km 1767 and Radvan LB, river km 1748). Concentration c$_{90}$ (with probability of non-exceedance 90 %) was higher than qualitative limit (0.11 and 0.12 mg/l – see Tab. 6) in both profiles.

Based on above mentioned facts, the concentration values of petroleum hydrocarbons in the range 0.1-0.2 mg.l^{-1} were considered as background values in the given section of the Danube river. It is evident from Tab. 4, that average value (period 2003-2006) of petroleum hydrocarbons concentration 0.05 mg/l can be treated as a background value. This value was also considered in the modelling of accident scenarios.

2) *Eco-toxicological viewpoint* – harmful effects on the water organisms. Published works were used in the evaluation (database of ESIS system - European Chemical Substances Information System and cards of safety data KBU), based on which toxic conditions can be defined with following harmful parameters (indicators):
- concentration of dissolved components in the range from 2–3 mg.l^{-1} up to 8 mg.l^{-1} and higher values,
- occurrence of oil substances phase or oil substances film of larger extent.

4. Discussion

Travel times computed in the first scenario of pollution migration (Tab. 1) represent average values, which were determined, based on simulated average cross-sectional flow velocities. They have to be treated with care, as approximate values. Real distribution of flow velocity in the cross-section is uneven. Maximum flow velocities in the river streamline may differ substantially from the average value. The maximum average cross-sectional velocity simulated at the given section of Danube river in the mentioned studies of Water Research

Institute is around 2 m.s^{-1} (river km 1736). Field measurements at the Danube during real floods indicate, that flow velocities higher than 2.5-3 m.s^{-1} were measured locally. On the other hand, flow velocities in shallow parts (usually near the river bank) are much lower than the average value.

More reliable estimate of travel times would require simulations with detailed 2-dimensional numerical model, which provides better information on the flow velocity distribution and flow direction.

Results indicate, that under simplified assumptions (scenario 1) when contaminants (phase or film of oil substance) migrate at the water surface with velocity equal to flow velocity, transport of oil spill pollution into the end profile of investigated river section (river km 1708.5, end of Slovak-Hungarian section, approximately 55.6 km away from the oil spill site) can be expected in the time range from about 23 hours at a discharge 1140 m^3.s^{-1} to about 10 hours at a flood discharge 9000 m^3.s^{-1}. Occurrence of oil spill at a lower discharge can be expected with higher probability. Discharge of 1140 m^3.s^{-1} was exceeded in the given section of Danube river for about 330 days in the average year (evaluated period 1931-1980).

Fast migration of oil substances film in the case of oil spill in the investigated industrial plant, as well as its relatively large impact can be documented with further facts. Pollution – film of oil substances, could reach distance of 6 km in 2.4 hours at lower discharges or in 1 hour during 100-years flood (Q = 9000 m^3.s^{-1}). Details are summarized in Tabs. 1, 2 and 7.

It has to be emphasized, that in this concept contaminant behaves as water molecule. Several characteristics of contaminant are not taken into account, like solubility of solid phase, evaporation of volatile components, contaminant sorption at the suspended load, film fragmentation as a consequence of turbulent flow, as well as emulsion creation. For instance, Pitter (1990) reports fuel oil solubility value of around 6 mg.l^{-1}.

Real migration of oil substances (in the form of film) in the river can differ to some extent from the assumptions. Our model concept does not take into account different characteristics of both evaluated media due to lack of information. It can be assumed, that petrol would evaporate intensively especially in the summer period.

Due to several uncertainties and simplifications, results on the migration of oil substances phase/film in the case of accidental oil spill should be considered as rough estimates.

In the second scenario, where migration of dissolved oil substances was simulated using 1-dimensional model of advection-dispersion transport (Nordin and Troutman, 1980) and (Hellweger, 2005), the results (concentration of petroleum hydrocarbons in mg.l^{-1}) summarized in Tabs. 8-10 were obtained.

River channel morphology was taken into account along the whole evaluated river section (from oil spill site in Komárno down to Chľaba/Szob) based on the results of water level regime modelling for different discharge

Tab. 7. Travel times of pollution along Danube at discharges 1140, 5530 and 9000 m³.s⁻¹.

D (distance from oil spill site)	Site	Q = 1140 m³.s⁻¹		Q = 5530 m³.s⁻¹		Q = 9000 m³.s⁻¹	
		Travel time					
		min	hours	min	hours	min	hours
cca 6 km	Iža	145	2.4	75	1.25	60	1
cca 10 km	Patince	260	4.3	130	2.2	100	1.7
cca 15 km	Stará Žitava	385	6.4	195	3.2	150	2.5
cca 20 km	Moča	505	8.4	265	4.4	205	3.4
cca 48 km	Štúrovo	1200	20	670	11.1	525	8.8
cca 56 km	Chľaba	1400	23.3	775	12.9	610	10.1

Tab. 8. Maximum values of petroleum hydrocarbons (mg.l⁻¹) in Danube, discharge 1140 m³.s⁻¹

Km from oil spill site	Site	Rkm	Var. 1a 117 kg FO	Var. 1b 460 kg FO	Var. 2a 212 kg P	Var. 2b 420 kg P	Var. 3a 180 kg FO	Var. 3b 587 kg FO	Var. 4a 163 kg FO
1.1	Szony	1765	0.096	**0.230**	**0.133**	**0.214**	**0.120**	0.279	**0.114**
3.2	Szony	1763	0.076	**0.151**	0.096	**0.142**	0.089	**0.179**	0.086
7.3	Iža - Almasfuzito	1758.8	0.066	**0.114**	0.080	**0.109**	0.075	**0.132**	0.073
11.6	Patince	1754.8	0.063	0.099	0.073	0.095	0.069	**0.113**	0.067
16.8	Radvaň - Neszmely	1749.5	0.060	0.088	0.068	0.085	0.065	0.099	0.063
26	Kravany - Labaztjan	1738	0.058	0.080	0.064	0.078	0.062	0.089	0.061
46	Štúrovo - Esztergom	1720	0.055	0.071	0.060	0.069	0.058	0.077	0.058
55.6	Chľaba - Szob	1710	0.055	0.068	0.058	0.067	0.057	0.073	0.056

Km from oil spill site	Site	Rkm	Var. 4b 530 kg FO	Var. 5 98 kg FO	Var. 6 35 kg P	Var. 7a 199 t FO	Var. 7b 79,7 t FO	Var. 8 180 t P
1.1	Szony	1765	**0.257**	0.088	0.064	*7.831*	*3.163*	*7.081*
3.2	Szony	1763	**0.166**	0.071	0.058	*4.412*	1.795	*3.991*
7.3	Iža - Almasfuzito	1758.8	**0.124**	0.064	0.055	*2.825*	1.160	*2.558*
11.6	Patince	1754.8	**0.107**	0.060	0.054	*2.178*	0.901	*1.973*
16.8	Radvaň - Neszmely	1749.5	0.094	0.058	0.053	1.697	0.709	1.538
26	Kravany - Labaztjan	1738	0.085	0.056	0.052	1.365	0.576	1.238
46	Štúrovo - Esztergom	1720	0.074	0.055	0.052	0.968	0.417	0.880
55.6	Chľaba - Szob	1710	0.071	0.054	0.051	0.835	0.364	0.759

Explanations: **0.10** – exceedance of limit concentration 0.1 mg/l in accordance with Act Nr. 296/2005; 2.6 mg/l – toxic effects on water organisms can be assumed; FO – fuel oil, P - petrol

Tab. 9. Maximum values of petroleum hydrocarbons (mg.l⁻¹) in Danube, discharge 5350 m³.s⁻¹

Km from oil spill site	Site	Rkm	Var. 1a 117 kg FO	Var. 1b 460 kg FO	Var. 2a 212 kg P	Var. 2b 420 kg P	Var. 3a 180 kg FO	Var. 3b 587 kg FO	Var. 4a 163 kg FO
1.1	Szony	1765	0.077	**0.154**	0.098	**0.145**	0.091	**0.183**	0.087
3.2	Szony	1763	0.064	**0.105**	0.075	**0.100**	0.072	**0.121**	0.070
7.3	Iža - Almasfuzito	1758.8	0.060	0.088	0.067	0.084	0.065	0.098	0.063
11.6	Patince	1754.8	0.057	0.079	0.063	0.077	0.061	0.087	0.060
16.8	Radvaň - Neszmely	1749.5	0.056	0.073	0.061	0.071	0.059	0.079	0.058
26	Kravany - Labaztjan	1738	0.054	0.067	0.058	0.066	0.057	0.072	0.056
46	Štúrovo - Esztergom	1720	0.053	0.062	0.055	0.061	0.055	0.065	0.054
55.6	Chľaba - Szob	1710	0.053	0.060	0.055	0.059	0.054	0.063	0.054

Slovak Geol. Mag., 12, 2 (2006), 103 – 116

112

Km from oil spill site	Site	Rkm	Var. 4b 530 kg FO	Var. 5 98 kg FO	Var. 6 35 kg P	Var. 7a 199 t FO	Var. 7b 79.7 t FO	Var. 8 180 t P
1.1	Szony	1765	**0.170**	0.072	0.058	*4.568*	*1.857*	*4.133*
3.2	Szony	1763	**0.114**	0.062	0.054	*2.444*	1.008	*2.214*
7.3	Iža - Almasfuzito	1758.8	0.093	0.058	0.053	1.682	0.703	1.525
11.6	Patince	1754.8	0.084	0.056	0.052	1.315	0.556	1.193
16.8	Radvaň - Neszmely	1749.5	0.077	0.055	0.052	1.050	0.450	0.954
26	Kravany - Labaztjan	1738	0.070	0.054	0.051	0.807	0.353	0.734
46	Štúrovo - Esztergom	1720	0.063	0.052	0.051	0.548	0.249	0.500
55.6	Chľaba - Szob	1710	0.062	0.052	0.051	0.487	0.225	0.445

Explanations: **0.10** – exceedance of limit concentration 0.1 mg/l in accordance with Act Nr. 296/2005; *2.6 mg/l – toxic effects on water organisms can be assume;* FO – fuel oil, P - petrol

Tab. 10. Maximum values of petroleum hydrocarbons (mg.l^{-1}) in Danube, discharge 9000 $m^3.s^{-1}$

Km from oil spill site	Site	Rkm	Var. 1a 117 kg FO	Var. 1b 460 kg FO	Var. 2a 212 kg P	Var. 2b 420 kg P	Var. 3a 180 kg FO	Var. 3b 587 kg FO	Var. 4a 163 kg FO
1.1	Szony	1765	0.071	**0.132**	0.088	**0.125**	0.082	**0.154**	0.079
3.2	Szony	1763	0.061	0.094	0.070	0.090	0.067	**0.106**	0.065
7.3	Iža - Almasfuzito	1758.8	0.058	0.080	0.064	0.077	0.062	0.088	0.061
11.6	Patince	1754.8	0.056	0.073	0.061	0.071	0.059	0.080	0.058
16.8	Radvaň - Neszmely	1749.5	0.055	0.069	0.059	0.067	0.057	0.074	0.057
26	Kravany - Labaztjan	1738	0.054	0.064	0.057	0.063	0.056	0.068	0.055
46	Štúrovo - Esztergom	1720	0.052	0.060	0.054	0.059	0.054	0.062	0.053
55.6	Chľaba - Szob	1710	0.052	0.058	0.054	0.058	0.053	0.061	0.053

Km from oil spill site	Site	Rkm	Var. 4b 530 kg FO	Var. 5 98 kg FO	Var. 6 35 kg P	Var. 7a 199 t FO	Var. 7b 79.7 t FO	Var. 8 180 t P
1.1	Szony	1765	**0.144**	0.067	0.056	*3.596*	1.468	*3.254*
3.2	Szony	1763	**0.100**	0.059	0.053	*1.934*	0.804	*1.752*
7.3	Iža - Almasfuzito	1758.8	0.085	0.056	0.052	1.351	0.571	1.226
11.6	Patince	1754.8	0.077	0.055	0.052	1.064	0.456	0.966
16.8	Radvaň - Neszmely	1749.5	0.072	0.054	0.051	0.861	0.374	0.783
26	Kravany - Labaztjan	1738	0.066	0.053	0.051	0.662	0.295	0.603
46	Štúrovo - Esztergom	1720	0.061	0.052	0.051	0.465	0.216	0.425
55.6	Chľaba - Szob	1710	0.060	0.052	0.051	0.417	0.197	0.382

conditions (from low flow to flood flow) in the Danube (Szolgay et al., 1994; Mišík et al., 1994; Szolgay et al., 1996). On the other hand, pollution decay and influence of tributaries (Váh, Hron, Stará Žitava, Ipeľ) were not considered.

5. Conclusion

Travel times computed in the first scenario of pollution migration, when contaminant (oil substances phase/film) migrates at the water surface depending on the flow velocity, represent average values, which were determined by simulated average cross-sectional flow velocities. They have to be treated with care, as approximate values. Real distribution of flow velocity in the cross-section is uneven. Maximum flow velocities in the river streamline may differ substantially from the average value. More reliable estimate of travel times would require simulations with detailed 2-dimensional numerical model, which provides better information on the flow velocity distribution and flow direction.

The results of simulations of contaminant dissolved component migration, presented in Tabs. 8 to 10 and Figs. 6a, b, c and 7a, b, c can be concluded as follows:

• Oil spills from pipelines or hoses (from 35 kg up to 587 kg - further marked as variants 1-6) can be indicated as "minor oil spills", the total occurrence frequency of which ranges in the interval 1.2 . 10^{-3}/year-6.1 . 10^{-4}/year.

- Oil spills from vessels (mobile tanks) (from 80 t up to 199 t - further marked as variants 7-8) can be indicated as "major oil spills", the total occurrence frequency of which is around $4.1 \cdot 10^{-7}$/year.

In the cases of "minor" oil spills (from pipelines and hoses) model simulations indicated maximum concentrations of petroleum hydrocarbons in the range of about *0.27-0.06 mg.l⁻¹, in the distance around 1.1 km from the oil spill site* (see Fig. 6a, b, c). Concentrations of contaminant decreased gradually with increasing distance

from the pollution source, due to dissolution in the water (see Tabs. 8-10). Such values are similar to annual maximums, when comparing with statistical evaluation of Danube water quality (Danube water quality monitoring in the period 2002-2005 – see Tabs. 3-4). In several sections of Danube the maximum values of petroleum hydrocarbons$_{UV}$ concentrations in the range 0.1-0.4 mg.l⁻¹, locally even 0.6-0.7 mg.l⁻¹ were recorded every year (Mucha et al., 2003-2006; see Tab.3).
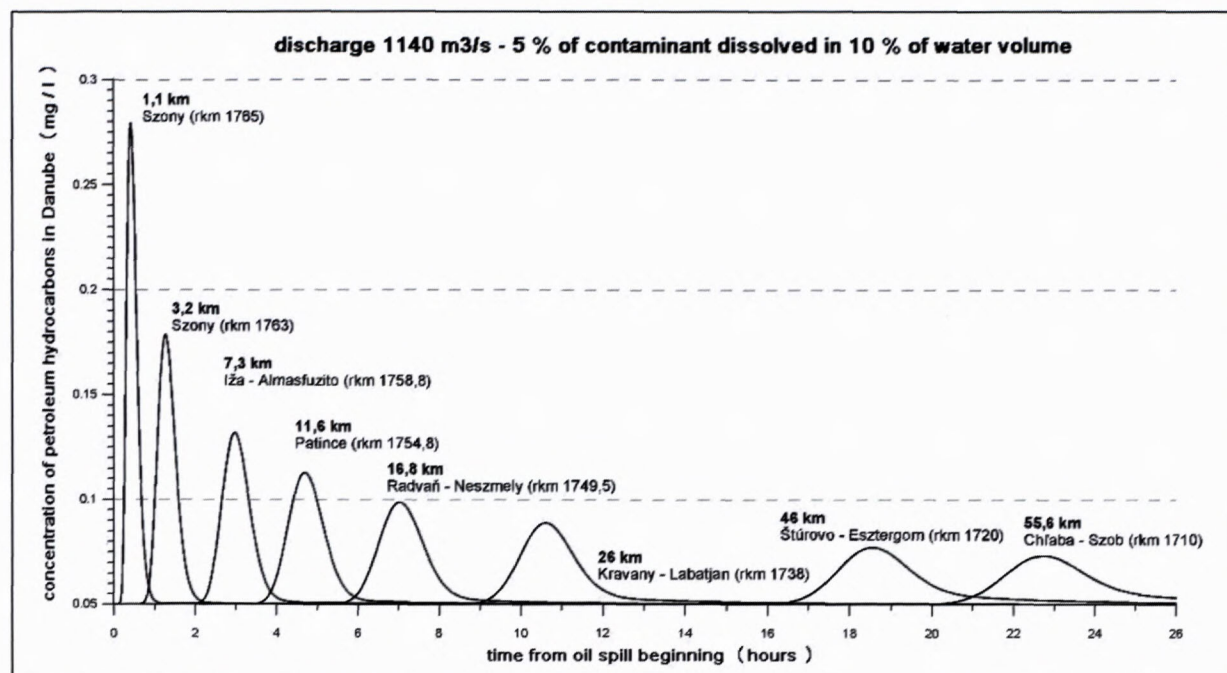
Fig. 6a. Calculated concentrations of petroleum hydrocarbons in Danube as a result of fuel oil spill in the quantity of 587 kg.

Fig. 6b. Calculated concentrations of petroleum hydrocarbons in Danube as a result of fuel oil spill in the quantity of 587 kg.

114

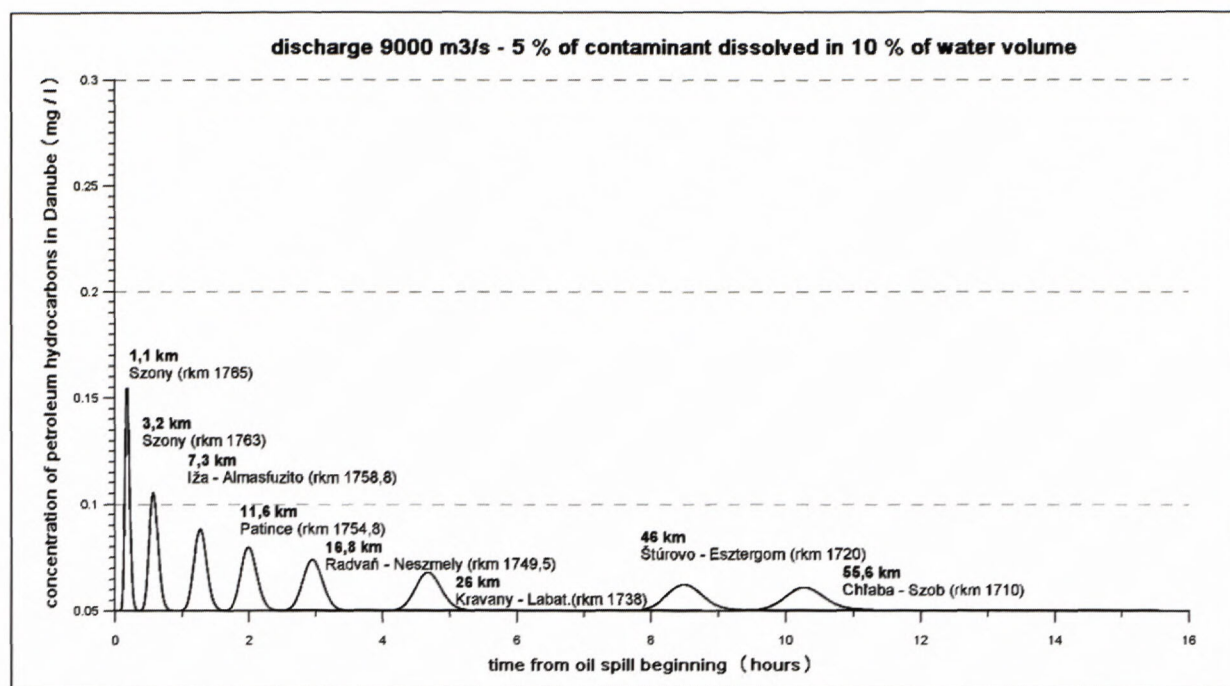*Slovak Geol. Mag., 12, 2 (2006), 103 – 116*
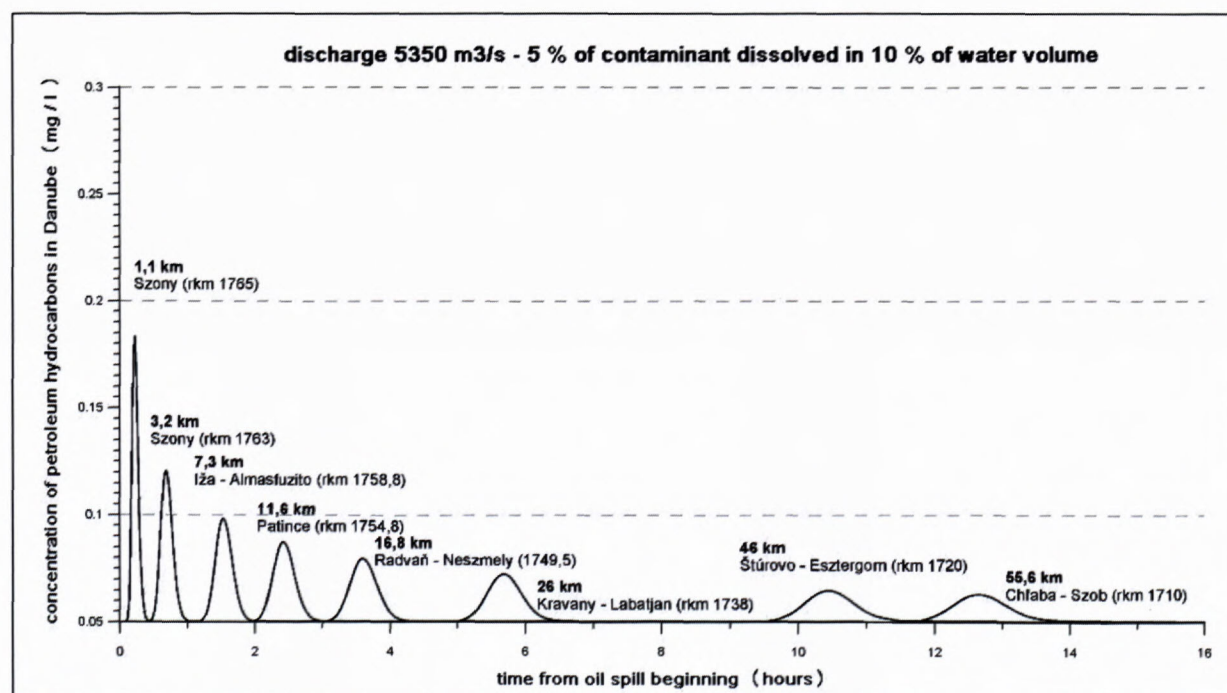
Fig. 6c. Calculated concentrations of petroleum hydrocarbons in Danube as a result of fuel oil spill in the quantity of 587 kg.

In the cases of "minor" oil spills (from pipelines and hoses, quantity of about 35-600 kg of oil substances) total frequency of these events reaches relatively higher values $F=1.2 \cdot 10^{-3}\text{-}6.1 \cdot 10^{-4}$/year according to the analysis of "failure trees" (Kminiaková and Jelemenský, 2006). Serious harmful effects on water organisms life are not assumed. Values in the range $0.06\text{-}0.27 \ m.l^{-1}$ (see Tabs. 8-10) are comparable with normal maximum values in each year. Higher concentrations of petroleum hydrocarbons in the order of several mg/l can be expected in the close surrounding (around 500 m) of the oil spill site. Toxic effects of such pollution can not be excluded from considerations.

In the case of this scenario, assuming partial dissolution of contaminant, output concentrations of petroleum hydrocarbons in the ranges 0.05-0.09 mg/l at lower discharges and 0.05-0.07 mg.l^{-1} at higher discharges were achieved (profile Chľaba-Szob, 55.6 km away from oil spill site).
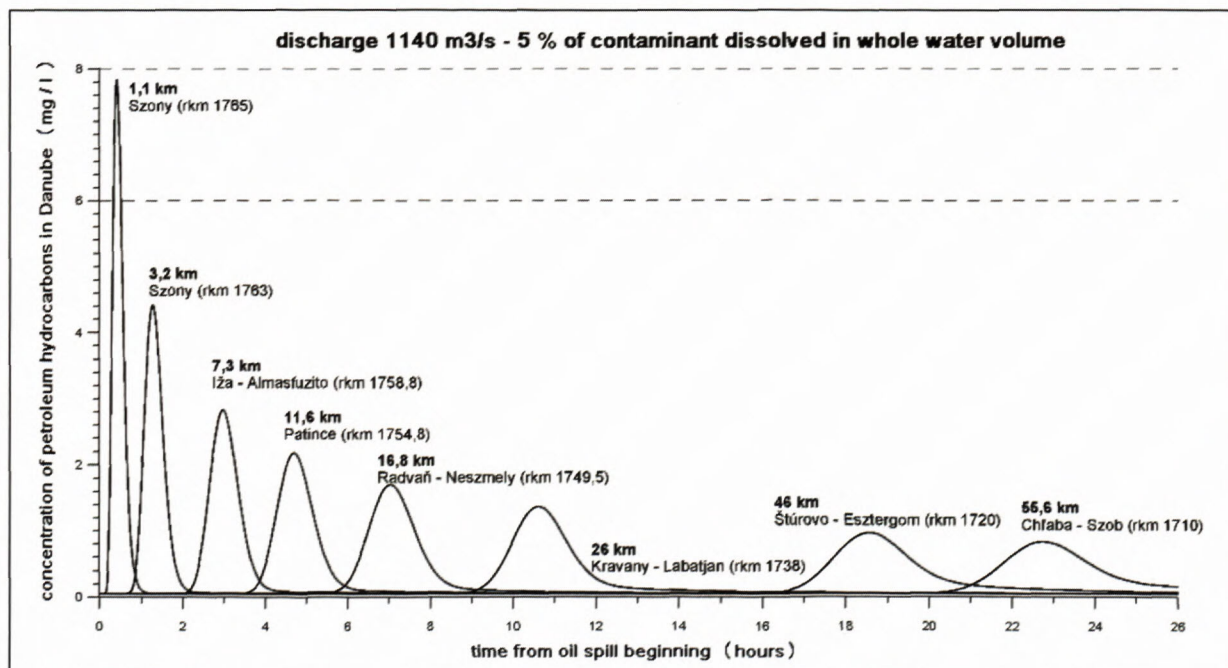

Fig. 7a. Calculated concentrations of petroleum hydrocarbons in Danube river as a result of fuel oil spill in the quantity of 199 tons.

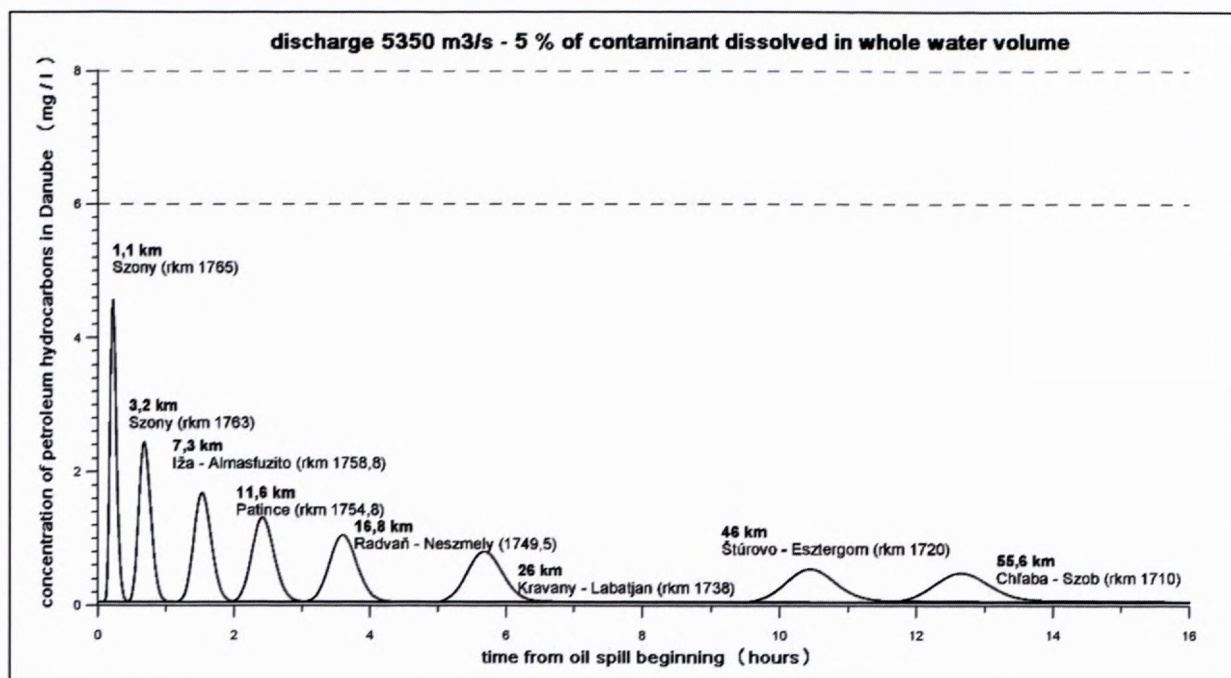K. Kminiakova and M. Lukáč: Modelling of oil substances migration...

115

Fig. 7b. Calculated concentrations of petroleum hydrocarbons in Danube as a result of fuel oil spill in the quantity of 199 tons.

Fig. 7c. Calculated concentrations of petroleum hydrocarbons in Danube as a result of fuel oil spill in the quantity of 199 tons.
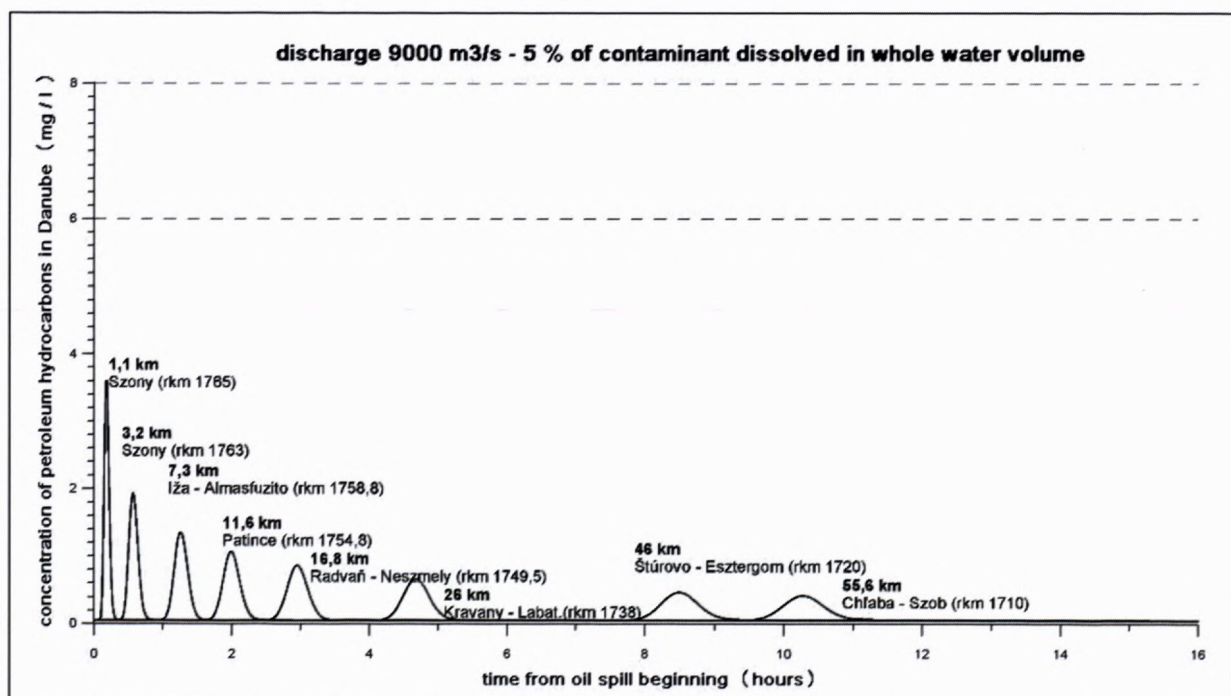
In the cases *of "major" oil spills* (from mobile tanks – vessels, assumed quantities 80-199 t) model simulations indicate maximum concentrations of petroleum hydrocarbons in the range 1.5–7.8 mg.l^{-1} at various discharges, around 1.1 km away from oil spill site (see Fig. 7a, b, c). As in the previous cases, concentration will decrease gradually with increasing distance from oil spill site, due to dissolution of contaminant in the water (see Tabs. 8-10). Assuming partial dissolution of contaminant, output concentrations of petroleum hydrocar-

bons in the ranges 0.36-0.84 mg.l^{-1} at lower discharges and 0.2-0.42 mg.l^{-1} at higher discharges were achieved (profile Chlaba-Szob, 55.6 km away from oil spill site).

Harmful effects of contamination with regard to *assumed toxic impacts at water organisms* (concentrations of petroleum hydrocarbons in the range 2-3 mg.l^{-1} and higher) can be expected:

• in 11 km long river section from oil spill site (profile Patince) at the discharge of 1140 m^3.s^{-1} (petroleum hydrocarbons concentrations in the range 2.0-7.8 mg.l^{-1})

116

- in 3 km long river section from oil spill site (profile Szony) at the flood discharges 5350–9000 $m^3.s^{-1}$ (petroleum hydrocarbons concentrations in the range 2.0-4.6 $mg.l^{-1}$)
- in the close surrounding of oil spill site (around 500 m) even higher concentrations of petroleum hydrocarbons can be expected.

Total frequency of "major" oil spills in the estimated quantity 80–199 t as a consequence of the mobile tanks (vessels) failure (collision with other vessel, or leakage) is substantially lower than in the case of "minor" spills. Analysis of "failure tree" (Kminiaková and Jelemenský, 2006) indicates that all possible sources of basic failures are of very low probability (frequency in the order $F=n.10^{-7}$ up to $n.10^{-8}$/year), comparable with meteor impact.

It has to be pointed out, that all mobile tanks (vessels) meet all necessary technical requirements for transport and manipulation with dangerous substances (of ADN type), as well as standards according to valid legislation in the field of shipment. Vessels are certified, capable to transport dangerous load of classes III and K1n.

Transport of similar vessels with identical load (petrol, fuel oil) of comparable volume is routine, in concordance with the Agreement on the navigation regime at the Danube river. Agreement was signed on 18th August 1948 in Belgrade and put in force on 11th May 1949 after ratification with member states parliaments. Agreement declared international navigation regime along the whole Danube section between Ulm (Germany) and Danube mouth to Black Sea in Romania (via Sulina branch and Sulina canal).

International navigation safety at the Danube river should be solved in a complex way along the whole river, not only in the form of case studies for individual potential sources of oil substances contamination.

6. References

DHI: MIKE 11 1-Dimensional surface water modeling software - Reference manual

Hellweger, F. L., 2005: Measuring and modeling large-scale pollutant dispersion in surface waters. Northeastern University Boston, MA 02115.

Chapra, S., 1997: Numerical methods for engineers: With programming and software applications. McGraw-Hill, Inc., New York, ISBN 0070109389, 1-916.

Kminiaková, K. & Jelemenský, Ľ., 2006: Risk assessment – port of mineral oils, DPT plant, Komárno. AQUIFER Ltd.

Mišík, M., Szolgay, J., Capeková, Z., Kľúčovská, J. & Holubová, K., 1994: Evaluation of the Danube river channel capacity at large discharges in the section between the tailrace canal end and Ipel river mouth. WRI Bratislava.

Mucha, I., Rodák, D., Banský, Ľ., Hlavatý, Z., Kučárová, K. & Lakatošová, E., 2003: Environment monitoring in the area of Gabčíkovo water structure effect. Summary report for 2002, Groundwater consulting Ltd.

Mucha, I., Rodák, D., Banský, Ľ., Hlavatý, Z., Kučárová, K. & Lakatošová, E.: Environment monitoring in the area of Gabčíkovo water structure effect. Summary report for 2003, Groundwater consulting Ltd.

Mucha, I., Rodák, D., Banský, Ľ., Hlavatý, Z., Kučárová, K. & Lakatošová, E., 2005: Environment monitoring in the area of Gabčíkovo water structure effect. Summary report for 2004, Groundwater consulting Ltd.

Mucha, I., Rodák, D., Banský, Ľ., Hlavatý, Z., Lakatošová, E. & Hlavatá, O., 2006,: Environment monitoring in the area of Gabčíkovo water structure effect. Summary report for 2005, Groundwater consulting Ltd.

Ministry of Environment of Slovak Republic, 1995: PHARE EC/WAT/01 Danubian Lowland: Ground Water Model, Final report, Vol.: I, II. III, Ministry of Environment of Slovak Republic, Commission of the European Communities.

Nordin, C. F.; Troutman, B. M., 1980: Longitudinal dispersion in rivers: The persistence of skewness in observed data. Water Resour. Res., 16(1), 123-128.

Pitter, P., 1999: Hydrochemistry. College of Chemical Technology, 309-315

PHARE EC/WAT/01: The Danubian Lowland Ground Water Model.

Sorentino, C., 2000: The Romanian cyanide spill. AusIMM Bull., 8/9, 26-27.

Szolgay, J., Capeková, Z. & Holubová K., 1996: Determination of the highest navigation water level at the Danube in the section of river kilometers 1880.2–1708.2 according to Recommendations of the Danube Commission. WRI Bratislava.

Szolgay, J., Capeková, Z., Mišík, M. & Holubová, K., 1994: Proposal of low regulation and navigation water level (HNR and PV-DK 1995) for the Danube river section between river kilometers 1880-1708. WRI Bratislava.

Slovak Hydrometeorological Institute, 1992: Hydrological bulletin 1986-1990. SHMI Bratislava

UNEP, 2000: Cyanide Spill at Baia Mare, Romania. United Nations Environment Program (UNEP), Geneva.

Decree Nr. 490 of the MoE SR, on the prevention of serious industrial accidents.

Act Nr. 261/2002 on the prevention of serious industrial accidents and on the changes and ammendments of selected Acts.

Act Nr. 277/2005 Dig. On the change and amendment of the Act Nr. 261/2002 Dig. On the prevention of serious industrial accidents.

Accumulation of moderate and highly soluble salts in soils: Implication for protection of underground steel structures in Slovakia

[1]Ján Milička, [2]Pavel Dlapa and [1]Ľubomír Jurkovič

[1]Comenius University, Faculty of Natural Sciences, [1]Dept. Geochemistry,
[2]Dept. Pedology, Mlynská dolina, G, 842 15 Bratislava, Slovakia

Abstract: Underground structures, represented by the steel constructions buried in depth 80-250 cm in soil, are the most important technological systems for transfer of strategic media like natural gas and crude oil in Slovakia. Among the most important of them belong Transit gas pipe-line, International gas pipe-line "Bratstvo" and oil pipe line "Družba". Operation and protection costs for trouble free use of these structures reaches enormous prices yearly. The most damages are caused by the degradation of protective coatings and consequently by the corrosion of metallic body. One of important factors negatively influencing both the protective coatings and the steel body corrosion is the natural inorganic salt occurrence in saline soils.

Key words: underground structures, porous protective coatings, natural soluble inorganic salts, Danube and East Slovakian lowlands

Introduction

One of the most principal protection technologies of buried steel pipe-lines is the application of protective coatings that should in the ideal case perfectly isolate the steel body against the direct contact to rocks and soils as well as to included media chemistry – mainly to soil solutions.

Soluble inorganic salts like natron, thermonatrite, and gypsum were identified using XRD (X-ray powder diffraction) in the form of efflorescence on bituminous protective coating of the high-pressure gas pipeline from southern part of the Danube Lowland. Besides these minerals typical for saline soil there were identified also mostly common clay minerals, calcite, dolomite and quartz. Depending mainly on groundwater level changes dynamics and on local climatic changes, the dissolution and re-crystallization of moderately ($CaCO_3$, $CaSO_4$ x $2H_2O$) and highly soluble (sodium) salts could cause considerable degradation of porous protective coatings. Consequently, the corrosion of steel underground structures is accelerated. Such conditions, i.e. saline soil environment often combined with agrochemical pollution could be expected in the most arid and hottest lowland areas of East Slovakian and Danube lowlands.

Characteristic of saline soils and their impact to protective coatings

Saline soils originate in various environmental conditions, however mostly in arid to semiarid climatic regions. Such conditions occur in our country often in local non-effluent terrain depressions situated on transitions from alluvia to uplands. The most frequent anions associated with the saline soils are chlorides, sulphates, carbonates and nitrates, while sodium, potassium, calcium and magnesium represent the common cations. The accumulation of easily soluble inorganic salts is characteristic for saline soils (e.g. Na_2CO_3 x H_2O, Na_2CO_3 x $10H_2O$, $CaSO_x$ x $SrSO_4$, $CaSO_x$ x $2H_2O$, Na_2SO_4, $MgSO_4$, NACl, $MgCl_2$, $NaNO_3$) and their active participation in biological and geological cycle and migration. Based on the quantity and nature of contained salts the soils can be divided into three groups. This classification depends on total amount of dissolved salts expressed by their electric conductivity, soil pH value and percentage of exchangeable natrium (Szabolcz, 1991):

Soil classi- fication	El. conductivity [mS/cm]	pH of soil	% of exchan- geable Na
Saline	> 4.0	< 8.5	< 15
Sodic	< 4.0	> 8.5	> 15
Salsodic	> 4.0	< 8.5	> 15

Corrosion processes running on the surface of metallic body in contact with various types of environments cause a continual degradation of material due to chemical and/or physical-chemical effects. Corrosion processes have various character in various environments, and that it is important to define in detail factors mostly influencing the corrosion.

Potential risk of degradation of bituminous protective coating is highest in the case of porous materials, e.g. bituminous coatings. Seasonal cycles of dissolution of moderately and highly soluble inorganic salts during wet and colder periods and their re-crystallization, when evaporation is dominant over precipitations (Fig. 1), occur also in Slovak lowlands.

Migration of these salts in dissolved state depends mainly on drainage conditions, dynamics of groundwater
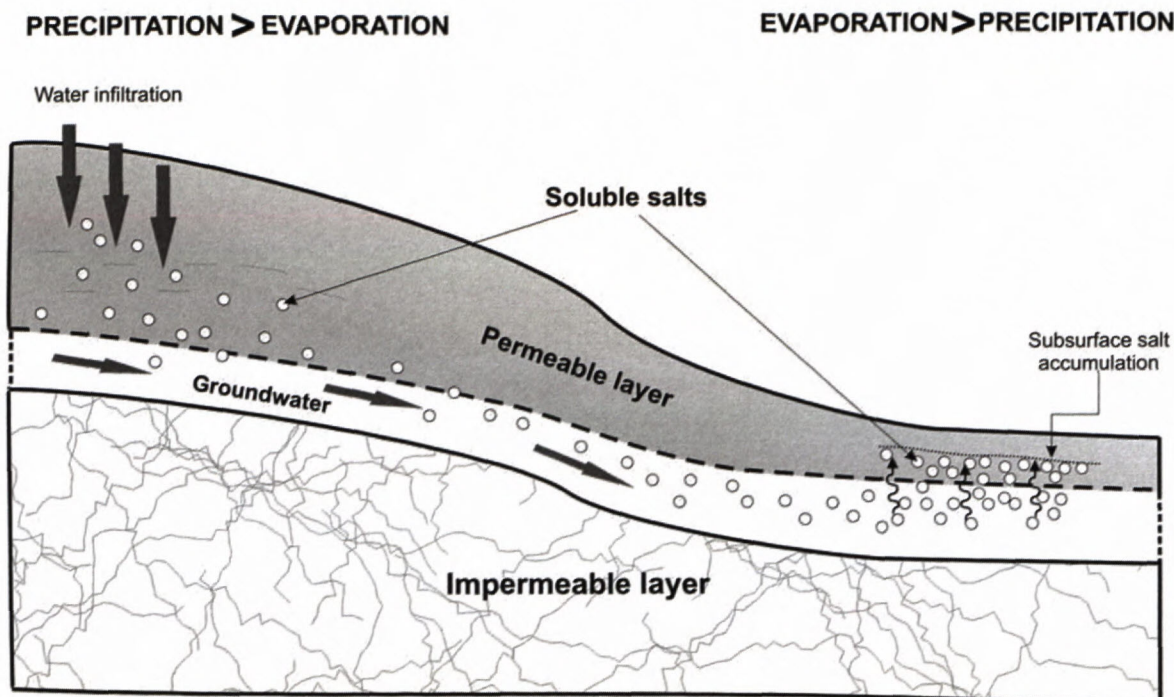
Slovak Geol. Mag., 12, 2 (2006), 117 – 121

118

PRECIPITATION > EVAPORATION

EVAPORATION > PRECIPITATION

Fig. 1. Scheme of subsurface salt accumulation in soils.

flow, local geomorphology and the presence of porous permeable layers and/or seal impermeable layers. Beside climatic regime the dissolution and re-crystallization processes depend mainly on the dynamics of groundwater level changes. Corrosion affects mostly on places with failed pipeline isolation. As shown in Tab. 1, using the XRD method, the nearly mono-mineral white efflorescence of thermonatrite (Na_2CO_3 x H_2O) was identified under following conditions: Powder diffractometer

DRON-3, Ni filtered $CuK\alpha$ radiation, measurement interval [°2Θ] of 4 to 64°. From other localities calcite, dolomite and gypsum were identified.

In natural condition the thermonatrite occurs often in association with natron Na_2CO_3 x $10H_2O$ and trona Na_2CO_3 x $2H_2O$ from which develops by partial dehydration. Under atmospheric pressure the thermonatrite precipitates from saturated solutions of soda by temperatures over 35 °C (Eugster and Smith, 1965; Last and Ginn, 2005).
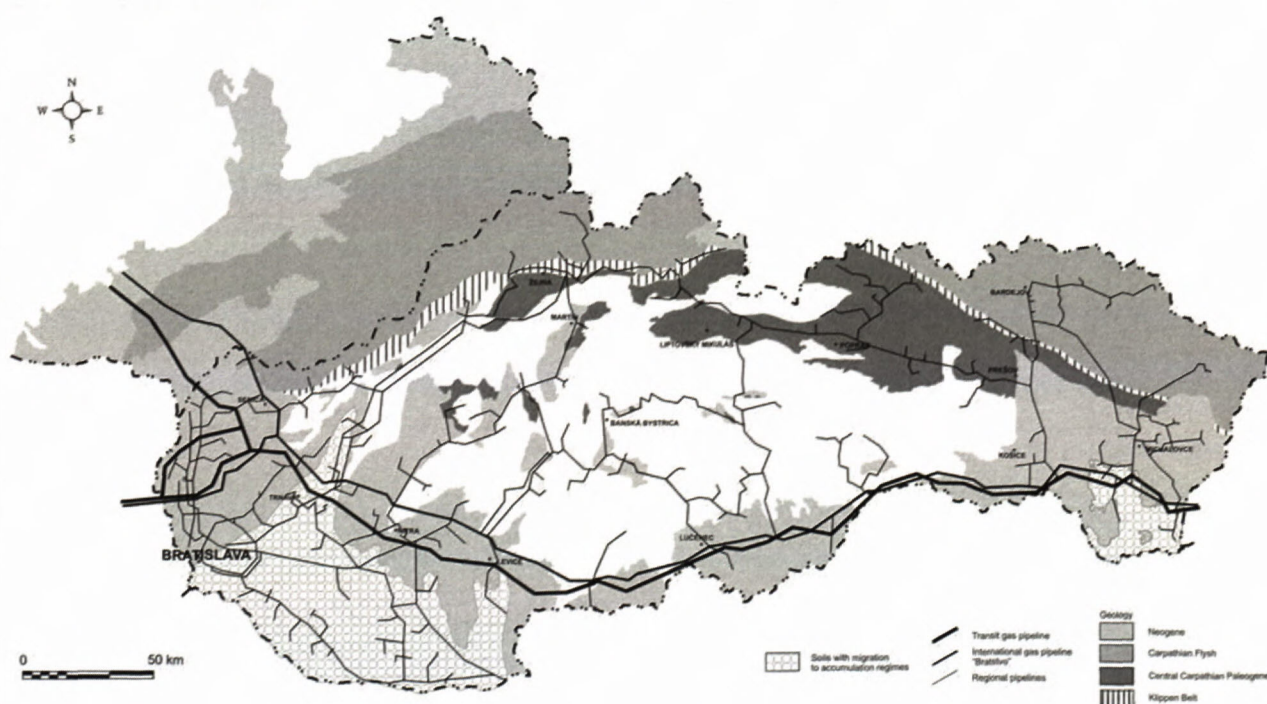

Fig. 2. Gas pipeline transfer system in Slovakia and the occurrence of soils with migration to accumulation salt regimes.

J. Milička et al.: Accumulation of moderate and highly soluble salts...

119

Tab. 1. Measured (m) and reference (ref) data of thermonatrite (JCPDS, 1974); d – interplanar distance, I – relative intensity.

d_{ref} [10^{-10} m]	I_{ref}	d_m [10^{-10} m]	I_m
5.352	20	5.335	33
5.240	20	5.278	30
4.720	2	4.691	12
4.120	10	4.119	23
3.240	4	3.240	12
2.768	100	2.760	100
2.753	55		
2.684	50	2.665	61
2.678	55	2.660	53
2.677	8		
2.622	8	2.638	17
2.550	2		
2.475	30	2.472	26
2.448	20	2.441	17
2.386	10		
2.372	60	2.366	57
2.238	20	2.236	18
2.181	16	2.175	14
2.065	18	2.060	18
2.026	2		
2.010	25		
2.004	20	2.004	28
1.985	4	1.984	9
1.961	4		
1.920	8	1.917	11
1.905	4		
1.875	4		

Problems of porous protective coating degradation are closely connected also by the anthropogenic, influencing the soil chemistry, i.e. mainly by the land use practice.

Occurrence of increased salt concentration in soils of Slovakia in relation to underground structures

There is up to 9 million km² of saline soils worldwide. The natural conditions for inorganic salt development exist in so-called saline countries with permanent or seasonal evapotranspiration regime, e.g. in Egypt and India. In EU countries the salinization influences about 1 million ha of soils mainly in Mediterranean region (Programma, 2001). In central Europe it is the case mainly in part of Hungary and Slovakia – mainly in parts of Danube and East Slovakian basins.

The accumulation of moderately and highly soluble salts and their active participation in biological and geological cycles and migration is characteristic for Slovakian lowlands. In geological conditions of alluvial regions the salt concentration is often connected with evaporative accumulation of inorganic salts. Such situations occur mostly in areas, where the groundwater level lies close to the soil surface and groundwater capillary rises to the surface. In anomalous situations the evaporative geochemical, or local redox barriers are developed. Due to the water capillary rise and evaporation the inorganic salts are accumulating near the surface residues in soil profile (Fig. 1). The extent of capillary rise is influenced mainly by the granulometry of soils and sediments (Kutílek 1978), however the whole process depends on several factors, from which the local climatic regime is the most important. More detailed criteria for mineralized water effect on secondary salt accumulation were introduced by Hraško and Bedrna (1988).

The application of agrochemicals and inconvenient irrigation water (Carter, 1969) also modify negatively the soil chemistry. Consequently, the negative effects related to underground structures became continuous. In respect to widespread and long termed agricultural activities, the increase of soil aggressiveness to steel underground constructions can reach a considerable dangerous extent. Such conditions, i.e. natural salinization combined with negative effects of salts originating from agrochemicals and irrigation are expected to occur in the most arid and hottest areas of Danube and East Slovakian lowlands (Fig. 2), especially in alluvial depressions with shallow groundwater level. The major media transfer system, i.e. oil pipe line and gas pipe line systems cross both these areas as shown in Fig. 2.

Based on the above mentioned, it is obvious that soils with accumulation of moderately and highly soluble salts (e.g. $CaCO_3$, Na-salts) in individual locations of the Danube- (Fig. 3) and East Slovakian lowlands (Fig. 4) are evaluated as potentially aggressive for porous protective coatings as shown in Fig. 5. Considering the date of steel constructions burial into the soil, the time changes of individual critical parameters are also very important.

Salt concentration changes could show long-time trends, but at the same time they would depend on seasonal changes of climatic conditions. The negative influence of mineralized soil solutions can be expected most expressive in Nové Zámky, Komárno, Kolárovo, Nitra, Trebišov, Michalovce and Kráľovský Chlmec districts. The soils in regions in Figs. 3 and 4 are of migration salt regime type according to Bedrna (1977) with alternating downward and upward movement of moderately (e.g. $CaCO_3$) and highly (sodium) soluble salts within the soil profiles. Accumulation of highly soluble sodium salts may occur especially in depressions with highly mineralized groundwater when evaporation exceeds rainfall. Occurrence of microcrystalline forms of $CaCO_3$ was described in detail by Čurlík (1992). These regions also reveal increased contents of calcium and sodium in A and C horizons of soils as shown by Geochemical atlas of the Slovak Republic (Čurlík and Šefčík, 1999).

In several localities mainly in Danube Lowland (e.g. Tvrdošovce, Nové Zámky, Komárno) the inorganic salts were identified using powder diffraction. The monomineral efflorescence of thermonatrite occurred in positions of external and internal crusts of the pipe line steel body (see Fig. 5). This section of high pressure gas pipeline was exhumed within the routine service works near
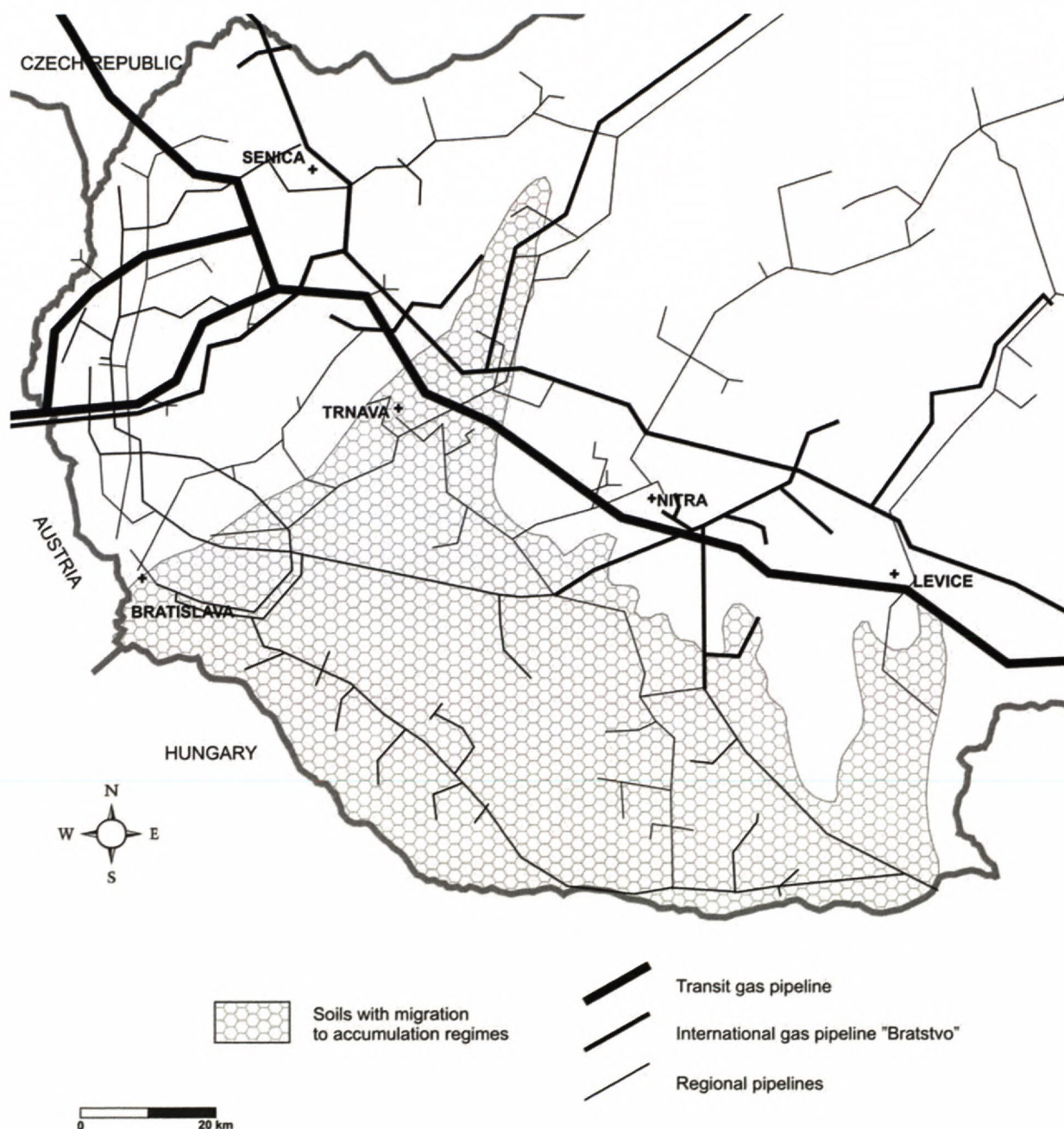
Fig. 3. Soils with migration to accumulation salt regimes in the Danube Lowland with respect to the gas pipeline system.

Tvrdošovce village in the Danube Lowland. Both, the degradation of bituminous coating and corrosion of steel body being caused also by the inorganic salts attack, are present.

Conclusions

The impact of increased salt accumulations in soil environment is in presented contribution evaluated in relation to underground structures e.g. gas- and oil pipelines. In the case of these constructions there can be distinguished a corrosion attack of inorganic salts against the metallic body as well as the degradation attack against the porous protective coatings.

Mechanism of repeated dissolution and re-crystallization of inorganic salts causes serious defects, eventu-

ally even destruction of porous protective coatings, especially in the case of bituminous isolation.

Based on the regional occurrence of soils with accumulation of moderately and highly soluble salts in Slovakia, the potential negative effect of increased salt concentrations to underground structures is expected mainly in following districts: Nové Zámky, Komárno, Dunajská Streda, Šaľa, Galanta and Senec in the Danube Basin and Michalovce and Trebišov districts in the East Slovakian Basin.

Acknowledgement

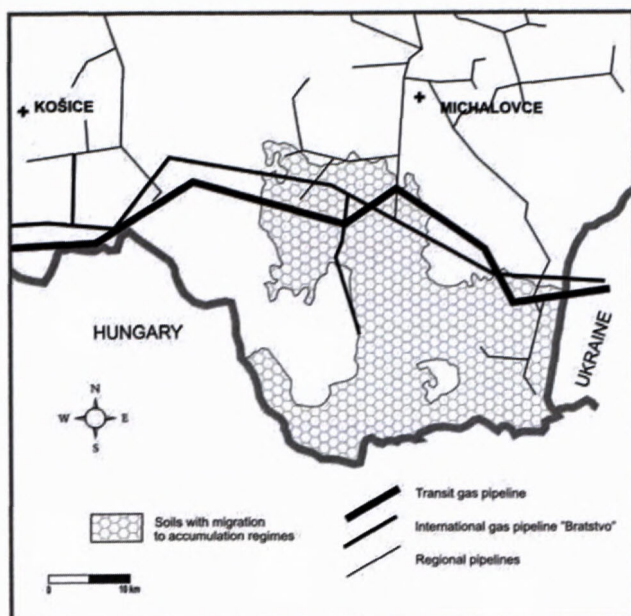J. Milička et al.: Accumulation of moderate and highly soluble salts...

121

Fig. 4. Soils with migration to accumulation salt regimes in the East Slovakian Lowland with respect to the gas pipeline system.

References

Bedrna, Z., 1977: Soil processes and soil regimes. Veda, Bratislava, 1-129. (In Slovak.)

Carter, D. L., 1969: Managing moderately saline (salty) irrigation waters. Univ. ID Curr. Inf. Ser., 1-107.

Čurlík, J., 1992: Carbonates in loess, their forms and distributions changes as influenced by pedogenesis in Slovakia. Vedecké práce VÚPÚ, 17, Bratislava, 30-59. (In Slovak.)

Čurlík, J. & Šefčík, P., 1999: Geochemical atlas of the Slovak Republic. Part V: Soils. Soil Science and Conservation Research Institute, Bratislava.

Eugster, H.P. & Smith, G.I., 1965: Mineral equilibria in the Searles Lake Evaporites, California. Journal of Petrology, 6(3), 473-522.

Hraško, J. & Bedrna, Z., 1988: Applied soil science. Príroda, Bratislava, 1-474. (In Slovak.)

JCPDS, 1974: Powder diffraction file: Joint Committee on Powder Diffraction Standards, Swarthmore, Pennsylvania.

Kutílek, M., 1978: Watermanaging pedology. Praha-Bratislava, 1-258. (In Czech.)

Last, W. M. & Ginn, F. M., 2005: Saline systems of the Great Plains of western Canada: an overview of the limnogeology and paleolimnology. Saline Systems, 1(10), 1-38.

Programma, 2001: Programma de Acción Nacional Contra la Desertificación. Ministerio de Medio Ambiente, Madrid.

Szabolcz, I., 1991: Soil classification related properties of salt affected soils. In: Characterization, classification and utilization of cold Aridisols and Vertisols. Proc. 6th Int. soil correlation meeting (ISCOM), Lincoln.
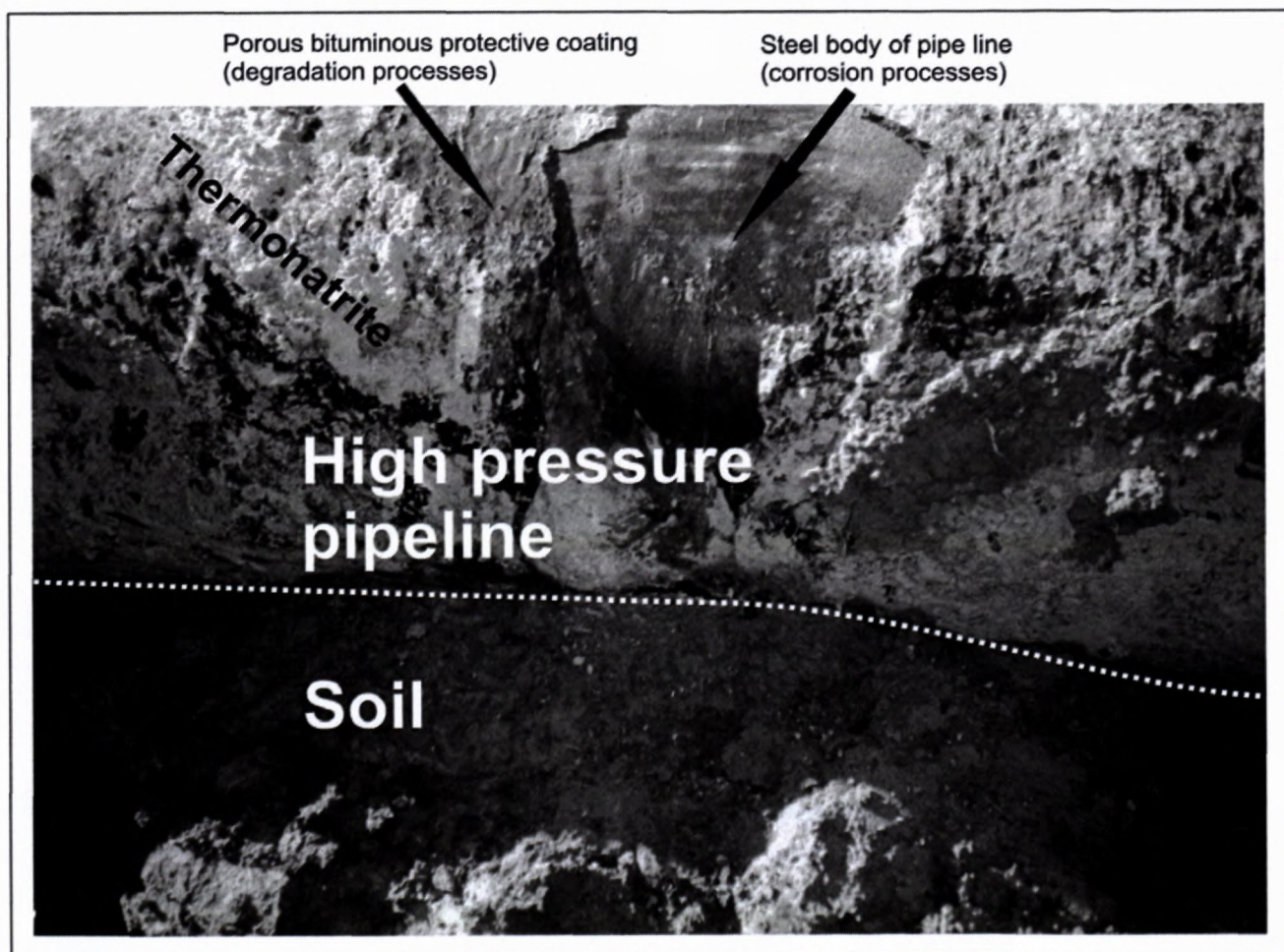

Fig. 5. Efflorescence of thermonatrite on high pressure gas pipeline in Danube Lowland.

Microbial boring activity in the Jurassic, Cretaceous and Tertiary limestones of the Western Carpathians

[1]Milan Mišík, [1]Daniela Reháková and [2]Ján Soták

[1]Department of Geology and Paleontology, Faculty of Natural Sciences, Comenius University,
Mlynská dolina G-1, 842 15 Bratislava, Slovak Republic
[2]Geological Institute, Slovak Academy of Sciences, Severná 5, 974 01 Banská Bystrica, Slovak Republic;
sotak@savbb.sk

Abstract. Microborings from bioclasts were selected and studied from several hundred thin sections of Mesozoic and Tertiary limestones. They were produced by cyanophyta, algae and fungi. Nine morphotypes were discerned especially from bivalves, crinoids, foraminifers; microborings from coralline algae and *Ethelia alba* were also preliminarily studied. The boring activity continued until the diagenetic stage. The cases of redeposition of terrestric microborings in the marine environment and retransportation of microborings from shallow marine waters to the deep water were considered. The density of microborings is proportional to the time of their exposition on the bottom, then to the rising of the sea-level and interruption of the transport from the sea-shore.

Key words: Jurassic, Cretaceous, Tertiary, Western Carpathians, microborings, diagenesis.

1. Introduction

Thin sections of limestones reveal very frequently thin channels of boring microorganisms in the skeletal fragments. In our collection they were abundant especially in pelecypod shells within the red Liassic limestones. They are well visible due to their filling by Fe-oxides and hydroxides. Microborings are especially dense in the hardgrounds where they affected not only fossils but also the lithified sediment. Microborings are common also in the skeletal parts of ammonites, belemnites, brachiopod shells, echinoderm ossicles, bryozoans and foraminifers. In the Tertiary limestones they perforate skeletal remains of algae like Corallinaceae and *Ethelia alba* what will be illustrated here.

Microorganisms produce their tiny tunnels by dissolution. The purpose of boring is protection and alimentation (organic matter contained in the skeletal particles). Microborings were defined by the span of the tunnel diameters from 1 μm to 100 μm. Therefore, borings of the worm *Potamilla*, sponge *Cliona* or traces of Cirripedia on the belemnite rostra should not be included here. Microborings are produced by Procaryota (cyanophytes/cyanobacteria) and also by Eucaryota like Chlorophyta, Rhodophyta and Fungi.

Repetition of some characteristic patterns of microborings is evidently produced by the same taxon. The key to their understanding is the study of recent microborings. The fossils are embedded by the resin and then the specimen is dissolved by an acid. Such artificial casts are studied using electron microscope (Golubic et al., 1970). According to our opinion this method should be completed by the study of these microborings in thin sections what will be documented here.

By comparison with recent endoliths it is necessary to take into account that the ancient fossils could contain also several died-out species of microendoliths. Glaub (1994) distinguished 34 ichnotaxa in 500 samples of Jurassic brachiopod and mollusc shells from different European basins. About 70 % of them show similarities with the modern microendoliths and 30 % have no analogy.

The type of tunnel is directed by the instinct mediated through the genus. There are some analogies with the manifold patterns of corridors bored in the tree by beetles or fucoids produced by worms. Seilacher (1967) compared the behaviour of a limnivore animal *Helmintoida labyrinthica* with the computer programme which renders the best possible extraction of nutrients. The programme contains four commands: 1. Move horizontally keeping within the single bed of sediment. 2. After advancing one unit of length make a U-turn. The length of the worm could serve as a measuring rod. 3. Always keep in touch with your own or some other tunnel (chemotaxis). 4. Never come closer to any other tunnel than the given distance „d" (phobotaxix) what prevents uneconomical crossing of tunnels.

2. Application of microborings in the facies studies

Glaub (1999) used microborings for the paleobathymetric reconstruction. From the samples of Jurassic limestones she discerned four zones according to the intensity of light:

1) Shallow euphotic zone II with *Fasciculus acinosus/ F. dactylus* ichnocoenosis. Cyanobacteria/Cyanophyta (Procaryota) prevail there. The borings are perpendicular to the surface of the substratum.

2) Shallow euphotic zone III with the ichnocoenosis *Fasciculus dactylus/Paleoconchocelis starmarchii* corresponding to the well illuminated part of subtidal environment. Besides mentioned microborings of Protista it contains also borings of chlorophyta and rhodophyta (Eucaryota).

3) Deep euphotic zone with *Reticulina elegans* and *Reticulina* sp. 1 with *Paleoconchocelis starmarchii* representing poor illuminated parts of subtidal environment (the intensity of light lowered to 1–10 % of the surface light. It contains eucaryote endoliths, especially of chlorophyta. The borings parallel to the substratum are dominant.

4) Aphotic zone with *Saccomorpha clava/Orthogonum lineare*. The ichnotaxa are similar to the recent chemoheterotrophic endoliths (e.g. fungi).

Olóriz et al. (2004) studied the relations among the microborings abundance of encrustation and the degree of fragmentation of skeletal remains in the Oxfordian limestones (Prebetic Zone of Spain). They discerned only two groups: simple and branching microborings. They found a higher index of microborings (MB_i) on the ammonites and serpulids. Lower occurrence of microborings had ostracodes, microforaminifers, bivalves, gastropods and echinoderms. There was a direct relationship between the index of microborings (MB_i) and the index of encrustation (E_1). No relation to the index of fragmentation was proved. Intervals with higher MB_i and E_1 corresponded to the periods of transgressive systems tract (TST), than to the periods of the growing distality.

3. Microboring morphotypes

In the following text we will try to catalogue well defined types of microborings from the numerous thin sections of limestones mostly in Liassic bivalves.

Morphotypes:

A – almost straight tunnels parallel with the surface of bioclasts (e.g. Pl. IX. Fig. 4).

B – undulating microborings (Pl. I. Fig. 1; Pl. VI. Fig. 4).

C – dichothom branching under the acute angle (Pl. IX, Figs. 1 and 2).

D – rectangular branching (Pl. I. Fig. 3).

E – stellate groups of tunnels (Pl. I. Figs. 3 and 5).

F – zig–zig microborings (Pl. I. Fig. 2)

G – cup-like borings (Pl. III. Figs. 1-3)

H – polygonal net-like borings (Pl. IV. Figs. 1 and 3; Pl. X. Figs. 1-3).

J – very thin borings perpendicular to the surface of the skelet (Pl. II. Fig. 7).

Similar essay concerning the definition of the morphotypes was carried out by Böhm et al., 1999 (p. 204 and Pl. 23, Figs. 3–9). They discerned following three morphotypes:

Morphotype 1 – "spotted" – dark dots circular and elliptical with a diameter about 0.32 mm. They are associated with smaller borings with a diameter of about 0.06–0.08 mm.

Morphotype 2 – straight or meandering unbranched borings with a diameter about 0.03 mm.

Morphotype 3 – covers the branched forms with three subtypes of branching: a) dichothom (Θ 0.03–0.05 mm), b) rectangular (Θ 0.06–0.08mm), c) zig-zag (Θ 0.016–0.025 mm).

These types were, however, poorly illustrated. On the Pl. 23, Figs. 4 and 5 there is a faulty explication "unbranched, elongated", meanwhile the microborings are clearly branched.

4. Bivalves

Perhaps, the most frequent microendoliths occur in the bivalvian fragments. Bivalves construct their shells from the calcite or aragonite. During the diagenesis aragonite shells are dissolved and replaced by fine-grained secondary calcite. Traces of microendoliths may be preserved in them. Aragonite shells are rarely replaced by calcite mosaic recrystallized "in situ". Up till now we did not succeed to find relicts of microendoliths in them.

The most frequent type of microborings is **undulated and simultaneously branched** (Pl. I. Fig. 1). Extreme types are **zig-zag tunnels** (Pl. I. Fig. 2). Interesting types are **rectangular branching** (Pl. I. Figs. 3-4) and **stellate aggregates** (Pl. I. Figs. 3 and 5). Very dense concentration of microendoliths is typical for bioclast accumulations exposed on the bottom for a long time (condensed sedimentation, Pl. I. Fig. 6). Another type represents thicker tunnels with the **club-like branching** (Pl. II. Fig. 1) corresponding to siphonate green algae. **Barrel-like borings** (Pl. II. Fig. 2) with a characteristic articulation correspond to the microendolith *Fasciculus dactylus* Radtke 1991. They were produced by cyanophyta in the euphotic zone (Glaub, 1998). Traces of borings in the thick shells of rudists (Pl. II. Fig. 3) were evidently produced by metazoans and will be not included in our study.

Bivalves with original aragonitic shell were filled after their dissolution by fine-grained pseudosparite. Microborings may be preserved in them like ghosts (Pl. II. Fig. 5-6). Remnants of tunnels are sometimes bordered by Fe-oxides (Pl. II. Fig. 4).

Fragments of bivalves, perforated perpendicularly to the surface of the shell by very tiny straight fungal microborings (Pl. II. Fig. 7) were rarely found.

5. Foraminifers

Lenticulina. Characteristic microendoliths resembling the tiny "cups" densely ranged were found on the numerous specimens of *Lenticulina* (Pl. III. Figs. 1-4). They begin from the outside by a narrow neck and end by a cup with elliptical to circular cross section. They can be identified with *Cavernula zancobola* Schmidt 1992. Glaub (1994, p. 73, Tab. I. Fig. 3) described them as globular spheroids with a diameter 10 μm. The contact with surface forms a thin corridor (only 1–3 μm) perpendicular to the surface. Glaub (l. c.) cited this taxon from the brachiopod shells of the Kimmeridgian and Tithonian age. One of our specimens (Pl. III. Fig. 4) displays even triangular cross-sections. Maybe it represents another species of that genus. Some thicker borings with irregu-

M. Mišík et al.: Microbial boring activity in the Jurassic...

125

larly changing diameter were associated with them (Pl. III. Fig. 2).

Large foraminifera. Rotalids often display the characteristic **net-like microendoliths** (Pl. IV. Fig. 1). A case of tiny corridors forming a tight spiral occurred (Pl. IV. Fig. 2). Thicker corridors with irregularly branched patterns were found in nummulites and discocyclinas (Pl. IV. Figs. 3–5).

6. Crinoids

The crinoidal ossicles from the red crinoidal limestones frequently contain thicker, slightly undulated tunnels (Pl. V. Figs. 1-2). Their oscillating thickness is due to the undulations in the plane different from that of the thin section.

A rare stellate form with club-shaped ends of the "rays" is reproduced in the Pl. V. Fig. 3. Perkins and Halsey (1971, Fig. 11) described a similar endolith as a stellate growing form of green algae. Our Pl. V. Fig. 4 shows a tunnel penetrating already in the syntaxial rim formed during the diagenesis (see the twinning lamellae continuing from the crinoidal plate into the rim). The echinoderm plate on the Pl. VI. Fig. 2 contains various thin, mutually crossing microborings. In the sample Pl. VI. Fig. 1 they form an imperfect network. Peculiar traces bitten into periphery of pentagonal columnalium are visible on the Pl. VI. Fig. 3. It contains also some smaller circular microborings.

The cherts in crinoidal limestones contain abundant ghosts of microborings in the entirely silicified plates. They are filled by Fe-oxides (Pl. V. Figs. 4 and 5). The illustrated cases proceeded from the allodapic intercalations (calciturbidites) in the Berriasian–Valanginian pelagic limestones. The tunnels are thin and undulated. The boring activity took place in the shallow zone before the transport of the biodetritus into the deep water.

7. Algae

Corallinaceae – were studied from the thin sections of Paleocene and Miocene limestones. They contain larger holes, sometimes in peculiar groups filled by sparite, probably bored by metazoans (Pl. VII. Figs. 1-6). Their ends are sometimes thinned (Pl. VII. Figs. 5 and 6). Larger, elongated and elliptical holes are filled partly by micrite (Pl. VIII. Fig. 1). Circular traces with dark borders (Pl. VIII. Fig. 2) and thin straight microborings with haphazard orientation are rare (Pl. VIII. Fig. 3). In a tunnel, five sickle-like partition was found (Pl. VIII. Fig.4); it reflects probably the progressing of the boring. The specimen illustrated in the Pl. VIII. Fig. 5 proves that the boring activity continued in the diagenetic stage (the microboring penetrated from the lithified sediment into the algae).

Ethelia alba is another alga frequently attacked by boring organisms. Dichothomically branched fan-like tunnels with faint articulation reflecting the stages of progress were present at two localities (Pl. IX. Figs. 1 and 2). Interesting phenomenon is a group of microendoliths which are subparallel in spite of considerable mutual distances (Pl. IX. Fig. 3). The Pl. IX. Fig. 4 displays a long, slightly undulated tunnel passing through the centre of the thallus (Pl. IX. Fig. 4). The course of the tunnel is not accommodated to the course of algal fibres.

8. Some examples of microborings in bryozoans, belemnites and ammonites

The sample of a bryozoan contains tunnels of various diameter perpendicular to the bioclast surface (Pl. X. Fig. 5). The belemnite rostrum (Pl. X. Fig. 6) is penetrated by small circular holes, a part of them belongs to the microborings parallel with the surface rostrum.

The aragonite shell of ammonite succumbed to the rare spot-like dissolution in several stages (Pl. XI. Figs. 1 and 2). The openings formed by the dissolution were filled by sparite and then, already in diagenetic stage, bored by tiny tunnels (Pl. XI. Fig. 1).

9. Peculiar types of microborings in the bioclasts of an unknown appurtenance

The borings of the genus *Dictyoporus* Mägdefrau in the *Orbitolina*-bearing Cenomanian limestones (an exotic pebble) resemble a net with pentagonal openings (Pl. X. Figs. 1-3).

Tiny tunnels forming a net with "knots" occurred in a silicified distal turbidite (Pl. X. Fig. 4) amidst the radiolarites, they were transported into the deep-water sediment.

10. Comparison with the terrestric microborings

Rocky surface covered by lichens is usually penetrated by straight, very thin tunnels of cyanophyta (Pl. XI. Fig. 3). Sometimes they occur in thin sections of limestones as artefacts from the contamination, if the sample was collected with negligence. If such microborings are limited to one clast only, the redeposition of a terrestric fragment in the marine environment may be admitted (Pl. XI. Fig. 4).

11. Some aspects connected with microborings

Microboring activity continues sometimes still in the diagenetic stage. They occur also in bioclasts which were evidently not loose but occurred already in the solidified sediment. On the Pl. VIII. Fig. 5 it can be seen that the microboring organism penetrated in the coralline alga from the solidified sediment. Microborings from the advanced diagenetic stage in the voids filled by sparite in the dissolved aragonite shell of ammonite were already mentioned (Pl. XI. Figs. 1-2). Peculiar microborings in the sparitic cement can be seen on the Pl. X. Fig. 7.

Microendoliths are preserved and expressed in chert nodules due to their filling by Fe-oxides even in the case that their silicified bioclasts totally disappeared from thin section (Pl. I. Fig. 3; Pl. VI. Fig. 5).

Redeposition of the microborings to the deep-water environment. Microendoliths originated in the shallow marine water were sometimes transported to the deep

126

Slovak Geol. Mag., 12, 2 (2006), 123 – 137

water and occur within the turbidite intercalations (Pl. VI. Figs. 4-6). Typical case of distal turbidite with bored bioclasts amidst the radiolarites was already mentioned (Pl. X. Fig. 4).

The possibility of redeposition of clasts with terrestric microborings into shallow marine environment is supposed in Fig. XI. Fig. 4.

The abundance of the borings is proportional to the length of time during which the bioclasts were exposed on the sea bottom. Their accumulation is interpreted in terms of sequence stratigraphy as a period of deepening (rising of the sea-level) and the interruption of the transport from the shore (Óloriz et al., 2004). The extreme density of microborings is in the hardgrounds from the periods of growing distality.

12. Conclusion

Cyanophyta/cyanobacteria, algae and fungi produced microborings in bioclasts (shells) for shelter and nutrients (aminoacids). The microborings are distinguished by somewhat different patterns dictated by the genetic inheritance. Some selected examples of microborings from bivalves, crinoids, foraminifers and algae are illustrated. Preliminary nine morphotypes except for algae were discerned. Two species: *Fasciculus dentatus* Radtke (in bivalve) and *Cavernula zancobola* Schmidt (in *Lenticulina*) were identified.

Acknowledgement

References

Böhm, F., Ebli, O., Krystyn, L., Lobitzer, H., Rakús, M. & Siblík, M., 1999: Fauna, stratigraphy and depositional environment of the Hettangian – Sinemurian (Early Jurassic) of Adnet (Salzburg, Austria). Abhandlungen Geol. Bundesantalt, Bd. 56, 2., 143–271.

Glaub, I., 1994: Mikroborspuren in ausgewählten Ablagerungsbereichen des europäischen Jura und Unterkreide (Klassifikation und Palökologie). Courier Forschungsinstitut Senckenberg 174, 1–324.

Glaub, I. 1999: Paleobathymetric reconstructions and fossil microborings. Bull. Geol. Soc. Denmark, 45, 143–146.

Golubic, S., Brent, G. & Le Campion, T., 1970: Scanning electron microscopy of endolithic algae and fungi using a multipurpose casting embedding technique. Lethaia, 3., 203–209.

Olóriz, F., Reolid, M. & Rodríguez-Tovar, F. J., 2004: Microboring and taphonomy in Middle Oxfordian to Lowermost Kimmeridgian (Upper Jurassic) from the Prebetic Zone (southern Iberia). Paleogeography, Palaeoclimatology, Palaeoecology , 212, 181-197.

Perkins, R. D. & Halsey, S. D., 1971: Geologic significance of microboring Fungi and Algae in Carolina shelf sediments. Journ. Sedim. Petrography vol. 41, No. 3, 843–853.

Radtke, G., Hofman, K. & Golubic S., 1997: A bibliographic overview of micro- and macroscopic bioerosion. Courier Forschungsinstitut Senckenberg 201, 307–340.

Seilacher, A., 1967: Fossil behavior. Scientific American 217, 2, 72–80.

M. Mišík et al.: Microbial boring activity in the Jurassic...

127
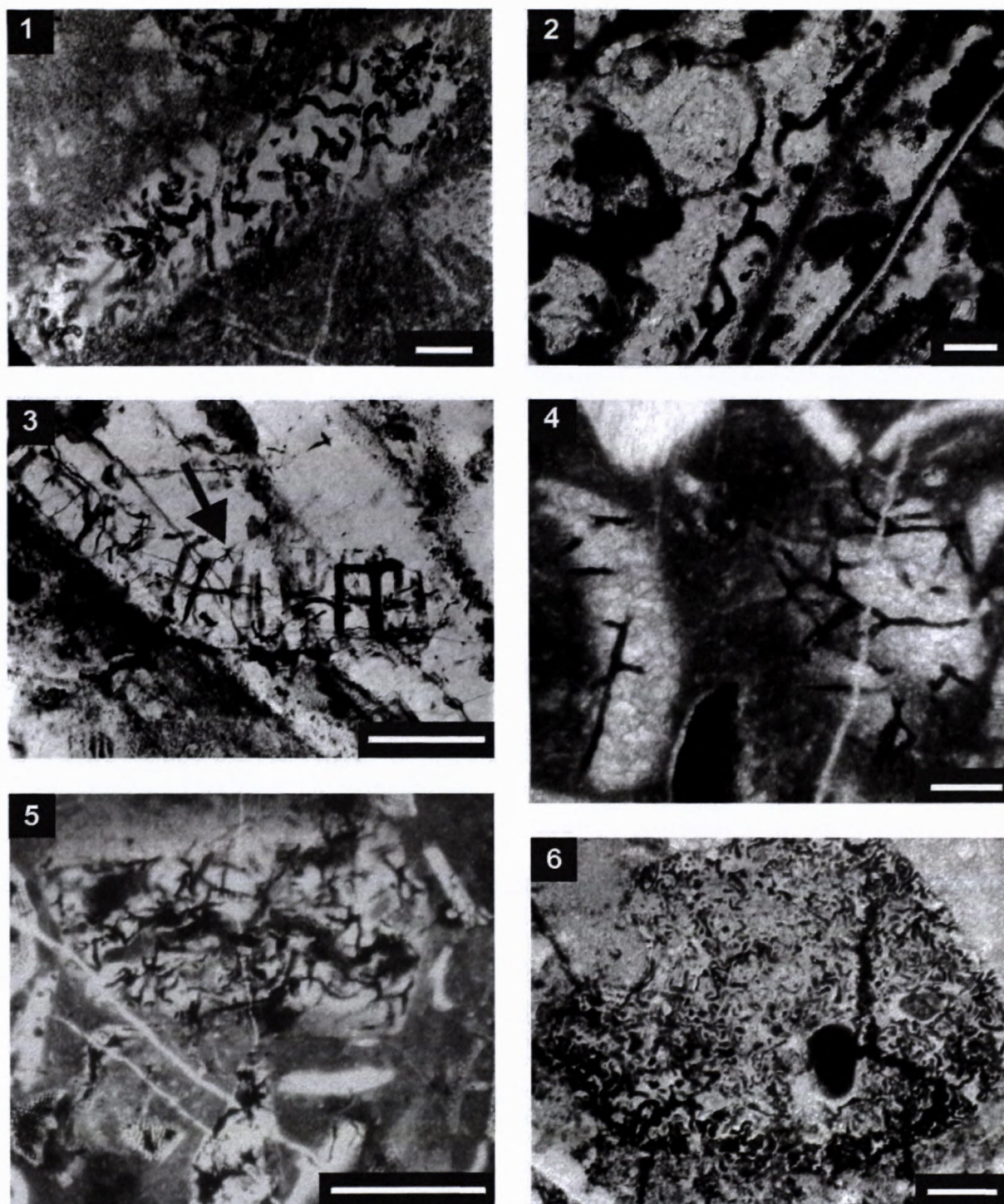
Plate I.

Fig. 1. Undulated and branched microendoliths in bivalve, filled by Fe-hydroxides. Liassic limestone with *Involutina liassica*. Krížna nappe, Donovaly, Veľká Fatra Mts. Scale bar = 20 μm.

Fig. 2. Microboring of "zig-zag" type in bivalvian clasts; tunnels filled by Fe-hydroxides. Callovian limestone, Czorsztyn succession of the Pieniny Klippen belt, Mikušovce. Scale bar = 100 μm.

Fig. 3. Two types of microborings in the silicified bivalvian shell: thicker rectangular and thin stellate tunnels (arrow). Red chert in red crinoidal limestones of Liassic age, Choč nappe, between Pružina and Predhorie, Strážovské vrchy Mts. Scale bar = 100 μm.

Fig. 4. Rectangular branching of microborings. Red Toarcian limestone, Solisko near Donovaly, Nízke Tatry Mts. Scale bar = 20 μm.

Fig. 5. Stellate arrangement of microendoliths in the bivalve shell of the Fe-hardground. The same locality as in Fig. 4. Scale bar = 100 μm.

Fig. 6. Microendoliths in a bioclast from the Fe-Mn hardground. Toarcian, Choč nappe, quarry near Bzince, Čachtické Karpaty Mts. Scale bar = 20 μm.

Slovak Geol. Mag., 12, 2 (2006), 123 – 137

128
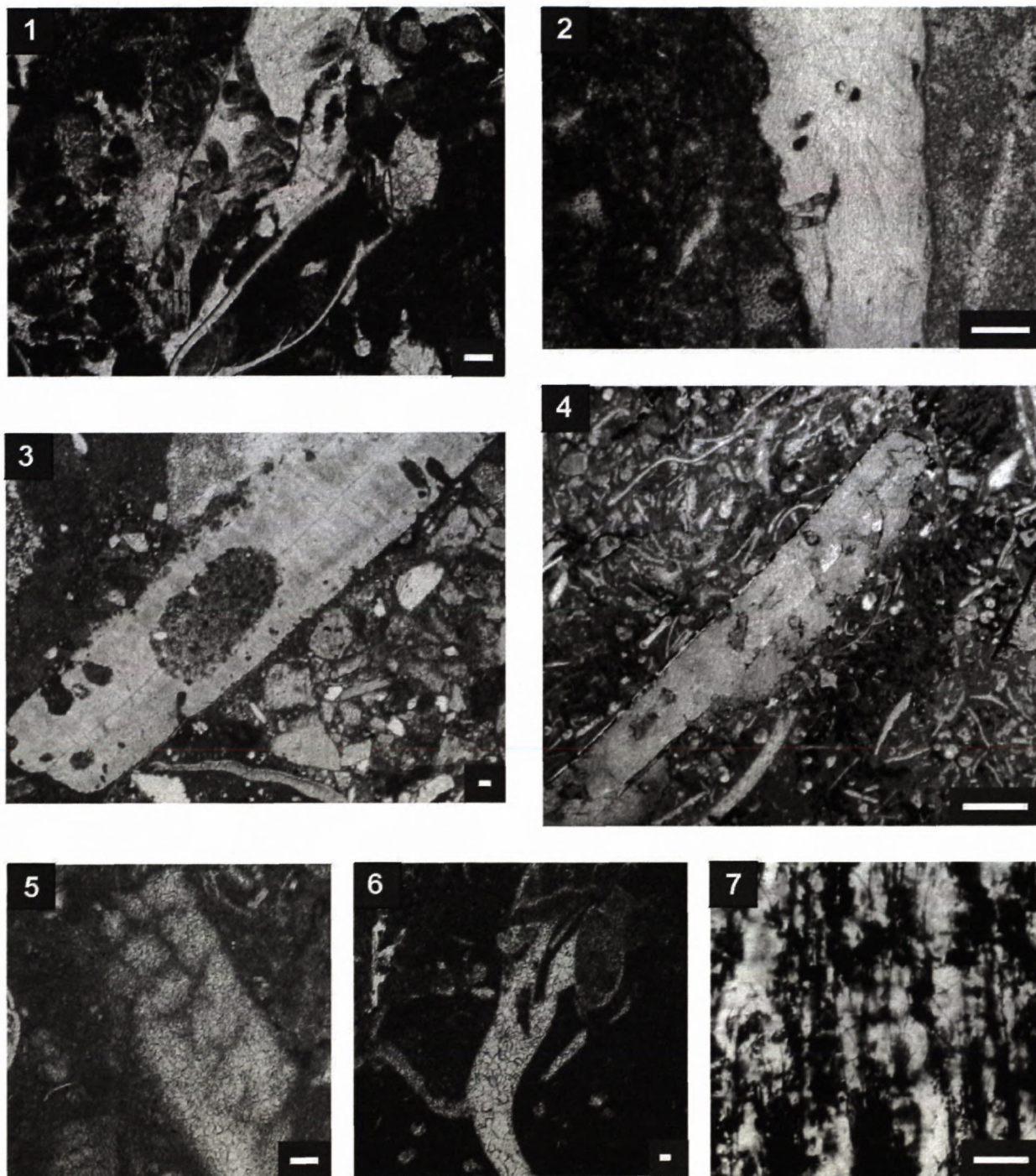
Plate II.

Fig. 1. Club-shape branched microendoliths from siphonate green algae in a bivalve. Upper Lotharingian limestone, Choč nappe, Chtelnica, Čachtické Karpaty Mts. Scale bar = 100 μm.

Fig. 2. "Barrel-like" microboring of *Fasciculus dactylus* in a bivalve. According to Glaub (1998) it is a sign of shallow euphotic zone III. Toarcian limestone, Krížna nappe, Horná Turecká, Veľká Fatra Mts. Scale bar = 20 μm.

Fig. 3. Two types of microborings in a bivalvian shell. Senonian limestone, Zemianska Dedina, Orava. Scale bar = 100 μm.

Fig. 4. Corroded aragonite bivalve with Mn-Fe coating have been filled after dissolution by fine-grained sparite. Borings after perforating organisms have been preserved to their early filling by calcite mud. Upper Kimmeridgian – Lower Tithonian of the Czorsztyn Unit. Kyjov – Pusté Pole. Scale bar = 100 μm.

Fig. 5. Bivalve shell originally composed of aragonite was filled by fine-grained calcite aggregate. Corridors of the boring organism preserved as ghosts. Kambühel limestone, Paleocene, settlement Rovná, Brezovské Karpaty Mts. Scale bar = 100 μm.

Fig. 6. Originally aragonite shell filled by fine-grained calcite aggregate contains relicts after the boring organisms. Upper Berriasian limestone, Czorsztyn Unit, Ďurčova valley near Stará Turá, Čachtické Karpaty Mts. Scale bar = 100 μm.

Fig. 7. Tiny tunnels bored by fungi in a bivalve shell. Mn-hardground. Lower Tithonian limestone, Czorsztyn Unit, klippe of Vršatec castle. Scale bar = 20 μm.

M. Mišík et al.: Microbial boring activity in the Jurassic...

129
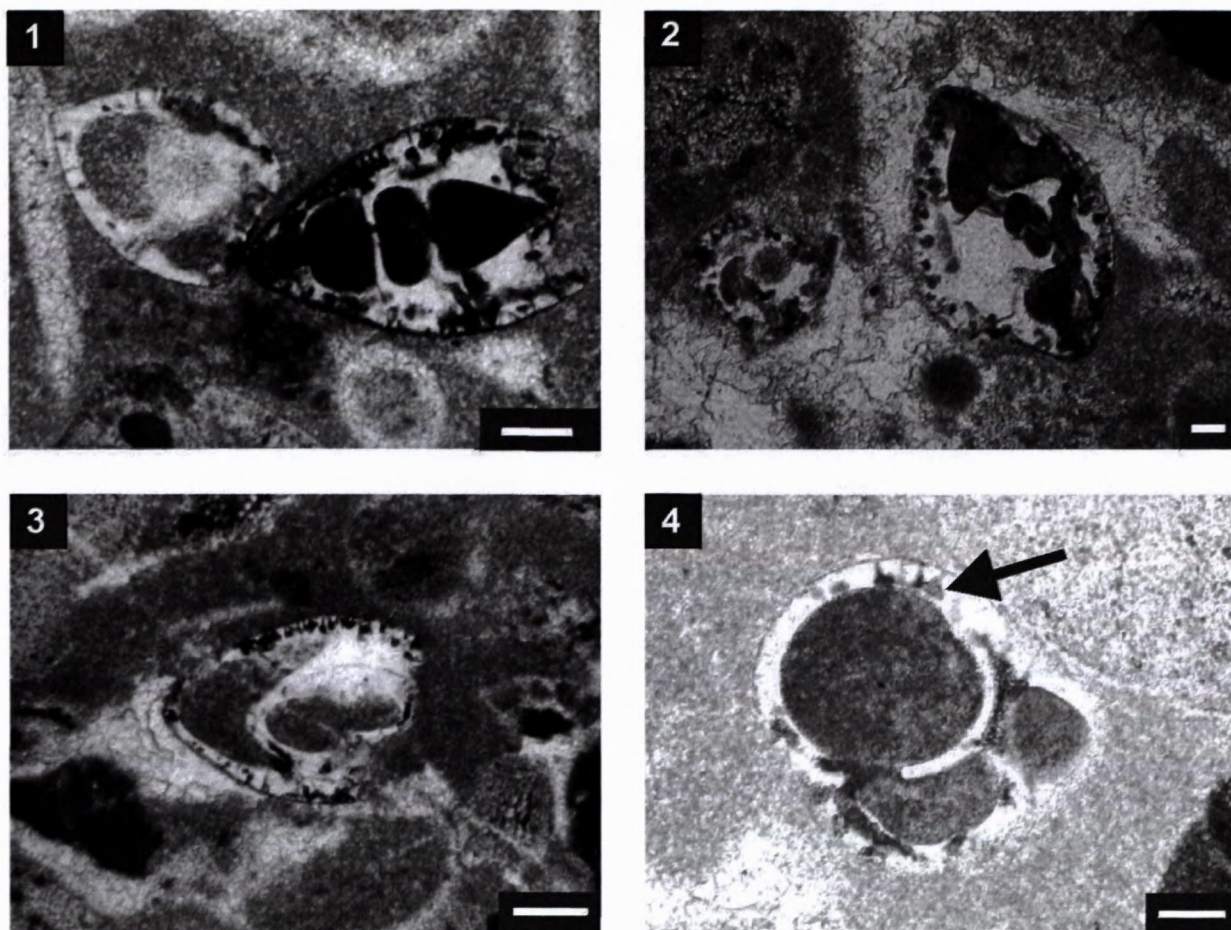
Plate III.

Figs. 1 and 2. Spheroidal microborings in the test of *Lenticulina* conformable to *Cavernula zancobola* Schmidt, 1922. Neocomian limestone, Czorsztyn Succession, quarry Dolný Mlyn near Lubina, Čachtické Karpaty Mts. Scale bar = 20 μm.

Fig. 3. Tiny sections of *Cavernula zancobola* with thick club-like borings probably from siphonate green algae. Neocomian limestone, Czorsztyn Succession, quarry Dolný Mlyn near Lubina, Čachtické Karpaty Mts. Scale bar = 100 μm.

Fig. 4. Microborings of *Cavernula* type; probably new species with triangular section. Locality as in the figs. mentioned above. Scale bar = 100 μm.

Slovak Geol. Mag., 12, 2 (2006), 123 – 137

130
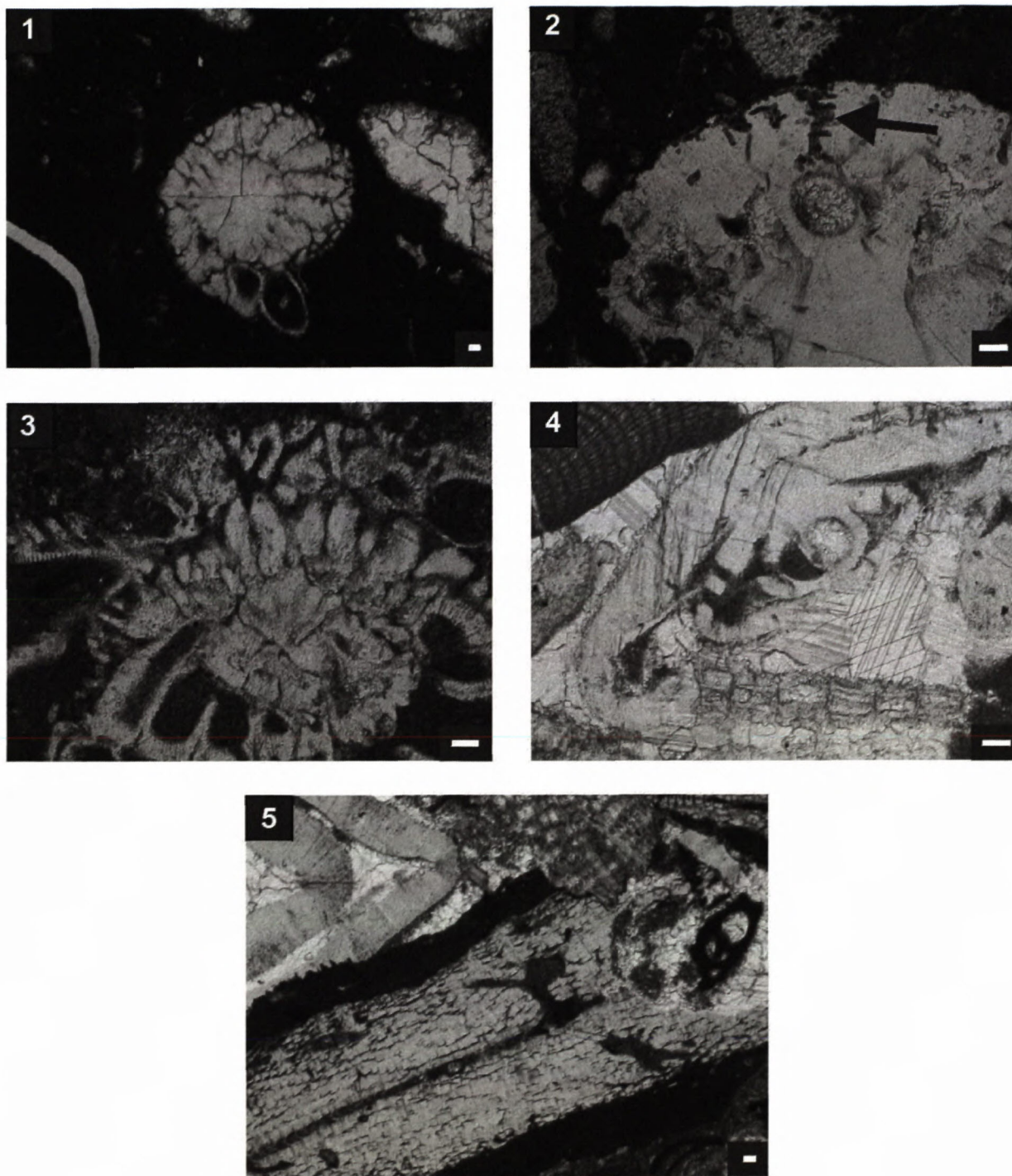
Plate IV.

Fig. 1. Net like microendoliths in *Rotalia*. Kambühel limestone, Paleocene, Ladziny, Brezovské Karpaty Mts.
Fig. 2. Tiny spiral microborings in a larger foraminifera. The same locality as in Fig. 1.
Fig. 3. Group of corridors in the test of *Rotalia*, Kambühel limestone, Paleocene, Rúbanice near Ovčiarske, Middle Váh valley.
Fig. 4. Microborings partly rectangular in the *Nummulites* test. Paleogene limestone, Ježov hill, Oravice.
Fig. 5. Microborings in the test of *Discocyclina*. Paleogene limestone. Bratancov stream near Žilina.
Scale bars = 100 µm.
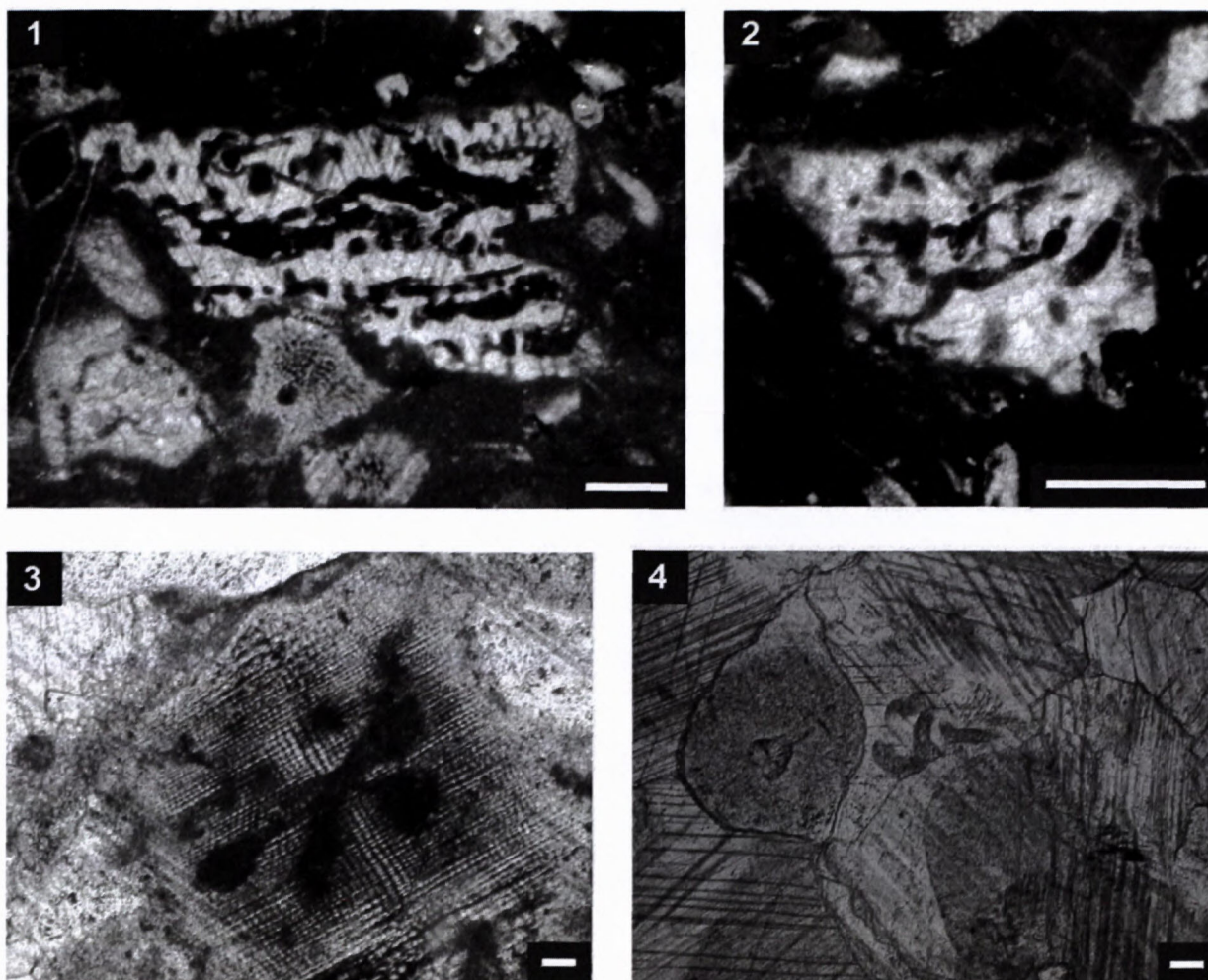
Plate V.

Figs. 1 and 2. Microendoliths in the crinoidal plate filled by Fe-oxides. Toarcian limestone, Krížna nappe, Solisko near Donovaly, Nízke Tatry Mts. Scale bar = 20 µm.

Fig. 3. Stellate boring from the siphonate green alga in a crinoidal plate. Middle Jurassic limestone, Czorsztyn Succession, quarry Krasin near Dolná Súča. Scale bar = 100 µm.

Fig. 4. Microendoliths in the crinoidal limestone. The boring continued in the diagenetic stage; the tunnels penetrated also in the syntaxial rim of the plate. Middle Jurassic limestone. Vysoké Tatry Succession, Javorová valley, Vysoké Tatry Mts. Scale bar = 100 µm.

132

Slovak Geol. Mag., 12, 2 (2006), 123 – 137
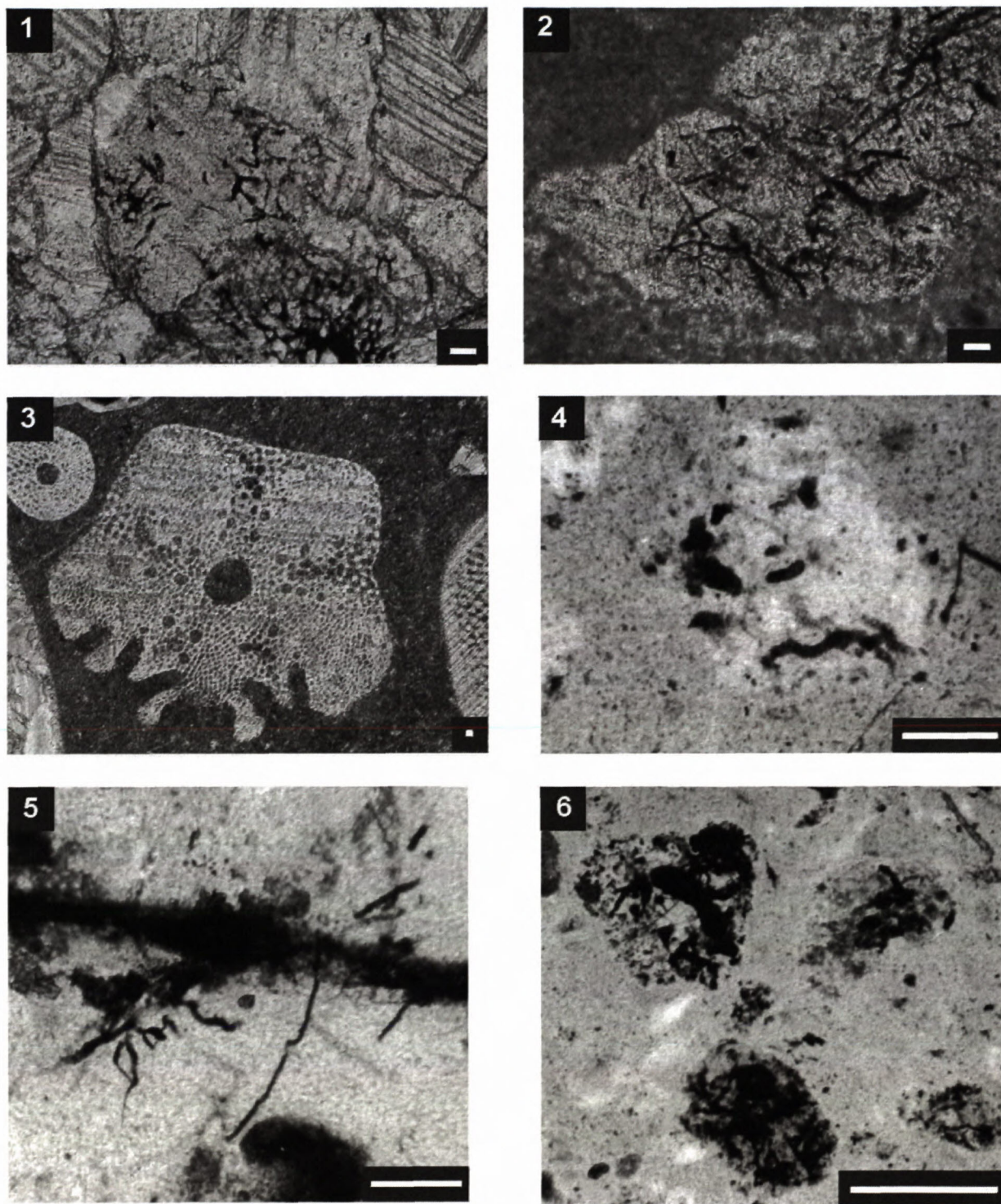
Plate VI.

Fig. 1. Reticular aggregate of microborings in the crinoidal ossicle. Crinoidal limestone, Middle Jurassic, Choč nappe. Quarry Kolíňany, Tríbeč Mts. Scale bar = 100 μm.

Fig. 2. Partly stellate microborings in the crinoidal ossicle. Bathonian limestone, Kostelec Succession of the Pieniny Klippen Belt, Kostelec by Považská Bystrica. Scale bar = 100 μm.

Fig. 3. Two types of microendoliths in a pentagonal columnalium. Liassic limestone, Krížna nappe, Donovaly, Veľká Fatra Mts. Scale bar = 100 μm.

Fig. 4. Undulated tunnels probably in an echinoderm ossicle within the chert. Berriasian limestone of Kysuca (Horná Lysá) Succession, Vršatec, Horná Lysá. Scale bar = 20 μm.

Fig. 5. Undulated corridor in the chert nodule. Turbiditic intercalation in the Berriasian limestone. Vršatec, Horná Lysá. Scale bar = 20 μm.

Fig. 6. Microborings in the crinoidal ossicle and lithoclasts in a chert nodule. Vršatec, the same locality as Figs. 4 and 5. Scale bar = 100 μm.

M. Mišík et al.: Microbial boring activity in the Jurassic...

133
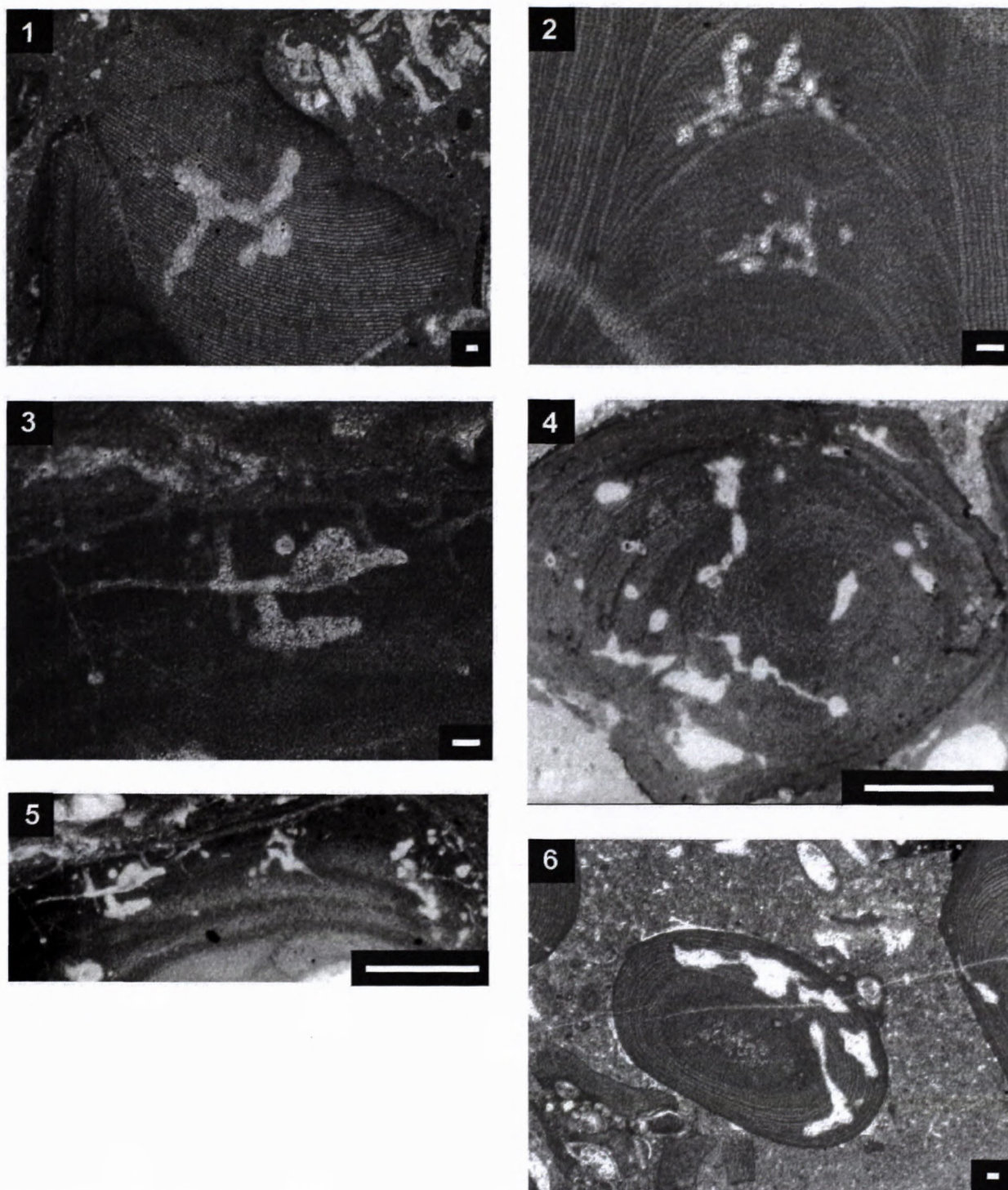
Plate VII.

Fig. 1. Club-shape branched microborings in a coralline alga. Badenian limestone, Rohožník, the margin of Vienna Basin.

Fig. 2. Aggregate of tunnels in the coralline alga. Kambühel limestone, Paleocene. Svätá Helena near Považská Bystrica.

Fig. 3. Boring organism in the coralline alga. Badenian limestone, Strelnica near Štúrovo.

Fig. 4. Borings in a coralline alga. Badenian biohermal limestone, Rohožník, the margin of Vienna Basin.

Fig. 5. Traces of boring organisms with fastigate endings in a coralline alga. Badenian limestone, Strelnica near Štúrovo, Danube Basin.

Fig. 6. Borings in the coralline alga. Kambühel limestone, Paleocene. Makovec near Považská Bystrica.

Scale bars = 100 μm.

Slovak Geol. Mag., 12, 2 (2006), 123 – 137

134
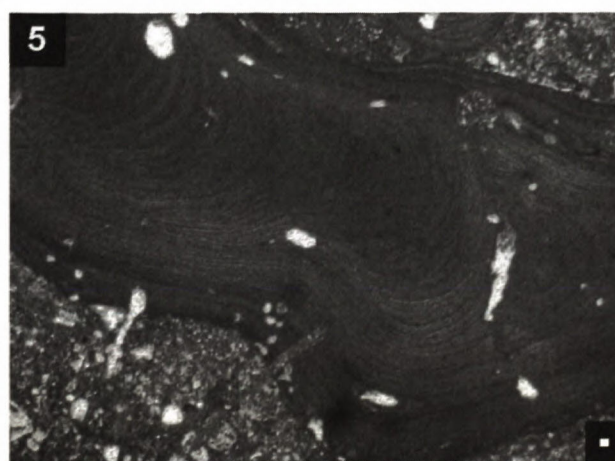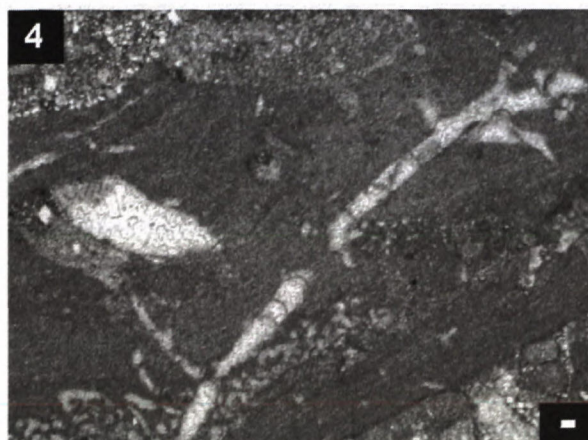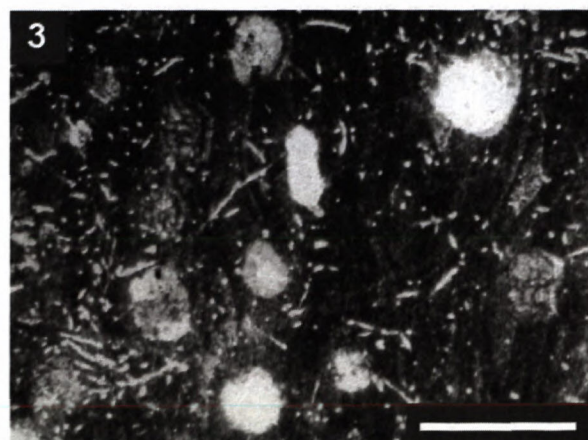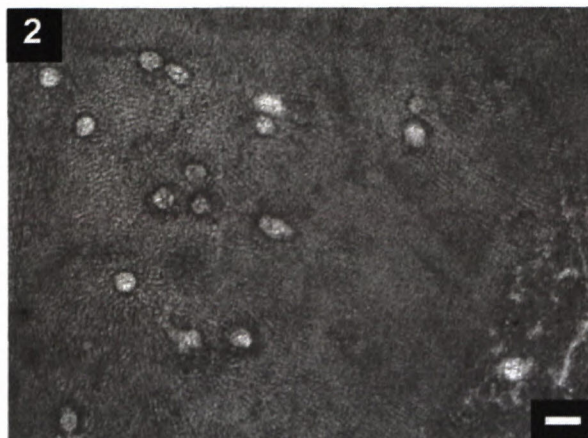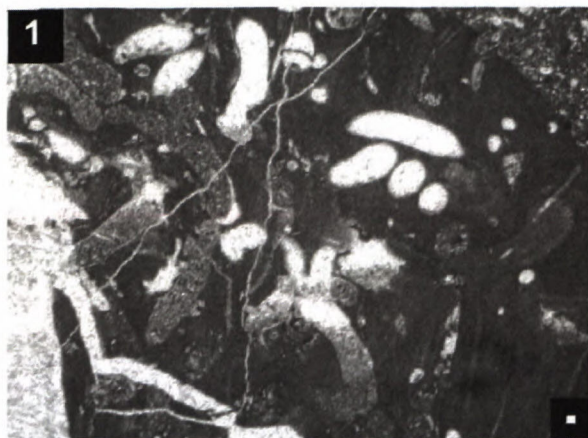
Plate VIII.

Fig. 1. Thicker corridors partly filled by micrite in a coralline alga. Kambühel limestone, Paleocene, Makovec near Považská Bystrica.

Fig. 2. Circular borings in the coralline alga. Kambühel limestone, Paleocene. Cinkov hill, Brezovské Karpaty Mts.

Fig. 3. Two types of borings in a coralline alga. Badenian limestone. Modrý Majer near Štúrovo, Danube Basin.

Fig. 4. Corridor with the sickle-like partitions in the coralline algae. Paleogene limestone. Ground elevation 316, Brezovské Karpaty Mts.

Fig. 5. Perforation from the lithified surrounding mass into the coralline alga. Kambühel limestone, Paleocene. Makovec near Považská Bystrica.

Scale bars = 100 µm.

M. Mišík et al.: Microbial boring activity in the Jurassic...

135
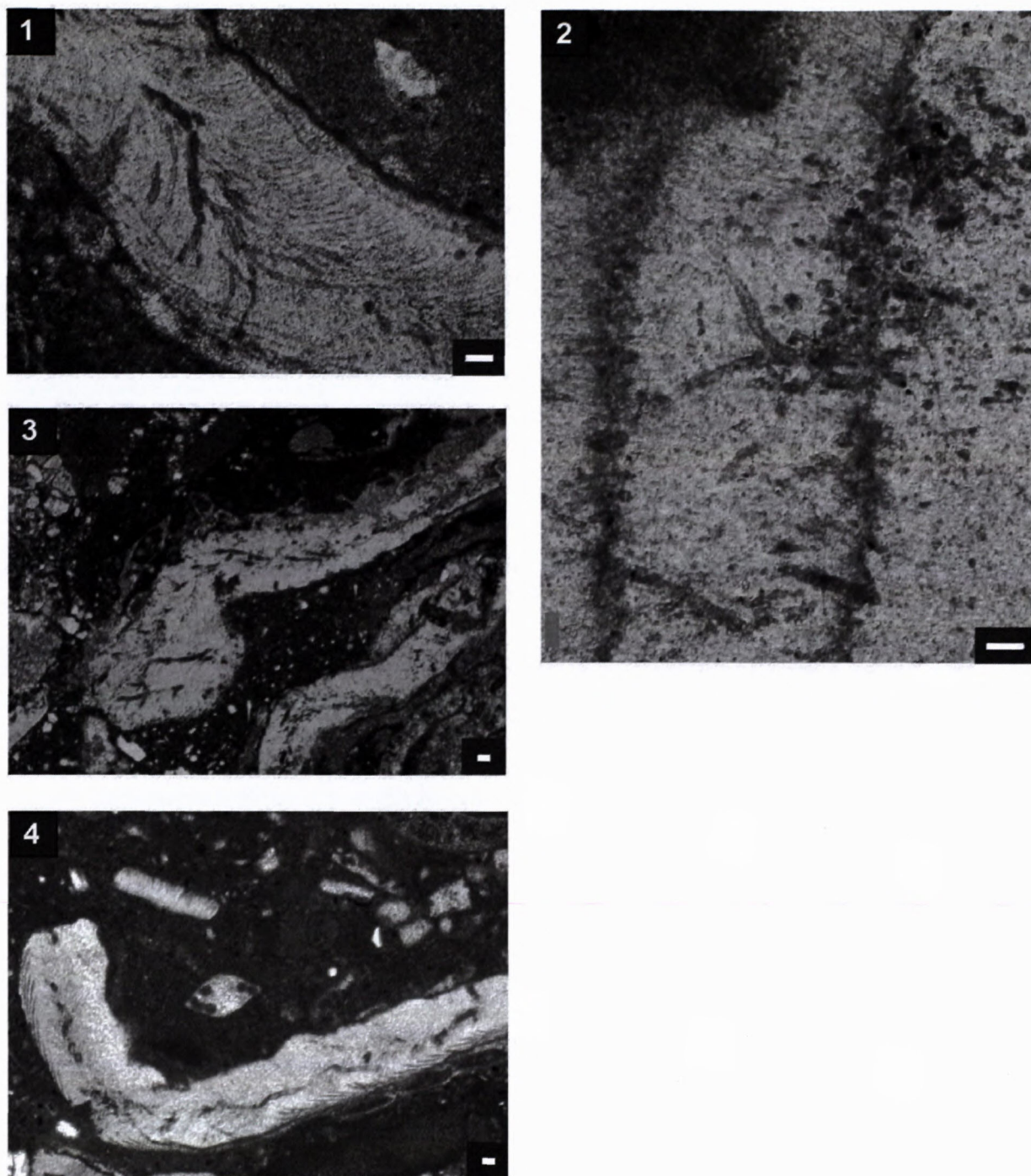
Plate IX.

Fig. 1. Corridors with dichothom fan-like branching with internal articulation in the alga *Ethelia alba.* Paleocene limestone. Saddle over the village Zázrivá.

Fig. 2. Dichothom branching in the alga *Ethelia alba.* Paleocene limestone. Settlement U Černých, Brezovské Karpaty Mts.

Fig. 3. Subparallel microborings in *Ethelia alba.* Santonian limestone. Zemianska Dedina, Orava.

Fig. 4. Long tunnel bored in the axis of the thallus *Ethelia alba.* Paleocene limestone. Brezová pod Bradlom.

Scale bars = 100 μm.

Slovak Geol. Mag., 12, 2 (2006), 123 – 137

136
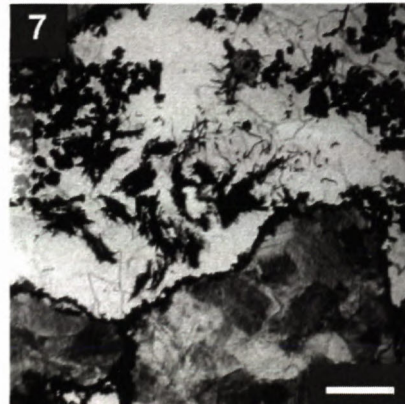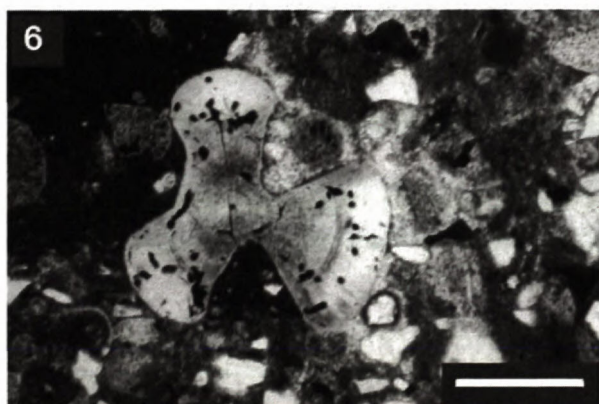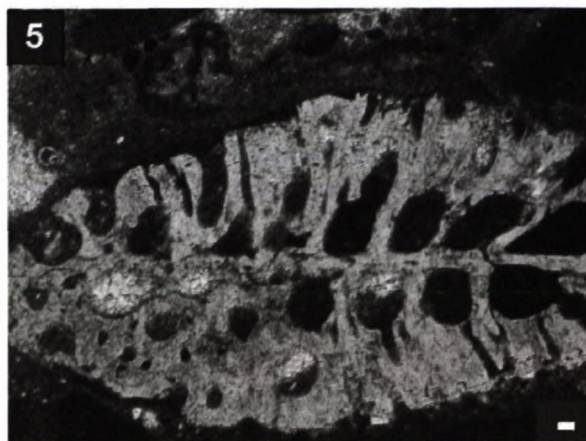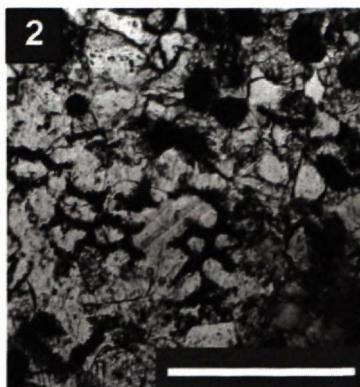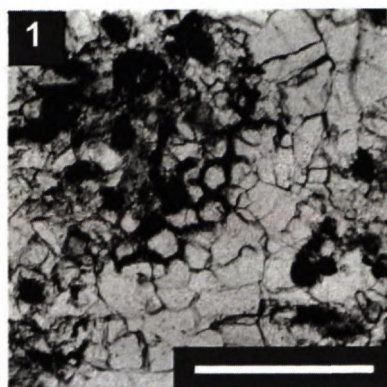
Plate X

Figs. 1.–3. Microboring forming a net with pentagonal loops, probably *Dictyoporus* Mägdefrau in a bioclast of uncertain appurtenance. Sandy *Orbitolina* – bearing Cenomanian limestone. Pebble from the Proč conglomerate with exotic rocks. Proč, Eastern Slovakia.

Fig. 4. Tiny net-like microborings in a bioclast of uncertain appurtenance. Distal turbidite in the Oxfordian radiolarites, Pieniny Succession of the Klippen Belt. Trstená bowling-alley.

Fig. 5. Two types of tunnels bored in bryozoan. Paleocene limestone, Bradový stream, Brezovské Karpaty Mts.

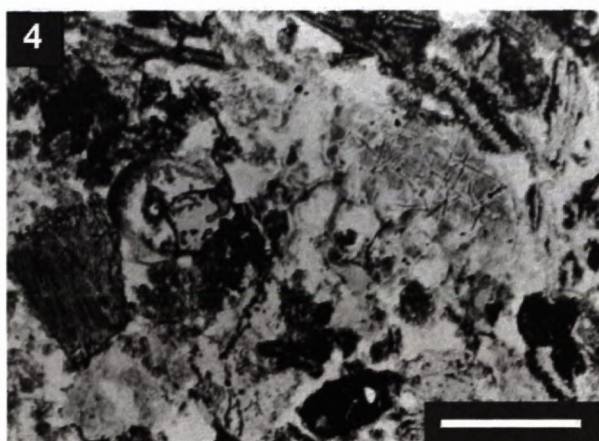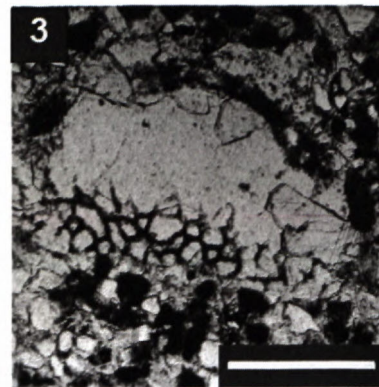Fig. 6. Borings in the belemnite rostrum. Callovian–Oxfordian limestone, Czorsztyn Succession quarry Krasin near Dolná Súča.

Fig. 7. Tiny tunnels of boring algae in the newly-formed calcite cement within Mn-hardground (dark aggregates). Jurassic limestone, Choč nappe. Quarry between Belušské Slatiny and Mojtín, Strážovské vrchy Mts.

Scale bars = 100 μm.

M. Mišík et al.: Microbial boring activity in the Jurassic...

137
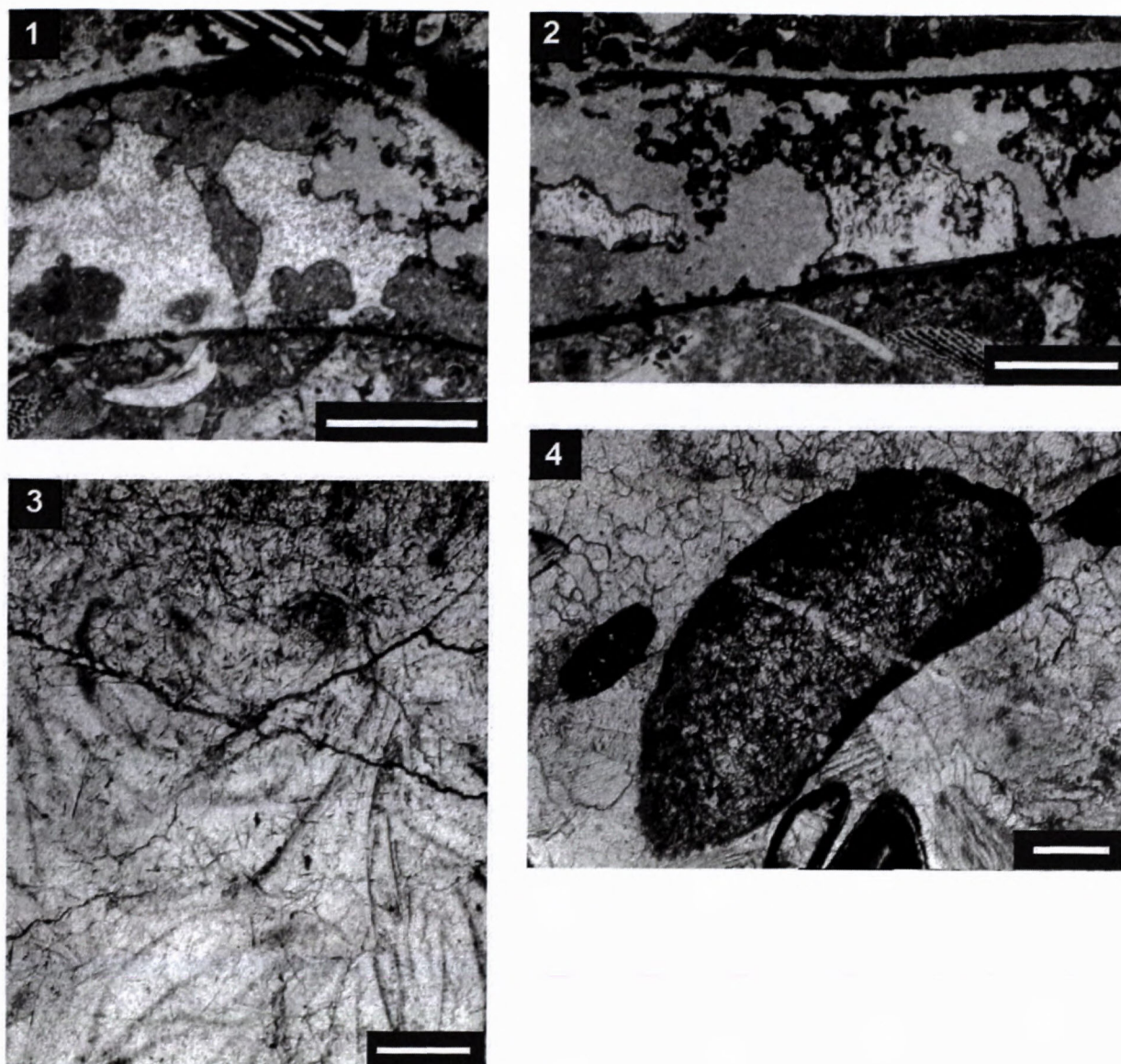
Plate XI

Figs. 1. and 2. Spot-like dissolution of the aragonite shell of an ammonite. The dissolution proceeded selectively according to the accretionary zones of the shell. The voids were formed and filled in three stages. The oldest voids were filled by sparite (clear). Further spaces were filled by dark micrite and the youngest voids of dissolution by clear micrite. In the sparitic voids abundant tiny microborings from the fungi are visible. It is an evidence that the boring activity continued until the diagenetic stage. The shell margins are impregnated by Fe–hydroxides. Upper Lotharingian limestone, Choč nappe. Holý hill near Chtelnica, Čachtické Karpaty Mts. Scale bar = 100 μm.

Fig. 3. Microborings in the terrestric conditions. The surface of Wetterstein limestone covered by lichens. Tiny tunnels belong to the boring fungi. Scale bar = 100 μm.

Fig. 4. Bioclast with a dense cluster of straight tunnels, perhaps redeposited from the continental environment. Lower Liassic biosparitic limestone, Manín Succession. Trenčianske Teplice. Scale bar = 20 μm.

The Fehér hegy Formation: Felsitic ignimbrites and tuffs at Ipolytarnóc (Hungary), their age and position in Lower Miocene of Northern Hungary and Southern Slovakia

[1]Dionýz Vass, [2]IgorTúnyi and [3]Emő Márton

[1]Matičná 5, 831 03 Bratislava, Slovakia; dionyz.vass@ zoznam.sk
[2]Geophysical Institute SAS, Dúbravská cesta 9, 845 28 Bratislava, Slovakia; geoftuny@savba.sk
[3]Etvös Lórand Geophysical Institute, Colombus Str. 17-23, 1145 Budapest, Hungary; paleo@elgi.hu

Abstract. The paleomagnetic study shows that the Gyulakészi Formation of felsitic volcanic rocks and those rocks in Bukovinka Formation have different paleomagnetic properties compared to the ignimbrites and tuff in the vicinity of Ipolytarnóc. They differ in magnetic polarity and size of rotation, and thus must be of different age. The new volcanic formation the Fehér hegy Formation includes the felsic volcanic rocks in the vicinity of Ipolytarnóc village.

Introduction

In the Lower Miocene of the Southern Slovakia and Northern Hungary the felsitic ignimbrites and tuffs (volcanic rocks of rhyolite/rhyodacite composition) occur. On the territory of Southern Slovakia such rocks outcrop in the frame of the Bukovinka terrestrial Formation together with gravel/conglomerate, sand/sandstone and mottled clay. In the Northern Hungary felsitic volcanic rocks have been described in terms of an independent formation the Gyulakeszi Formation. Terrestrial deposits as gravel/conglomerate, sand/sandstone and mottled clay are included into the Zagyvapálfalva Formation. The ignimbrites and tuffs at Ipolytarnóc building up the Fehér hegy hill have been considered as a part of Gyulakeszi Formation. It was evident that the Bukovinka Formation is an equivalent to both Zagyvapálfalva and Gyulakeszi formations. Both, the Bukovinka Formation and the Zagyvapálfalva Formation in Hungary are considered to be Upper Eggenburgian in age. The Gyulakeszi Formation is considered to be Lower Ottnangian in age (Vass in Vass ed., 1983; Hámor, 1974, fide Bartkó, 1985).

Results of paleomagnetic study of the ignimbrites and tuffs occurring nearby Ipolytarnóc (Fehér hegy) studied in detail, pointed out that those rocks had completely different paleomagnetic properties, and do not belong to Gyulakeszi and Bukovinka formations (Márton et al., 2007).

The paper methodically refers the paleomagnetic studies of the Lower Miocene felsitic volcanics of the area of interest published by several authors (Márton and Márton, 1996; Márton et al., 1996; Pécskay and Karatson et al., 1998; Karatson et al., 2000; Póka et al., 2004; Márton et al., 2007). Data are critically evaluated and conclusions important for the topic of the paper are drawn from the data.

Geological background

As described above, the main portion of the Lower Miocene ignimbrites and tuffs occur in Bukovinka Formation of Cerová vrchovina Highland together with gravel/conglomerate, sand/sandstone and mottled clay. The formation is correlated with the Upper Eggenburgian. In Hungary the felsitic volcanic rocks are gathered into Gyulakeszi Formation, considered to be Lower Ottnangian in age and terrestrial deposits are included in the another formation – Zagyvapálfalva Formation, Upper Eggenburgian in age. Both Bukovinka and Zagyvapálfalva formations discordantly cover the Fiľakovo and/or Pétervásara formations attributed to Eggenburgian (Hámor, 1974, fide Bartkó, 1985; Vass in Vass et al., 1979, 1983; Bartkó, 1985). Detailed paleomagnetic study of felsitic ignimbrites and tuffs had shown that those rocks may be subdivided according to paleomagnetic properties into two groups. The first group consists of almost all ignimbrite and tuff bodies in Bukovinka and Gyulakeszi formations with an exception of the Fehér hegy and surrounding ignimbrite and tuff bodies. Former belong to the second group.

The ignimbrite and tuff bodies in Bukovinka Formation have reverse magnetic polarity and their declination exhibits rather large counter-clockwise (CCW) rotation compared with recent magnetic field. The angle of rotation varies from 66° to 97°. The measured sites are as follows: at villages Pleš, Čakanovce and NE of Lipovany village (samples Nos. 1–3, Fig. 1, Tab. 1). Identical paleomagnetic properties have been measured on felsitic volcanic bodies of Gyulakeszi Formation, sites: at villages Gyulakeszi, Nemti, Kisterénye, at abandoned coal mine Rákoczitelep and in Mátraszele – Kazár quarry. (Nos. 4–9, Fig. 1, Tab. 1). Polarity is reverse and angle of declination varies CCW 64° to 120°.
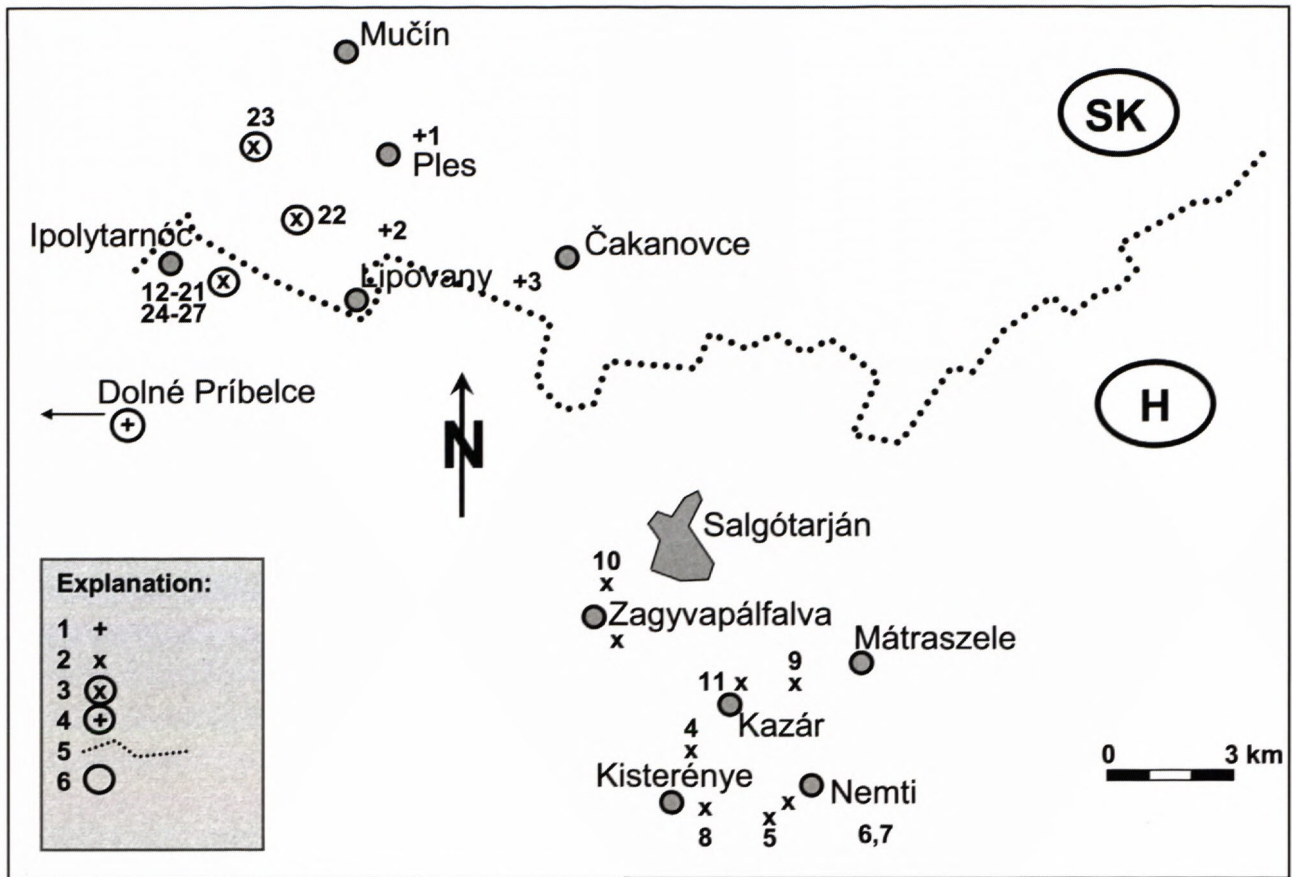
Slovak Geol. Mag., 12, 2 (2006), 139 – 145

140

Fig. 1. Situation scheme of sampled sites. 1 – samples of Bukovinka Formation, 2 – samples of Zagyvapálfalva and Gyulakeszi formations, 3 – samples of Fehér hegy Formation, 4 – sample of a siltstone, Karpatian in age, 5 – state boundary, 6 – villages.

Similar paleomagnetic properties appear in the mottled clays of the Zagyvapálfalva Formation measured on sites: at villages Zagyvapálfalva and Kazár (Nos. 10 and 11, Fig. 1, Tab. 1). The polarity is reverse and CCW rotation varies between 63° and 76°. The felsitic volcanics of Bukovinka and Gyulakeszi formations as well as Zagyvapálfalva Formation most probably originated either during the reverse event of the chronozone C5D, having numeric age of 17.235–18.056 Ma and correspond with the Lower Ottnangian (No. 3 in Fig. 3 left side). Another possibility is that mentioned rocks came to origin during the chronozone C5E (18.056–18.748 Ma) more exactly during its lover reverse event corresponding to Upper Eggenburgian (18.500–18.748 Ma, No. 2 in the left side of the Fig. 3) and/or during the chronozone C 6 its lower event 19.70–20.04 Ma B.P. (No. 1 in the left side of Fig. 3). Numeric time calibration is after Strauss et al. (2006). The last possibility is convenient with the reliable radiometric age 19.6 Ma of a layer of felsitic tuff inside the Bukovinka Formation (Kantor et al., 1988, Fig. 3).

Felsitic ignimbrites and tuffs, outcropping at village Ipolytarnóc and building up the Fehér hegy hill, occur directly above the sandstone bench with the Mammalian foot prints on the surface. They are of normal magnetic polarity and of CCW rotation by 32° (an average value of measured varying between 20° and 38°, Nos. 12–21, Fig. 1). Such paleomagnetic properties clearly show that volcanic rocks originated by another volcanic activity as

above mentioned ignimbrites and tuffs. Because of relatively small CCW rotation, those rocks originated after the first Lower Miocene rotation (approx. 50°-60° CCW) and before the second rotation, so they must by younger in comparison with felsitic volcanic rocks of the Bukovinka and Gyulakeszi formations.

The ignimbrites originated from the hot clouds of volcanic ash. The temperature of the clouds achieved 800–1100 °C, which was enough for the heating of the subjacent rocks and lost of their remanent magnetization by the overprint with the new one from the time of overheating. The bench of sandstone with foot prints is located beneath thin layer of tuff and 4 to 5 m thick mass of ignimbrite (the original thickness was probably reduced by intravolcanic erosion) should be heated enough to lose its remanent magnetization and obtained actual magnetization in the time of hot clouds eruptions. Because of this the paleomagnetic properties of the sandstone bench are the same as properties of overlaying ignimbrite. The sandstone is of normal magnetic polarity and CCW rotation varies between 21° and 48°. Four measurements of the sandstone were done (Tab. 1, Nos. 24–27, Fig. 1). The flora studied by many authors associates with the foot prints bearing sandstone. Hably (1985) concludes that the flora association, represented by the leaves of raining forest trees, is the same as flora association from the site Lipovany (NE from the village, Tab. 1, No. 3) occurring in the frame of Bukovinka Formation and des-

D. Vass et al.: The Fehér hegy Formation: Felsitic ignimbrites and tuffs...

141

Tab. 1   Magnetic polarity and rotation angle of sampled rocks.

	Site of Sapling	Chronostratigraphy	Litostratigraphy and Rock Type	Polarity	CCW Rotation
1.	Pleš	Late Eggenburgian	Bukovinka Fm. Felsitic Ignimbrite/Tuff	R	57°
2.	Lipovany NE	Late Eggenburgian	Bukovinka Fm. Felsitic Ignimbrite/Tuff	R	66°
3.	Čakanovce	Late Eggenburgian	Bukovinka Fm. Felsitic Ignimbrite/Tuff	R	84°
4.	Rákoczi Telep	Early Ottnagian (Late Eggenburgian)	Gyulakeszi Fm. Ignimbrite	R	89°
5.	Gyukeszi	Early Ottnagian (Late Eggenburgian)	Gyulakeszi Fm. Ignimbrite	R	83°
6.	Nemti	Early Ottnagian (Late Eggenburgian)	Gyulakeszi Fm. Ignimbrite	R	97°
7.	Nemti	Early Ottnagian (Late Eggenburgian)	Gyulakeszi Fm. Ignimbrite	R	120°
8.	Kisterénye – Nemti	Early Ottnagian (Late Eggenburgian)	Gyulakeszi Fm. Ignimbrite	R	107°
9.	Matraszele - Kazári Quarry	Early Ottnagian (Late Eggenburgian)	Gyulakeszi Fm. Ignimbrite	R	77°
10.	Zagyvapálfalva	Late Eggenburgian	Zagyvapálfalva Fm. Mottled clay	R	107°
11.	Kazár	Late Eggenburgian	Zagyvapálfalva Fm. Mottled clay	R	77°
12.	Borókás Creek	Late Ottnamgian	Fehérhegy Fm. Tuff	N	28°
13.	Borókás Creek	Late Ottnamgian	Fehér hegy Fm.Ignimbrite	N	37°
14.	Borókás Creek	Late Ottnamgian	Fehér hegy Fm.Ignimbrite	N	35°
15.	Borókás Creek	Late Ottnamgian	Fehér hegy Fm.Ignimbrite	N	32°
16.	Puhakő Quarry	Late Ottnamgian	Fehér hegy Fm.Bentonite	N	28°
17.	Puhakő Quarry	Late Ottnamgian	Fehér hegy Fm.Ignimbrite	N	24°
18.	Puhakő Quarry	Late Ottnamgian	Fehér hegy Fm.Ignimbrite	N	29°
19.	Bokrókás Creek	Late Ottnamgian	Fehér hegy Fm.Ignimbrite	N	21°
20.	Botos Creek	Late Ottnamgian	Fehér hegy Fm.Ignimbrite	N	26°
21.	Learn. Path	Late Ottnamgian	Fehér hegy Fm.Ignimbrite	N	38°
22.	Lipovany NW	Late Ottnamgian	Fehér hegy Fm.Ignimbrite	N	28°
23.	Mučín	Late Ottnamgian	Fehér hegy Fm.Ignimbrite	N	20°
24.	Borókás Creek	Late Eggenburgian	Zagyvapálfalva Fm. Foot print Sandstone	N	37°
25.	Borókás Creek	Late Eggenburgian	Zagyvapálfalva Fm. Foot print Sandstone	N	36°
26.	Borókás Creek	Late Eggenburgian	Zagyvapálfalva Fm. Foot print Sandstone	N	31°CW
27.	Borókás Creek	Late Eggenburgian	Zagyvapálfalva Fm. Foot print Sandstone	N	46°
28.	Dolné Príbelce	Karpatian	Siltstone	R	30°

For detail paleomagnetic data see paper Márton et al. in press (Tab. 1) and Túnyi et al. (2003).

cribed by Němejc (1967) and Knobloch in Papp et al., eds. (1973). The age of flora association is Upper Eggenburgian in age. Between felsitic volcanics of Fehér hegy hill and Zagyvapálfalva/Bukovinka formations including the sandstone with Mammalian foot prints and tuff layer with rich flora of rain forest seams to be a relatively large stratigraphic gap and the Pôtor coal bearing Member / Kisterénye Member and lower part of the Plachtince Member are missing (Fig. 3).

Definition of the Fehér hegy Formation

Different paleomagnetic properties and different age of felsitic volcanics near the village of Ipolytarnóc (Nos. 12–21 and 24–27 including the tuff and/or ignimbrites outcropped NW of Lipovany and SW of Mučín villages (Nos. 22 and 23, Fig. 1) should be excluded from the Gyulakeszi and Bukovinka formations, respectively. In accordance with the Codex of Stratigraphy we suggest for
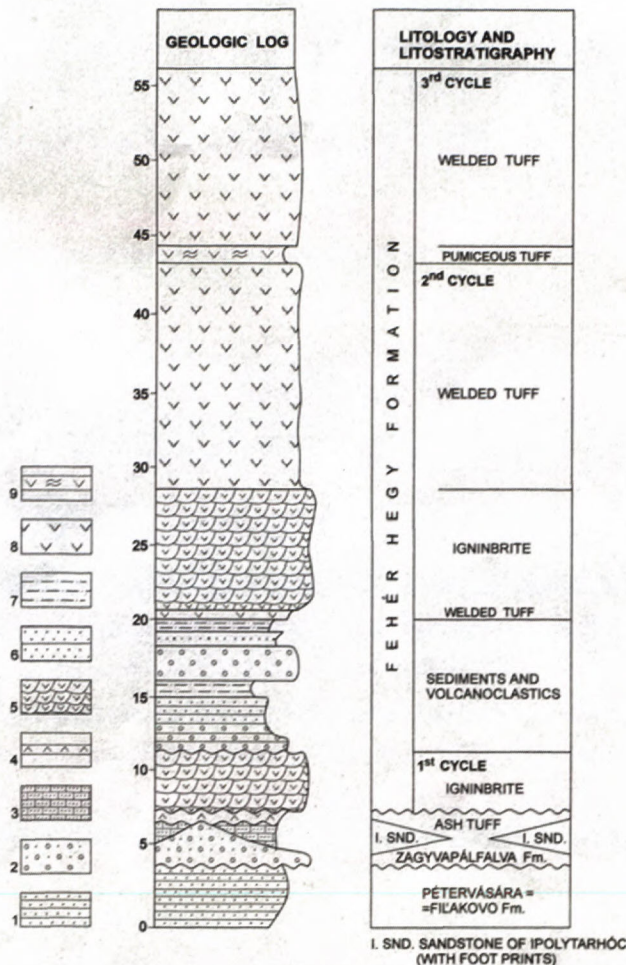
Fig. 2. Geological log at Ipolytarnóc foot prints site and Fehér hegy hill (according to Korpás 1998–2003, modified). 1 – friable glauconitic sandstone, 2 – conglomerate, 3 – sandstone with foot prints, 4 – ash tuff rich in leaf imprints, 5 – ignimbrite, 6 – tuffaceous sandstone, 7 – tuffaceous siltstone, 8 – welded tuff, 8 – pumiceous tuff.

those rocks the status of a new formation called after type section Fehér hegy Formation.

The type section of the Fehér hegy Formation is situated on the southern slope of the Gyartánykö Hill, 2.3 km E of railway station Ipolytarnóc, Ipolytarnóc village The access to the type section is from the Borokás árok Creek, 100 m WSW from Natural museum hall (conservation hall) protecting the footprints sandstone outcrop.

The reference section is on the SE slope of Fehér hegy Hill in a gorge 0.8 km WSW of the type section. The access to the section is from the Botos árok Creek (Fig. 3).

Lithology of the Fehér hegy Formation in its stratotype locality 0.8 km NE from the eastern margin of the village Ipolytarnóc on the SE slopes of Fehér hegy hill was described by Bartkó (1985) and Korpás (2003). The formation is laying directly on the sandstone of Zagyvapálfalva Formation, bearing the Upper Eggenburgian Mammal foot print covered by a layer of ash tuff thick less than 1 m. The Fehér hegy Formation is subdivided into 3 cycles generated by the different short volcanic pulses (Fig. 2).

The first cycle is built up by the ignimbrite thick up to 5 m. The ignimbrite is followed by the sediments or volcanosedimentary rocks thick up to 10 m. The sediments are represented by the conglomerate, sandstone and siltstone. The sediments contain volcanic admixtures being formed mostly by the fragments of volcanic rocks.

The second cycle of volcanic rocks starts with the layer of welded tuff thick 0.5 m, overlaid by the ignimbrite thick as much as 10 m, being followed by felsitic biotitic welded tuff thick 19 m.

The third cycle starts with a layer 1 m thick of pumiceous tuff, followed by 10 m thick mass of welded tuff. The whole sequence is thick up to 42 m.

Age of Fehér hegy Formation

From the above description it follows that Fehér hegy Formation came into being at times between the 1st Lower Miocene CCW rotation by 50° to 60° and 2nd one by 30° CCW. The first rotation occurred at 17.7 Ma, which dates it to the Ottnangian after or at the end of sedimentation of the Pôtor/Kisterénye members of the Salgótarján Formation and second rotation took place at 16.5 Ma in the Upper Karpatian or after the Karpatian (Fig. 4). Because of it the Miocene rocks older as 17.7 Ma show the 80°-90° CCW rotation. In the time interval between 17.7 and 16.5 Ma beside the sedimentary rocks, at least two horizons of felsitic tuff, or tuffaceous rocks occur. The first is in Plachtince and/or Mátranováki members of the Salgótarján Formation and the second is in Sečianky Member of the Modrý Kameň Formation corresponding to the Garáb Schlier Formation in the Hungary, both Karpatian in age.

The siltstone of the Sečianky Member was sampled at Dolné Príbelce village (No. 28, Tab. 1, Fig. 1). The paleomagnetic properties of the sample show the reverse polarity and CCW rotation by 30° (Túnyi et al., 2003). The tuff occurring in the Sečianky Member could not be an equivalent of ignimbrites of the Fehér hegy Formation. On the other hand the Plachtince Member originated during the Upper Ottnangian and the normal magnetic polarity event. So the tuff inside the Plachtince Member may be an equivalent of the Fehér hegy Formation. The Fehér hegy Formation is younger by at least 0.5 Ma up to 2.5 Ma in comparison with the Gyulakészi and Bukovinka formations (Fig. 4).

After submitting this paper, another one dealing with the paleomagnetic properties and consequent age estimation of the Miocene pyroclastic rocks in the Bükk Mts. and their forelands appeared (Márton et al., 2007). Two rhyolite tuffs, studied paleomagnetically (sites Bukkszék Oldalfóke and Törokkréti patak, Nos. 15 and 16 in quoted paper), are of normal polarity and declinations are of 228° and 329° resp. Both tuffs by their paleomagnetic properties and supposed age (17.2 Ma) seam to be coeval with the Fehér hegy Formation. Our correlation indicates that volcanic activity forming the Fehér Hegy Formation was not a local one, but has the equivalents in the Bükk forelands.

D. Vass et al.: The Fehér hegy Formation: Felsitic ignimbrites and tuffs...
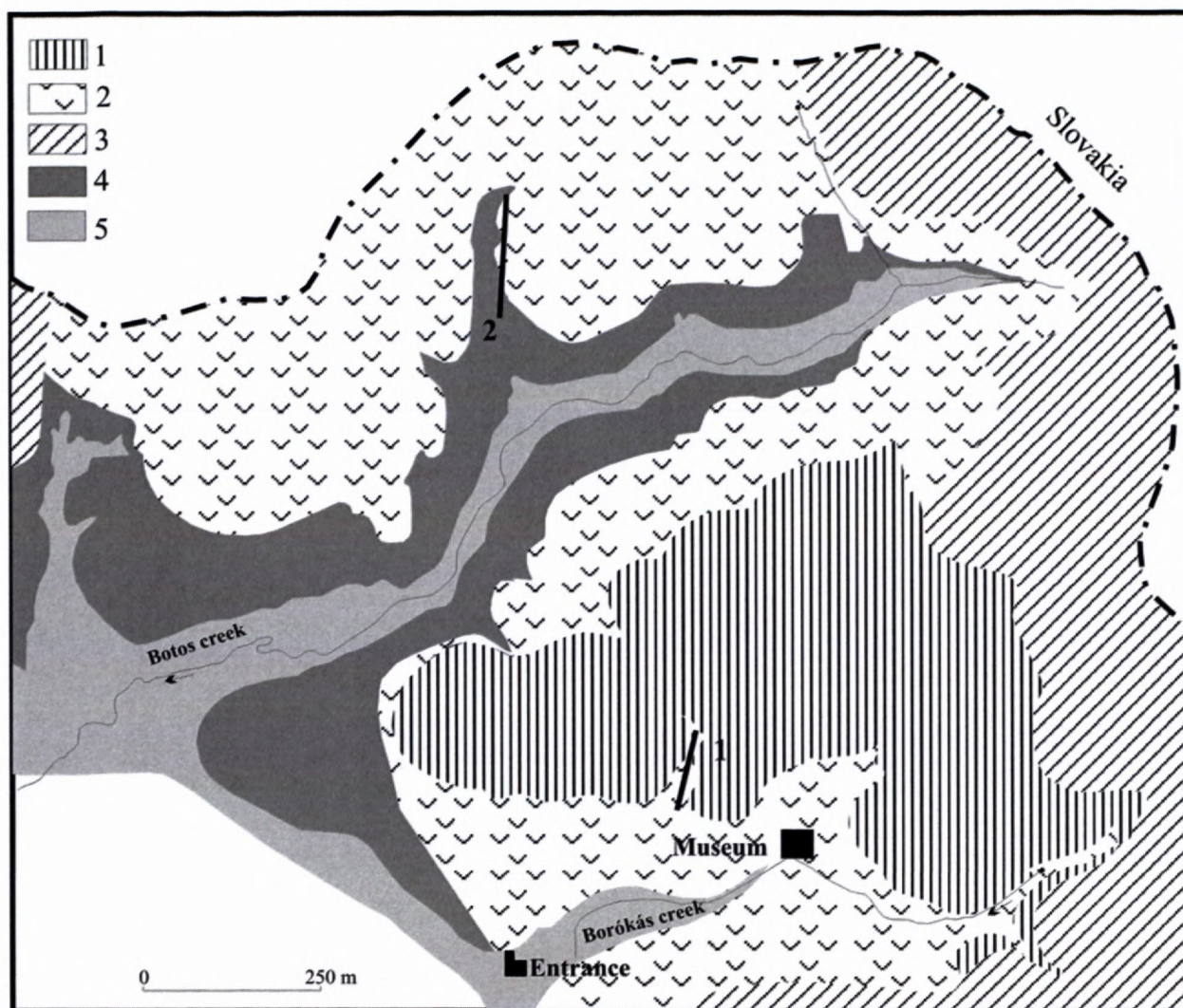
143

Fig. 3. Schematic geologic map of the surroundings of Ipolytarnóc footprints site (according to Bartkó 1985, simplified) and the situation of the Fehér hegy Formation type (1) and reference (2) sections.
Explanations: 1 – tuffaceous sandstone with pebbles of ignimbrite, conglomerate, Upper Ottnangian ?, 2 – ignimbrites of Fehér hegy Formation, Upper Ottnangian, 3 – mottled clay of Zagvapálfalva / Bukovinka formations, Upper Eggenburgian. 4 – sandstone of Pétervásara / Fiľakovo formations, Lower Eggenburgian, 5 – sandy claystone / siltstone of Pétervásara / Fiľakovo formations, Lower Eggenburgian.

Conclusions

The main portion of the Lower Miocene felsic tuff and ignimbrites occurs in the terrestrial Bukovinka Formation (gravel/conglomerate, sandstone, mottled clay and felsitic volcanic rocks) of the Upper Eggenburgian age. In the Northern Hungary, the terrestrial deposits are included into the Zagyvapálfalva Formation and felsitic volcanic rocks into Gyulakeszi Formation considered to be Lower Ottnangian in age. The paleomagnetic study of Lower Miocene felsitic ignimbrites and tuffs has shown that these rocks can be subdivided into two groups. First and older group has the reverse magnetic polarity and larger CCW rotation (80°–90°). The second one, occurs exclusively at the village of Ipolytarnóc, NW of the village Lipovany and SW of the village Mučín. The rocks of second group are of normal magnetic polarity and their

rotation is smaller (about 30°). Because of it the felsitic tuff and/or ignimbrite of the second group are separated from the Gyulakeszi and Bukovinka formations, and the new formation was described obtaining its name after the type locality Fehér hegy hill. This formation is younger than the first block rotation at 17.7 Ma and older than second rotation at 16.5 Ma. The normal polarity event occurred in the Upper Ottnangian, so the Fehér hegy Formation is of this age. The foot prints sandstone has the same paleomagnetic properties as the Fehér hegy Formation, but according the flora assemblage from overlying fine tuff layer it belongs to Zagyvapálfalva Formation of Eggenburgian age. Its original paleomagnetic properties are overprinted by slowly cooling hot ash clouds generating the ignimbrite.

144
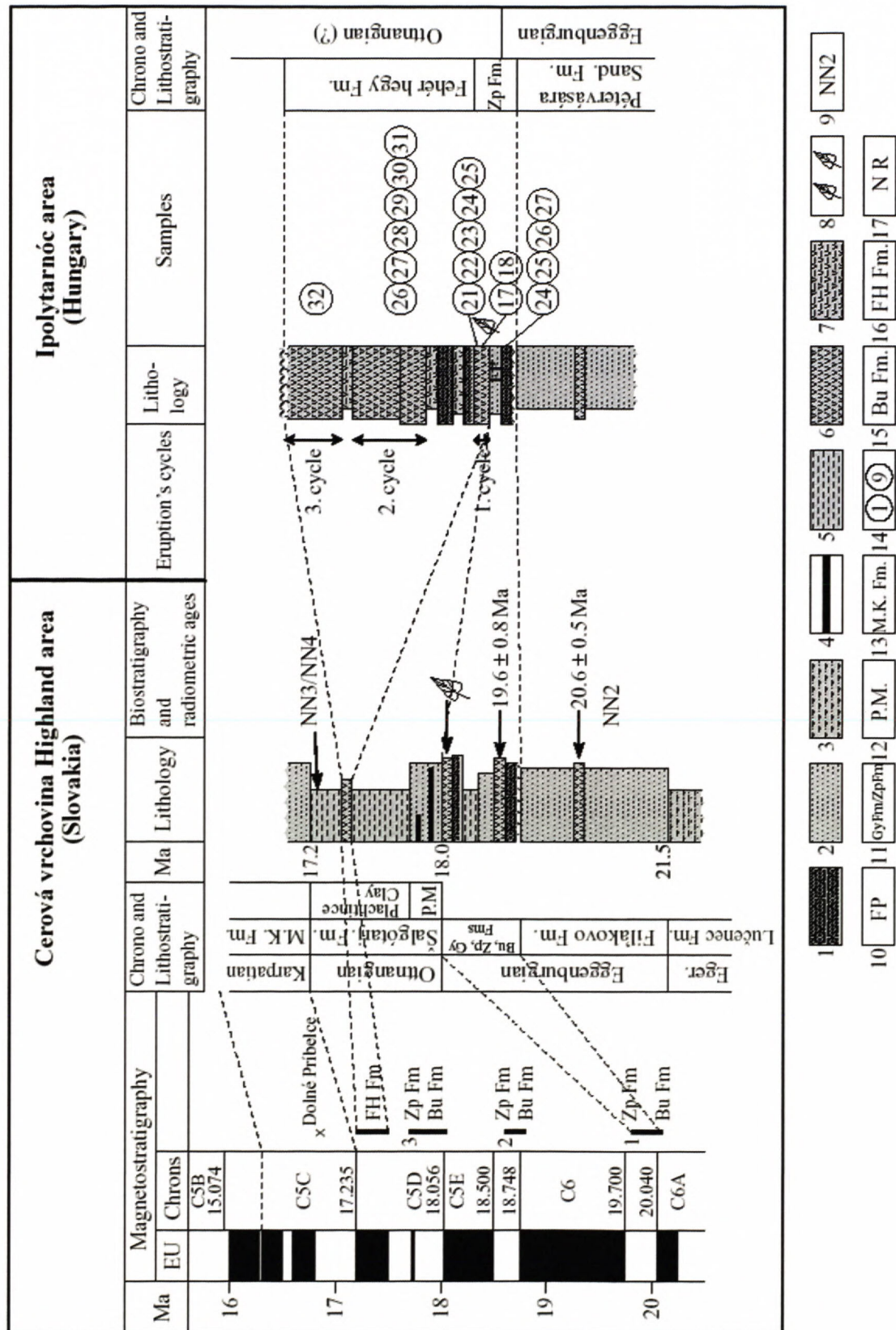
Fig. 4. Correlation chart of Lower Miocene rocks of the Cerová vrchovina Highland area in Slovakia (lithology after Vass, 2002) and Ipolytarnóc area in Hungary (after Bartkó, 1985 in Korpás, 2003). In the former major part the Ottnangian is missing. 1 – conglomerate, 2 – sandstone, 3 – siltstone , 4 – coal seams, 5 – clay/claystone, 6 – felsitic tuff and ignimbrite, 7 – tuffaceous siltstone/claystone, redeposited tuff, 8 – leaf imprints, 9 – nannoplankton zone, 10 – foot prints, 11 – Zagyvapálfalva and Gyulakészi formations, 12 – Pôtor Member coal seam bearing, 13 – Modrý Kameň Formation, 14 – number of sampled site, 15 – Bukovinka Formation, 16 – Fehér hegy Formation, 17 – N: normal polarity, R: reverse polarity.
Numbers 1, 2, 3 of Fig. 3. left side – explanation see in the text.

References

Bartkó, L., 1985: Geology of Ipolytarnóc. Geologica Hungarica, se. Paleontologica, 44, 49-71.

Hably, L., 1985: Early Miocene plant fossils from Ipolytarnóc, N. Hungary. Geologica Hungarica ser. Paleontologica, 45, Budapest, 77-255.

Kantor, J., Ďurkovičová, J., Wiegerová & Sládková, M.,1988: Radiometric age of the rhyolite tuff from the drill EV-2 at Ľuboriečka. Manuscript, Geofond, Bratislava, 1-7. (In Slovak.)

Karatson, D., Márton, M., Harangi, Sz. Józsa, Balogh, K. Pécskay, Z., Kovácsvölgy, S., Szakmány, Gy. & Dulai, A., 2000: Volcanic evolution and stratigraphy of the Miocene Börzsöny Mountains, Hungary. An integrated study. Geologica Carpathica, 51, 325-343

Knobloch, E., in Papp & Rögl, F., eds., 1973: Chronostratigraphie und Neostratotypen Miocen d. Zentralen Paratethys, M2 – Ottnangien, Veda, Bratislava, 1-841.

Korpás, L., 2003: Az Ipolytarnoci homokkö szedimentologiai modellje. A vulkani esemény kronológiája és közponzjának rekonstrukciója. Manuscript. Magyar Karst és Barlangkutató Társulat, Manuscript, 1-42.

Márton, E. & Márton, P., 1996: Large scale rotations in North Hungary during the Neogene as indicated by paleomagnetic data. In: A. Morris & D. H. Tarling (eds.): Paleomagnetism and tectonics of the Mediterranean Region. Geol. Soc. London, Spec. Publ. 105, 153-173.

Márton, E. & Pécskay, Z., 1998: Correlation and dating of the Miocene ignimbritic volcanics in the Bükk foreland, Hungary: Complex evaluation of paleomagnetic and K/Ar isotope data. Acta Geologica Hungarica 41, 467-476.

Márton, E., Vass, D. & Túnyi, 1996: Rotation of the South Slovak Paleogene and Lower Miocene rocks indicated by paleomagnetic data. Geologica Carpathica, 47, 1, 31-41.

Márton, E., Vass, D., Túnyi, I., Márton, P. & Zelenka, T., 2007: Paleomagnetic age assignment of the ignimbrites from the famous foot prints site of Ipolytarnóc (at the Hungarian – Slovak boundary). Geologica Carpathica, 58, 6, 531-540.

Márton, E., Zelenka, T. & Márton, P., 2007: Paleomagnetic correlation of Miocene pyroclastics of the Bükk Mts. and their forelands. Central European Geol., Budapest, 50, 1, 47-57.

Němejc, F., 1967: Paleofloristic studies in the Neogene of Slovakia. Sborník Narodního Muzea, 23, Praha, 1-32. (In Slovak.)

Póka, T., Zelenka, T., Seghedi, I., Pécskay, Z. & Márton, E.: Miocene volcanism of the Cserhát Mts. (N. Hungary). Integrated volcano–tectonic, geochronologic and petrochemical study. Acta Geologica Hungarica, 47, 221-246.

Túnyi, I., Vass, D. & Konečný, V., 2003: Anomalous paleomagnetic declinations of Karpatian and Badenian rocks, Southern Slovakia. Slovak Geol. Mag., 9, 1, 41-49.

Vass, D., 2002: Lithostratigraphy of Western Carpathians. Neogene and Buda Paleogene. Štát. geol. ústav D. Štúra, Bratislava, 1-202.

Vass, D., Konečný, V. & Šefara, J., eds., 1979: Geological setting of the Ipeľ Basin and Krupinská planina plateau. Geol. ústav D. Štúra, Bratislava 1-277. (In Slovak.)

Organic matter and fossil content in Serbian oil shales: Comparison with oil shales of Central Europe

[1,2]Dionýz Vass, [3]Nadeźda Krstić, [4]Ján Milička, [4]Mariana Kováčová-Slamková,
[5]Jelena Obradović and [3]Dradoljub Grgurević

[1]Faculty of Education, Catholic University, Námestie A. Hlinku 56, 030 41 Ružomberok, Slovak Republic;
dionyz.vass@zoznam.sk
[2]Geol. Institute of Slovak Acad. of Sci., branch Banská Bystrica, Severná 5, 974 01 Banská Bystrica, Slovak Republic
[3]Geoinstitut Rovinjska 12, Belgrade, Serbia; n_krstic@ptt.yu
[4]Faculty of Natural Sciences, Comenius University, Mlynská dolina, G, 842 15, Bratislava, Slovak Republic;
milicka@fns.uniba.sk, kovacova@fns.uniba.sk
[5]Faculty of Mining and Geology, University of Belgrade, Djušina 7, 110 00 Belgrade, Serbia; jeobrad@ptt.yu

Abstract: Serbian Cenozoic lacustrine deposits contain the oil shales beside other sedimentary rock types. Organic matter of five randomly selected oil shale samples was characterized using elementary analysis and Rock-Eval pyrolysis. Fossil content and paleoecological conditions are characterized by palynological study. According to results of analyses, the samples from Subotinac, Vranye and Sushevlynska Bela Stena correspond to aquatic kerogen type I, being rich in organic carbon content (10–30 wt.%), as well as in hydrogen content expressed by hydrogen index (HI = 740–840 mg HC/g TOC). Sample from Mionica represents kerogen type III derived from woody material. According to maximal pyrolytic temperature all investigated samples are in early mature relict stage.

The oil shales originated in relatively large and deep lakes well supplied by nutritive elements and the water was eutrophic. The oil shales of Miocene age originated under subtropical climate conditions. The oil shale from Vranye Depression, Oligocene in age, originated in tropical to subtropical climate. The laminated structure of oil shales testifies the seasonal climatic changes. Small size of Botryococcus cells indicates the high reproduction potential of the algae.

The comparison with the Cenozoic oil shales of Central Europe indicates the differences in paleolake size, in paleoheat flow intensity and in carbonate lamina origin. Particularly the maar lakes of Slovakia and Hungary were small. The paleoheat flow in surroundings of Drienovec (Slovakia) was significantly lower in comparison with the Central Serbia and Kosovo. The Drienovec oil shales differ from those of Shushevlyanska Bela Stena in the origin of organic matter free lamina. Those of Drienovec originated by the activity of calcareous algae, those of Shushevlyanska Bela Stena are of chemogene origin.

Key words: paleolakes, Serbia, Cenozoic, oil shales, Botryococcaceae, pollen spectra, Rock–Eval pyrolysis, TOC

Introduction

In July 2003 one of us (Vass), being invited by Serbian Geological Society and personally by Nadezda Krstić, took part on the workshop Paleolimnology of the Serbian Neogene. During the field trip the samples of oil shales from four localities were collected. The sampled localities were (Fig. 1):

- Subotinac at town of Aleksinac, samples Srb-1 and 2
- Vranye Depression, sample Srb-3
- Mionica – bridge in the town, sample Srb-4
- Shushevlyanska Bela Stena, west of town Mionica, sample Srb-5

The lacustrine deposits are typical for the Serbian Neogene, including the oil shales. The paleolakes with oil shales by Obradović, Djurdjević-Colson & Vasić (1997) have been subdivided into two groups:

The oil shales of the first group are represented by an alternation of carbonate and kerogen (rich in organic matter) lamina. Such type of rock occurs in Valyevo–Mionica, Yadar (Jadar) and Pranyani depressions.

In the oil shales of second group the clay, marl or shale lamina alternate with lamina rich in kerogen. This type of oil shales occurs in Vranye and Aleksinac depressions.

The main purpose for sampling the Serbian oil shales was to get some information about shale's organic matter and fossil contents. The Serbian oil shales were compared with several oil shales of Central Europe, namely with Slovak localities – Pinciná (maar type), Drienovec (sea costal lagoon type, data from Vass et al., 1997; Milička & Vass, 2001), further with Hungarian localities Pula and Gérce (maar type, data from Bruckner-Wein & Hetényi, 1993) and Czech oil shale from Sokolov Coal Basin (data from Müller, 1987).

Method of study

The organic matter of oil shales was characterized using elementary analysis and Rock-Eval pyrolysis. Total organic and inorganic carbon (TOC, TIC) was determined in Czech Geological Survey Prague, branch Brno. Rock-Eval pyrolysis was carried out in Oil and

Slovak Geol. Mag., 12, 2 (2006), 147 – 158

148

Fig. 1. Sampled sites of oil shales in Serbia. Srb-1, 2 – Subotinac (Aleksinac Depression), Srb-3 - Goć – Denotin Deposit (Vranye Depression), Srb-4, 5 - Mionica, bridge in town and Shushevlyanska Bela Stena.

with turbiditic sedimentation took place continuously from the Upper Cretaceous through Upper Oligocene what is corroborated by calcareous nannoplankton and dinoflagellate cysts (Capoa & Radoićić, 2002). Aside off the straight some lagoons were formed, like acidic Shumadia Lake (Krstic et al., 2003), being also dwelled by marine fishes (mugilid) except for the period of sprawling when they migrated to the sea water (Gaudant, 2002) of nearby straight. The closing of the straight had not stopped the sedimentation in these lagoons, but changed them into lakes, like lakes of Aleksinac and Polyanica (Goc-Devotin), deep enough to house meromictic lakes, their profundal filled by oil shales.

The Serbian Lake (Krstić, 1996) was formed along the postcollisional spreading area, further modified by bending of Carpathian-Balkan arc. Close to Belgrade conformably on the Serbian Lake sediments the Middle Badenian sequences lie. The lake, spotted by some islands, in its deeper subdepressions had the water stratification, thus the conditions convenient for the oil shale origin.

The most oil bearing is the Valjevo-Mionica Depression more than 20 km long and 10 km wide. Four depth zones were distinguished (Jovanovic et al., 2005):

• Lentic environment, in places with sedge, but mostly with fossiliferous Tolić Limestone around Paśtrić, Tolić and other villages was in the past the area of floating plants producing lacustrine chalk

• In the southeastern and northern parts of depression the moderately deep and well aerated portion of lake, with marly silt sedimentation, contains ostracodes *Ohridiella sabantae, Cypria* and, in rare places, *Congeria, Micromelania* (Jovanović et al., 2005) as some other molluscs from genera *Pisidium, Planorbis, Prosothenia, Nematurella (?), Lymnea, Theodoxus* (Dolić, 1983)

• Third is the belt where ostracode laminite indicates the ancient position of mesolimnion - there alternate ostracode-bearing lamina brought by seepage of warmer and more dense water from epilimnion with lamina deriving from hypolimnion pulsations – exactly the sample Srb-4 was taken there.

• To the fourth, the lake profundal winnow redundancy of *Botryococcus* algae when water was calm, while when water was agitated by the turbidites, the silt was settled - both together making lamina. Today the main oil shale body is 8 x 2.5 km large (Pantić et al., 1980) and covers the central and southern parts of the Valjevo-Mionica depression. It crops out again northward on the other side of Kolubrara fault.

Gas Institute Kraków and interpreted in the sense of Espitalié et al. (1986).

For palynological study the fine-grained sediment samples, about 20 g in volume, were treated using a standard palynological extraction technique involving HCl – HF – HCl and heavy liquid treatment (solution of cadmium iodide, potassium iodide of a specific gravity of 2.0), next the obtained organic matter was macerated in 30 % hydrogen peroxide solution, in KOH and subjected to acetolysis by Erdtman's (1943, 1960) method.

One to three microscopic preparations were made from each sample according to the amount of the palynomorphs. Samples were sieved on 10 µm sieves.

General characteristics of sampled depressions

Samples were taken from two very different geotectonic units. First group of samples is from Lower Miocene conformably topping Paleogene turbidite deposits of the Vardar Zone, this time the strait between Dinaric and Carpatho-Balkan islands. Others were taken from the deposits of Middle Miocene Serbian Lake situated in the middle of Balkan Land formed by uniting of mentioned islands.

The Vardar Zone was an area of deep sea deposition for very long time (since Carboniferous). The last phase

D. Vass et al.: Organic matter and fossil content in Serbian...

149

Sampled places are app. 7.5 km apart and belong to two depth zones: the mesolimnion (Mionica) and hypolimnion Shushevlyanska Bela Stena.

Aleksinac Depression

An exhausting geological description of the Aleksinac Depression was given by Stevanović (1964) including the story of the coal bearing depression investigation from the end of 18. century (list of papers see in Stevanović references).

The depression filled by Cenozoic deposits is surrounded and underlain, sometimes overthrusted, by the Lower Paleozoic metamorphic rocks (Krstić, B. et al., 1980) possibly Ordovician – Silurian in age (Kreutner & Krstic, B., 2003). The depression sedimentary fill containing the coal seams and oil shales, being Oligocene-Lower Miocene (Petković & Ćićulić, 1962) or Lower Miocene (Stevanović, 1964) in age is of lacustrine origin. According to Krstić, B. et al. (1980) these sediments are thick up to 900–1000 m. The profundal lake deposits are represented by oil shales. The marginal, or coastal facies are represented by paludal – lacustrine deposits including the coal seams. The depression fill is subdivided into three units (informal formations, Obradovič et al., 1997):

- Lower formation with three oil shale horizons of the total thickness 520 m,
- Middle formation contains the coal seam thick 2–4 m, exceptionally 15 m and oil shale thick up to 60–100 m.
- Upper formation consists of marlstone, its thickness is up to 200 m.

The basal deposits of the depression fill: conglomerate and sandstone with thin layers of conglomerate of alluvial origin transgressively lie on the crystalline basement. Above the fine-grained sandstone, the claystone, marl and oil shale occur. The coal of middle formation manifests the paludal–lacustrine or marsh–swamp origin. Directly over the coal the oil shale thick up to 100 m lies (representing marginal facies?). The upper member is built up by marlstone with 3–5 % of organic matter (kerogen) grading upward in white marlstone with thin intercalations of the marly clay and tuff.

The oil shales are laminated. The lamina rich in organic matter alternate with lamina of marl and/or clay, rarely of dolomicrite. The kerogen is of type I, less of type II (Obradovič et al., 1997). The huminite reflectance varies from 0.25 to 1.5 % R_o. The TOC contents range between 12 wt.% and 24 wt.%.

Valyevo–Mionica Depression

The depression elongated in direction W–E is surrounded on the north by the Paleozoic and Lower Triassic clastic rocks and on the south by Middle Triassic limestone. Simplified lithological column is in Fig. 2. The thickness of the depression fill is ca. 250 m. According to Andjelković (1989) the depression fill is Lower Miocene in age. According to new stratigraphy revision by Jovanović et al. (2005) the age of depression fill is Middle Miocene – Pliocene and the oil shale sequence occu-
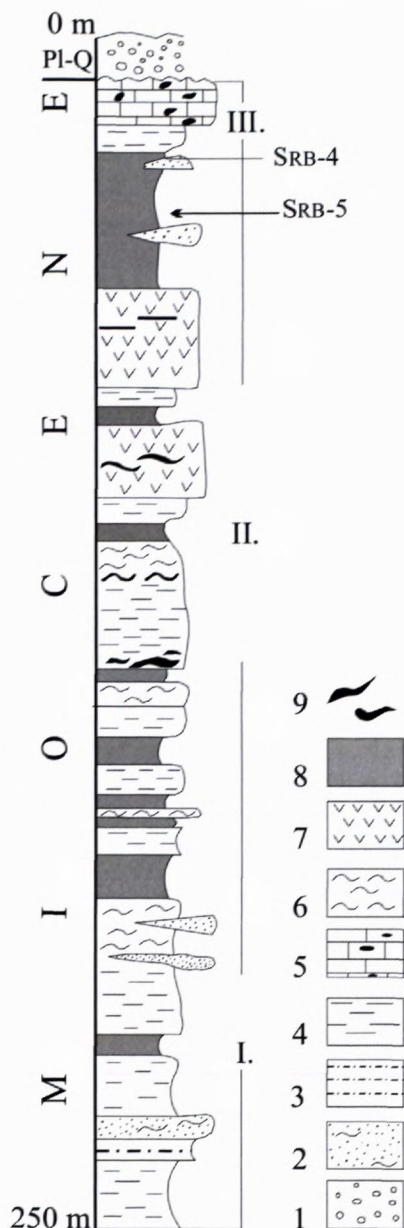

Fig. 2. Schematic lithological column of Valyevo–Mionica Depression fill. 1 – conglomerate, 2 – sandstone and marly sandstone, 3 – siltstone, 4 – claystone, 5 – limestone with chert concretions, 6 - marlstone, dolomitic marlstone, 7 – tuff, 8 – oil shale, 9 – searlesite and analcime bodies. I – marginal facies, II – intrabasinal facies, III – shallow water facies with chert concretions. (After Obradović, Djurdjević-Colson & Vasić, 1997).

pying approximately middle part of the column is considered to be Upper Miocene in age. The lower and marginal parts of the depression fill are built up by limestone, marlstone, sandy marlstone and clay marlstone with sandstone intercalations. The profundal (intrabasinal) sediments consist of the marlstone, oil shale, tuff with thin layers or bodies of searlesite ($NaBSi_2O_5(OH)_2$) and analcime. The thickness of the whole sequence is larger at Shushevlyanska Bela Stena, towards north the sequence is divided into two parts and is thinner. The uppermost part of depression fill deposited in shallow water and the dominant lithotype is limestone with chert. The oil shale is laminated, the lamina rich in organic matter alternate

Slovak Geol. Mag., 12, 2 (2006), 147 – 158

150

with lamina of dolomicrite, rarely calcite. In the dolomic-rite lamina the authigenic minerals searlesite and anal-cime appear. The lamination is often deformed by the authigenic minerals grow. The authigenic minerals mentioned, especially the trona, shortite and even gypsum occurring in same samples, indicating the salinity rise in the paleolake and interstitial brine. The ammoniacal nitrogen is present as a result of the organic matter decay (Obradovič et. al., 1997).

The kerogen of the Valyevo–Mionica depression belongs to the type I and II (Obradovič et al., 1997). The huminite reflectance R_o is 0.26 % (Ercegovac, 1990). Algae of *Botryococcus* type are well preserved.

Polyanica Depression north of Vranye

The Vranye Depression situated in Southern Serbia is surrounded and underlain by the Riphean–Cambrian crystalline schists of the Serbian–Macedonian Massif: gneiss, leptynolite, micaschist, amphibolite schists and quartzite. The deep borehole penetrates these rock types in the central part of depression in depth around 1500 to 2000 m (Krizak, 2003). The depression is divided into a smaller and older (Oligocene) Polyanica partial depression and a larger and younger (Middle Miocene) Vranye s. s. partial depression. The depression opened during the Paleogene and was filled by Paleocene–Eocene (its southernmost Pćinya part) and Oligocene deposits (Mihajlović, 1985) as well as by the Miocene and Pliocene deposits (Vukanović et al., 1977). The sedimentation was accompanied by volcanic activity culminating in the Middle Miocene.

The basin fill was subdivided by Jovanović and Novković (1988) into three formations or complexes:

Pćinya Formation: tuffaceous deposits, tuff, turbidites of total thickness of 400 m, Paleocene – Eocene in age, having the marine deep gulf origin. Far to the south the marine molluscs were found (at Ovće Polye, Macedonia).

Buśtranye – Polyanica Formation with the oil shales thick up to 1100 m, Oligocene in age, the formation is of lagoonal origin (marine Lower Oligocene corals were found westwards close to the town Gnyilane).

Vranye Complex containing several formations having the lithological contents: tuff, zeolite, bentonite, diatomite, oil shale and lignite. The age of the complex main part is Middle Miocene and the total thickness is 2 000 m or more. The complex is of volcanic and lacustrine origin.

The Oligocene lagoonal Polyanica Formation deposits lying unconformably on the Pćinya marine gulf/strait formation begin with the fluvial conglomerate, coarse sandstone and limestone originated on the river mudflats. The asphalt also occurs there. The lacustrine profundal and/or intradepressional deposits are marlstone, tuff, tuffaceous rocks and oil shales. The age was determined on the base of macroflora by Mihajlović (1985). The oil shales are developed in four horizons, their thickness varies from 4 to 15 m. The uppermost Oligocene consists of marlstone, shale, claystone and carbonates.

The Miocene Complex is composed by fluvial and marginal lacustrine deposits as conglomerate, gravel and sandstone. The intradepressional or profundal deposits

are composed of oil shales covered with lapilli tuff and tuffaceous deposits. The uppermost rocks of the Miocene complex are marlstone, claystone, tuff being often transformed in zeolite (Obradović & Vlasić, 1990), tuffaceous rocks, while diatomite and lignite may be Pliocene in age (Vukanović et al., 1977).

The Oligocene oil shales are laminated rocks. The lamina rich in organic matter alternate with the lamina of clay. The kerogen is mostly of type I, partly type II. Type III is randomly present, too. The reflectance of bituminite is 0.10–0.30 % R_o and of huminite is 0.35–0.45 % R_o (Ercegovac, 1990).

Results of collected samples study

Samples of Serbian oil shales collected in 2003 belong to both types defined by Obradović et al. (1997). The samples taken in town of Mionica and at the site Shushevlyanska Bela Stena are of the first group. The samples coming from village of Subotinac near town of Aleksinac and from Vranye Depression belong to the second group.

Characteristics of oil shale samples from Subotinac–Aleksinac Depression

The samples (Srb-1 and 2) have been collected in the abandoned pit near the village of Subotinac, where the main oil shale horizon in the hanging wall of the coal bearing horizon outcrops (Fig. 3). The sampled oil shale consists of alternating grey marl and dark lamina rich in organic matter.

The estimated TOC contents are of 25.9 and 28.6 wt.%. According to the Rock-Eval pyrolysis the free hydrocarbon (S1) contents are of 2.87 and 3.33 mg and fixed hydrocarbon (S2) contents are of 213.4 and 216.1 mg. The hydrogen index (HI) ranges from 747 to 835 g of TOC and the maximum pyrolysis temperature T max reaches 440 and 446 °C (Tab. 1).

The clay minerals were studied by X-ray diffraction method. The samples from all studied localities are characteristic by low reflexion intensity resulting from the low clay mineral contents and probably the low structural organization of clay minerals along with the increased background, signalizing the presence of amorphous organic matter. The clay minerals of the oil shale from Subotinac (sample Srb-2a) are illite, smectite, eventually I-S mineral of high expandability and possibly the clinoptilolite (one reflex only). The rock exchange capacity is of 232 and 238. The specific surface is of 359.41 and 347.32 $m^2 . g^{-1}$ (Uhlík, written com.).

The most common fossils in the oil shale are algae occurring in colonies. The channel like structures on the colonies margins resemble the colonies of the Botryococcaceae family with strongly reduced magnitude of the channels. The pollen spectrum is uniform, not diversified represented by gathered unidentified amorphous not coalfield organic matter and by few algae. The pollen grains of *Pinus*, *Cathaya* and *Quercus* type *ilex* are the very rare admixture in the pollen spectrum. They indicate a subtropical climate.
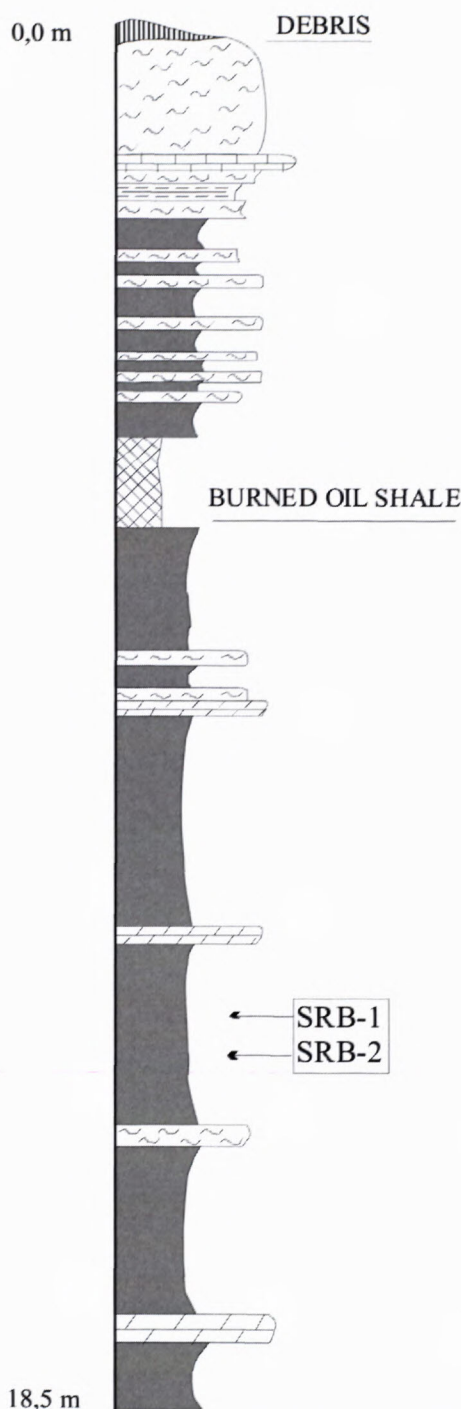
D. Vass et al.: Organic matter and fossil content in Serbian...

151

0,0 m   DEBRIS

BURNED OIL SHALE

SRB-1
SRB-2

18,5 m

Fig. 3. Lithological column of abandoned oil shale pit (a slope above the rivulet Moravica), Subotinac village at Aleksinac (Kaśanin – Grubin, 1996). For explanations see Fig. 2.

Characteristics of samples from Mionica – bridge and Shushevlyanska Bela Stena

In the valley of **Ribnica river** 2 km downstream of the town Mionica the oil shale bearing horizon outcrops. The outcropping rocks represent three different lake environments (Jovanović et al. 2005). At the village Pashtrić the shallow lacustrine deposits – massive and laminated carbonates (chalk) outcrop. The massive carbonate contains the molluscs Congeria sp., Planorbis sp. and Mi-

cromelania sp. as well as the ostracodes – Candoninae. At the bridge in Mionica town the thermocline belt occurs. Several kilometres downstream of the river the profundal laminites – oil shales outcrop. The light grey to white dolomicrite lamina alternate with dark lamina rich in algal organic matter. The flora indicates the Middle Miocene age (Pantić et al., 1980).

In the **Mionica town** near bridge on the Ribnica river thin bedded or laminated siltstone outcrops. The bedding planes are covered by valves of ostracodes. The horizon originated when the dense mineralized water from the lake water level submitted to evaporation seeps down the sublittoral bottom, struck the thermocline and the speed of seepage decelerated. The ostracodes sailing in the mineralized water fell down and recently occur on the siltstone bedding planes (Jovanović et al., 2005).

The sample taken from the rock (Srb-4) is relatively poor in organic matter. TOC content is of 1.11 wt.%. The content of free hydrocarbons (S1) is of 0.18 mg, the fixed hydrocarbon amount is 2.9 mg. The hydrogen index is 259 mg HC in g of TOC. The maximum pyrolysis temperature (Tmax) is of 439 °C (Tab. 1).

The clay minerals are represented by illite and smectite or by I-S mineral of a high expandability. The X-ray analyses indicate the low contents of chlorite, kaolinite and quartz. The rock exchange capacity is 118 and 131. The specific surface is 174.92 and 191.99 $m^2.g^{-1}$ (Uhlík, written com.)

The pollen spectrum is rich and extremely diversified. The warm - temperate arctotertiary elements are dominant and the paleotropical taxa are sub dominant. The thermophile elements are represented by Sapotaceae, Eng*elhardia, Platycarya, Castanea, Ilex, Distylium, Symplocos and Myrica*. The humid plants are represented by *Alnus, Ulmus, Salix, Nyssa and Osmunda*. The mesophytic taxa are represented by *Quercus, Fagus, Pterocarya, Carya, Zelkova, Carpinus and Juglans*. The mountain vegetation is represented by *Picea, Abies, Cedrus and Sciadopytis. Pinaceae* family is represented by *Pinus and Cathaya. Graminae* are present, too. The algae occur sporadically. According to the presence of evergreens *Engelhardia, Platycarya, Castanopsis, Sapotaceae*, the climate was subtropical.

Near the town of Valyevo the **Shushevlyanska Bela Stena** rocks are outcropping. The oil shale is laminated, the lamina rich in organic matter alternate with lamina of dolomicrite. The rock (Srb-5) is relatively rich in organic matter. TOC content is of 15.85 wt.% and the inorganic C content is of 2.47 wt.%. The content of free hydrocarbons is 3.76 mg fixed hydrocarbon amount is of 128.4 mg. The estimated hydrogen index (HI = 810) is considerably high. Tmax is of 439 °C (Tab. 1).

The clay minerals are represented by illite and kaolinite or chlorite of low concentration. Beside it the quartz, albite and K-feldspar are present. The rock exchange capacity is 132 and 142. The specific surface is 199.70 and 208.44 m^2. g^{-1}(Uhlík, written com.)

The palynospectrum is diversified. Beside the amorphous organic matter there are *Myrica, Engelhardia, Alnus, Nyssa, Pinus, Cathaya and Tsuga*. The climate was subtropical and humid.

Tab. 1 Organic-geochemical characteristic of Serbian oil-shales

Locality	Sample code	Stratigraphy	Depth m	TIC	TOC wt.%	S1 mgHC/g r.	S2 mgCO/g r.	HI mgCO/g TOC	OI mgCO$_2$/ TOC	PI	GP	T$_{max}$ °C	Kerogen type
Subonatic (a)	SRB1	Lower Miocene	surface	0.52	28.60	2.87	213.4	747	32	0.01	216.31	440	I
Subonatic (a)	SRB2	Lower Miocene	surface	0.05	25.89	3.33	216.1	835	35	0.02	219.39	446	I
Vranye	SRB3	Middle Miocene	surface	0.05	9.63	0.95	71.3	741	30	0.01	72.27	438	I
Mionica*	SRB4	Middle Miocene	surface	2.30	1.11	0.18	2.9	259	50	0.06	3.06	439	III
Shushevlyan-ska Bela Stena	SRB5	Middle Miocene	surface	2.50	15.85	3.76	128.4	810	34	0.03	132.15	439	I

TOC, S1, S2, HI, OI, PI, GPm, T$_{max}$ – Rock-Eval pyrolysis parameters: TOC – total organic carbon; S1 – free hydrocarbons; S2 – fixed hydrocarbons-residual hydrocarbon potential; HI – hydrogen index; OI – oxygen index; PI – production index; GP – genetic potential; Mionica: claystone with low organic matter content not representing an oil shale.*

Tab. 2 Comparison of selected organic-geochemical characteristics of Serbian oil-shales with other localities in Central Europe

Locality	Well	Depth m	TOC extent	x	S1 extent	x	S2 extent	x	HI extent	x	T$_{max}$ extent	x	Number of samples
Serbian oil shales Lower – Middle Miocene	outcrops	surface	9.63-28.6	19.99	0.95-3.76	2.72	71.30-216.10	157.29	741-835	783	438-466	440	4
Slovakia (Drienovec) Eocene – Oligocene	VD 2	577-622	1.23-5.6	3.49	0.10-0.38	0.20	7.02-32.56	21.19	571-667	606	418-434	426	5
Slovakia (Pinciná) Pontian	VPA 1, 3, 4, 5, 7	7.0-48.0	3.81-28.58	8.90	0.29-14.36	3.80	10.5-169.00	41.50	279-962	451	426-442	438	91
Hungary (Pula) Upper Pannonian – Pliocene	Put 30	6.3-50.5	2.50-31.00	15.30	0.29-13.74	6.10	7.49-265.54	100.83	293-769	569	438-444	440	93
Hungary (Gércse) Upper Pannonian – Pliocene	Gét 6	16.3-65.0	2.39-9.84	5.92	2.04-15.46	8.05	8.91-73.63	34.68	372-1007	566	391-433	422	23
Czech Republic (Sokolov Basin) Cypris Beds (Middle Miocene)	open coal-mine	subsurface		6.47		0.02		60.9		939		439	77

TOC, S1, S2, HI, Tmax – Rock-Eval pyrolysis parameters as in table 1: x – average value

D. Vass et al.: Organic matter and fossil content in Serbian...

153

Characteristic of samples from Polyanica Depression (north of Vranye)

The main occurrence of oil shales in **Vranye** surroundings belongs to Oligocene (Buśtranye – Polyanica Formation). The oil shales form four seams. The maximum thickness of the uppermost one (seam I) is 15 m and the quality concerning the crude oil content is the best – in average of 4.4 % (Novković et al., 1986).

From the Goć–Devotin oil shale deposit, borehole Dj-3, depth 3.0–8.0 m, the following pollen spectrum was described: *Laevigatoporitess haardti, Polypodiaceoisporites marxheimensis, Punctatisporites crassiexinus, Foraminisporites granoverrucatus, Monocolpopollenites tranquilus – Palmae, Monocolpopollenites tranquilus tranquilus – Palmae, Inaperturopollenites hiatus – Taxodium, Pityosporites microalatus – Pinus haplpxilon, Pityosporites labdctus – Pinus silvestris, Piceapolis planoides – Picea, Cedripites crassiunulicristatus – Cedrus Podocarpidites sp., Polyvestibulopollenites verus var. multiporatus – Alnus, Polyvestibulopollenites verus – Alnus, Tricolporopollenites dolium – Rhus, Tricolporopollenites pseudocingulum – Rhus, Tricolporopollenites megaexactus bruehlensis – Cyrillacea, Tricolporopollenites krushi pseudolaesus – Nyssacea, Ephedrites sp., Tricolpopollenites henrici – Quercus, Tetracolpopollenites macroechinatus – Sapotaceae, Tetracolpopollenites sapotoides – Sapotaceae, Tetracolpopollenites obscurus – Sapotaceae, Tetracolpopollenites sp., Tetradopollenites callidus – Ericaceae, Polyadopollenites multipartitus – Mimosaceae, Cercidiphylum sp.* (L. Dimić unpublished data). The assemblage indicates tropical to subtropical climate.

The sample (Srb 3) was taken from uppermost seam of the Goć-Devotin oil shale deposit (Fig. 4). The Rock-Eval pyrolysis yields the following data: TOC content 9.63 wt.%, free hydrocarbon content 0.95 mg, fixed hydrocarbon content 71.30 mg. The hydrogene index reaches to 741 and Tmax to 438 °C (Tab. 1).

The rock exchange capacity is 96 and 102. The specific surface is 140.97 and 145.18 $m^2.g^{-1}$ (Uhlík, written com.)

Discussion

The oil shale of Subotinac under the study similarly as the Cainozoic Middle European laminated oil shales (Fig. 13) originated in relatively deep lakes (about 40 m or deeper). In such lakes in humid and moderate warm or subtropic climate during the summer the water mass was stratified and the lake underwent a period of stagnation. The upper water layer – epilimnion – heated by solar radiation was relatively hot and well supplied by mineral nutrients swash down into lake from the weathered rocks of lake source area. The nutrients came particularly from the volcanic rocks of the intermediate or basic chemical composition rich in K, Ca, Mg and P. Such rocks, as from the geologic background of the lakes follows, have been present in the lakes surroundings. The lake water table was calm and quiet. In such conditions the water of epilimnion became quickly eutrophic and overpopulated
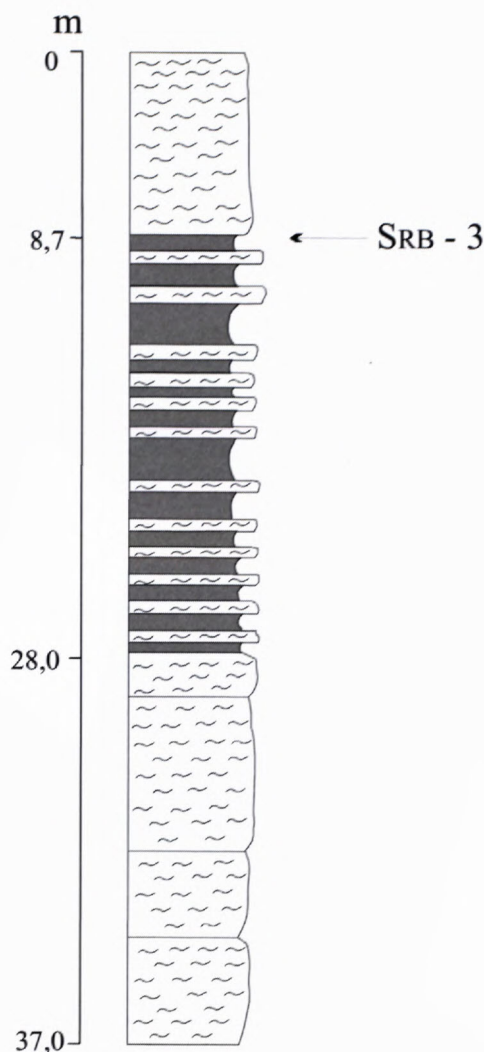

Fig. 4. Borehole D-3/82 lithologic profile, Goć – Devotin deposit, north of Polyanica, Vranye Depression. (After Novković et al., 1986). For explanation see Fig. 2.

by microflora, particularly by the Botryococcaceae. The dead clusters of *Botryococcus* fell down on the bottom and in anaerobic conditions of the hypolimnion, buried by fine clastics the organic matter has been fossilized. By this way the dark lamina rich in organic matter of the oil shale originated. With approaching of the late autumn and winter the water stratification collapsed. The period of lake stagnation was replaced by period of water circulation. The life conditions, as well as conditions of the organic matter fossilization at the lake bottom become worse and in such conditions the lamina poor in organic matter originated.

The oil shale of Vranye Depression, Oligocene in age, originated in tropical climate that is proved by the sporomorphs assemblage. The tropical lakes have different seasonal cycles in comparison with the temperate (and subtropic) ones. In recent meromictic Lake Malawi in Africa, laminated deposits originate. The lamination reflects the seasonal change: dry windy season (April – October) with high bioproductivity in the lake and wet, but calm season with low bioproductivity (Pilskaln & Johnson, 1991; fide Cohen, 2003).
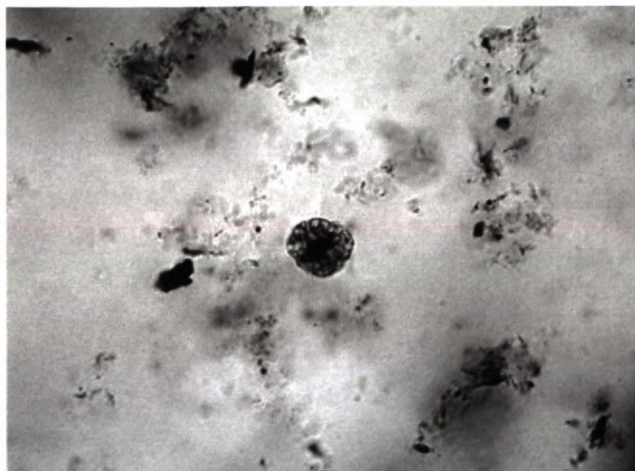
Slovak Geol. Mag., 12, 2 (2006), 147 – 158

154

Fig. 5

Fig. 8

Figs. 5–8. Clusters of Botryococcus braunii Kützing 1849, magn. 630x, Aleksinac. Individual forms are small as a result of excellent life conditions and of high reproduction potential.
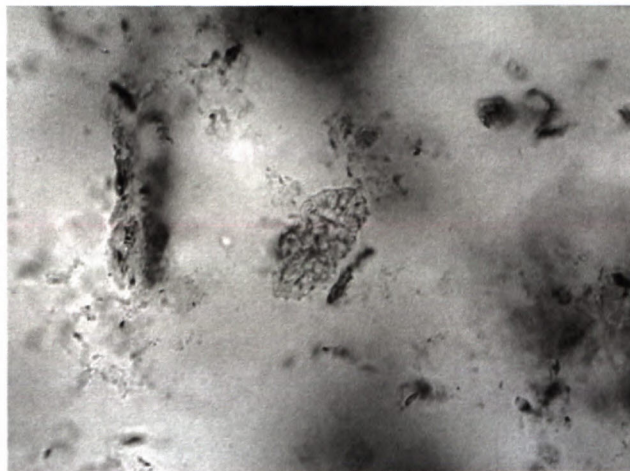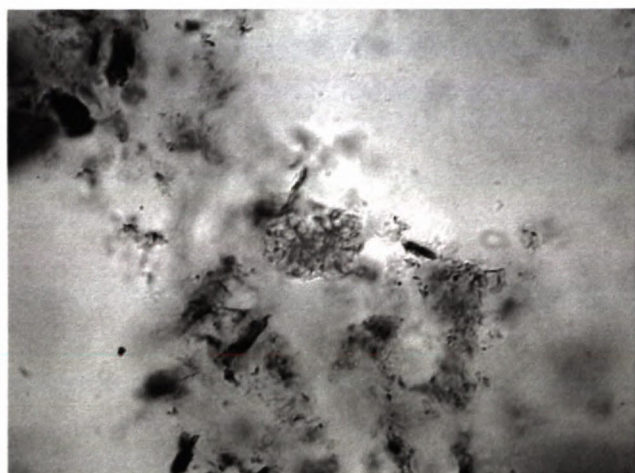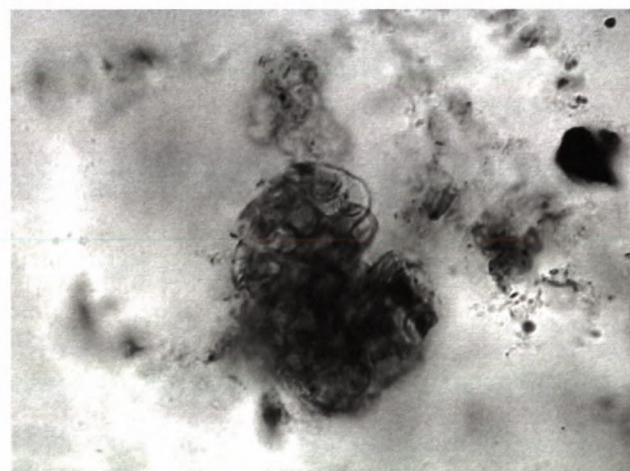

Fig. 6

Fig. 9. Botryococcus braunii Kützing 1849, magn. 630x, Pinciná, Slovakia. In comparison with the forms of Aleksinac, the forms of Pinciná are larger testifying slower growth in the slightly worse life conditions.
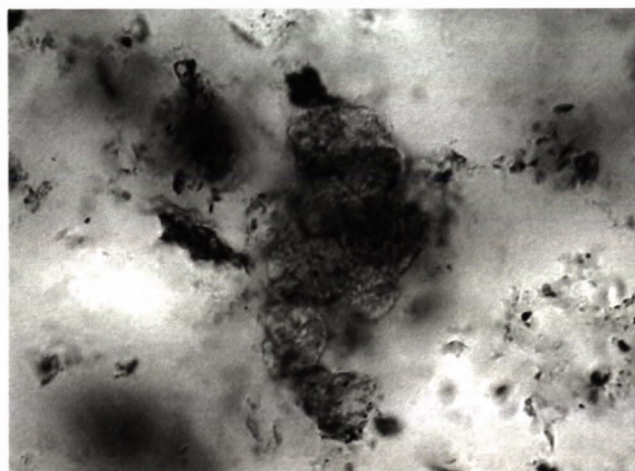

Fig. 7

According to Rock-Eval pyrolysis of the samples from Subotinac, Vranje and Shushevlyanska Bela Stena (Srb1, 2, 3 and 5 in Table 1) the kerogen of the sampled oil shales represents the aquatic kerogen type I (Fig. 11). The kerogen of the Middle Europe Cenozoic oil shales (alginite) originated in basalt maar lakes represents a mixed type I-II (the aquatic and aquatic/terrestrial). The reason of different kerogen type in compared paleolakes

may be the different lake extent. The paleolakes of Aleksinac, Vranye and Mionica (Shushevlyanska Bela Stena) have been of larger extent. Particularly the maar lakes where the alginite originated have been small. For example the maar lake at Pinciná (Southern Slovakia) has been only 0.25 km² large (Vass et al., 1997). In small lakes during the summer stagnation beside dominant Algae larger water plants vegetated being the source of kerogen type II in the organic matter of bottom sediment. The large lakes epilimnion especially at some distance of the coast was free of larger water plants and the Algae have had excellent life conditions producing the kerogen type I in the bottom sediment. This idea is supported by high contents of organic matter in the oil shales generated in large lakes (see Tab.1 and compare with Tab. 2) as well as the Botryococcus cells form testify the very good condition for Algae quick bloom. In the oil shales particularly from Aleksinac Depression exclusively small types of Botryococcus braunii Kützing have been found

D. Vass et al.: Organic matter and fossil content in Serbian...

155

(Figs. 5–8). Small forms of Botryococcaceae are typical for the biologically active water environment, when this algae have high reproduction potential. The large size of *Botryococcus brauni* cells from Pinciná testifies the slower grow of the algae (Fig. 9).

Obradović and Vlasič (2008), examined a set of oil shales from Aleksinac Depression using gas chromatography. According to these results the pristane/phytane ratio is generally less than 1, indicating an origin in a saline lake rich in dissolved carbonates (Rohrback, 1983). The n-alkanes range from n-C_{16} to n-C_{33}; n-C_{27} is generally the most abundant n-alkane.

The oil shale generation in large paleolakes is usually in genetic relation with the coal seams generation. The lakes before got deeper and perhaps larger they have been shallow swamps or bogs convenient for the coal generation. It is valid particularly for paleolake of Aleksinac Depression, the Sokolov Coal Basin in Bohemia and the oil shale from Šiatorská Bukovinka (Southern Slovakia) associated with the coal bearing Pôtor Member of Salgótarján Formation (Vass, 2001). The kerogen of oil shale from the Somodi Formation at Drienovec (SE Slovakia) being in genetic relation with glance brown coal (Vass et al. 1994) is at boundary between type I and II (Milička & Vass, 2001).

The inorganic carbon contents in the oil shale of Shushevlyanska Bela Stena (Srb. 5) is relatively high. The high contents of inorganic carbon also in oil shale from Drienovec (but almost 5 tens higher as in Srb. 5 sample, Fig. l) was measured. In both rocks the dark in organic matter rich lamina alternate with white carbonatic lamina. The carbonatic lamina in Drienovec oil shale are of organic origin being build up by "carpets" of calcareous Algae (thin stromatolites; Mello in Vass et al., 1994). The oil shale originated in a lagoon on the sea coast (Vass et al. 1994).

The carbonatic lamina in oil shale from Shushevlyanska Bela Stena, and/or in oil shale of the Valyevo–Mionica Depression are built up by the dolomicrite (rarely by calcite) with the authigenic minerals as searlesite, analcime, trona, shortite and gypsum. The minerals testify the relatively high salinity in paleolake and in interstitial brine (Obradović, Djurdjević-Colson & Vlasič, 1997).

The sample taken from the oil shale outcropping in the town of Mionica near the bridge on the Ribnica river is poor in TOC (1.11 wt.%) and the kerogen is of type III and II. The sampled rock facies originated under different conditions as other sampled Serbian oil shales. When the sampled rock originated, the paleolake was deep enough to enable the summer stagnation in the lake and the sediments originated in the lake are laminated. On the other hand in the epilimnion of the paleolake, and/or its marginal parts the conditions for the nannophytoplankton have not been optimal. The *Botryoccocacea* have been obliged to live together with higher water plants and even with woody plants growing nearby the lake coast. Because of it the kerogen generated from the mixed plant population is of type III and II.

Concerning the oil shales maturation stage the oil shale of Drienovec is less mature as sampled Serbian

ones despite the Drienovec oil shale older age. The age of former is Eocene – Oligocene while the age of Serbian oil shales is Lower and Middle Miocene. For instance the age of oil shale in Aleksinac Depression is Lower Miocene (Stevanović, 1964) and the samples of Subotinac (Srb-1 and 2) are in early mature relic stage. The significantly older Drienovec oil shale is in immature stage (Fig. 10). The reason may be the higher heat flow in the Aleksinac Depression. The recent one is about 100 mW.m^{-2} (Milivojević & Martinović, 2000) and the former heat flow was probably higher being elevated by contemporaneous volcanism in the area. The recent heat flow in surroundings of Drienovec is about 70 mW.m^{-2} (Franko et al., eds., 1995) and in the surroundings of Drienovec any manifestation of Cenozoic volcanic activity is missing, so there is no reason to suppose the higher heat flow during the Paleogene.
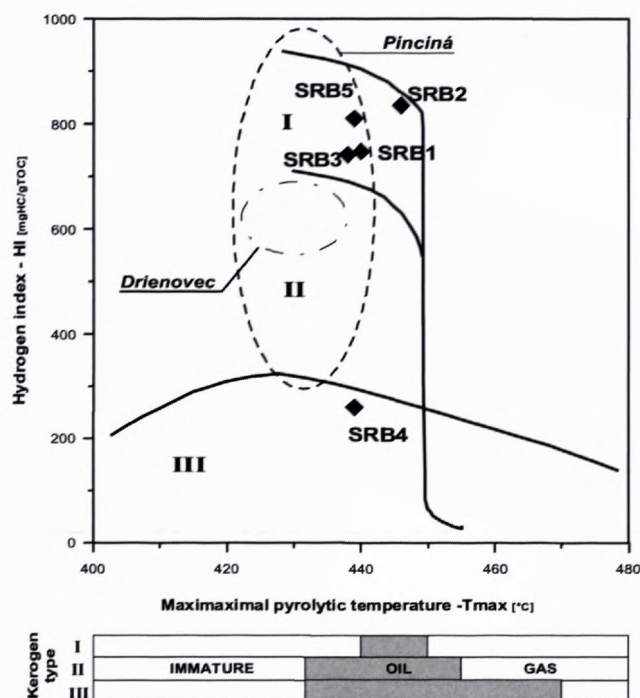

Fig. 10. HI – Tmax diagram showing kerogen type and maturation stage of investigated samples.

Another but less probable reason of the inverse maturity stage of the compared oil shales may be the relatively higher original overburden of the Serbian oil shales under study.

The alginite of Pinciná with prevailing kerogen of type II despite its young age (Pontian) is in early mature relic stage. It is the consequence of coeval elevated paleoheat flow caused by basalt volcanic activity in the Southern Slovakia, lasting from Pontian till the Quaternary.

The relation between total inorganic carbon and total organic carbon contents in the oil shales taken into consideration in this paper and presented in the Fig. 12, indicates the relation ship more TIC contents signify the drop of TOC in oil shales.

The inorganic carbon contents (TIC) of the Aleksinac and Vranye depressions oil shales, as well as of the alginite of Pinciná are low and similar. On the other hand
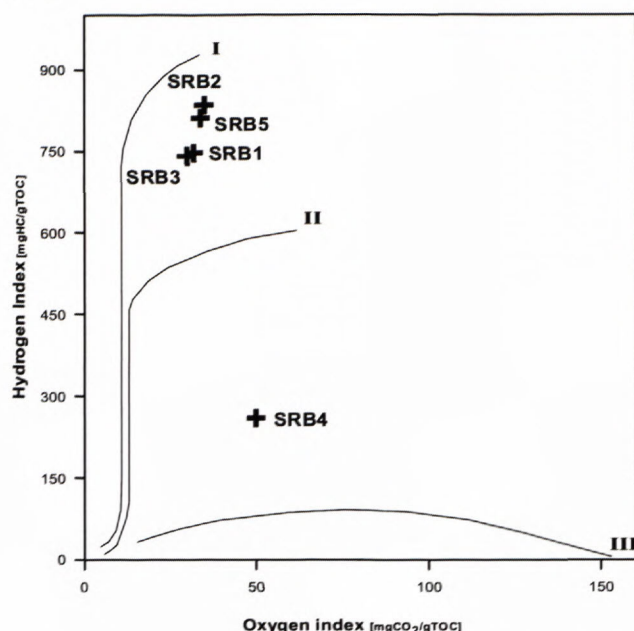
156

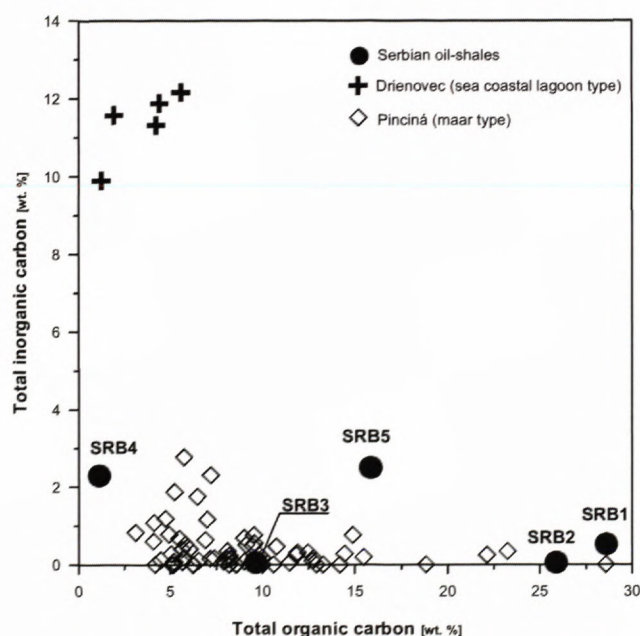Fig. 11. Kerogen type of Serbian oil shales in OI – HI diagram.

Fig. 12. Comparison of inorganic carbon content in Serbian and Slovak oil-shales.

the TIC contents of the Mionica Depression oil shales (Srb-4 and 5) are higher (by 2 wt.%) and of Drienovec oil shale much more higher (by 10 to 12 wt.%, Fig. 12). The TIC contents reflect conditions of deposition environment and the rock composition in the source area. The oil shales of Aleksinac and Vranye depressions and of Pinciná maar originated in paleolakes supplied by fine clastic material – by clay coming from weathered source rocks. The oil shales of Mionica Depression originated in the paleolake supplied by the carbonates in solution. The salinity of the lake was elevated and dolomicrite layers with the authigenic chemogene minerals after seasonal summer stagnation originated. The Drienovec oil shale origi-

nated in the sea costal lagoon, in condition resembling the carbonate shelf platform. After seasonal stagnation when the lagoon was crowded by the Algae rich in oil, the season of calcareous Algae growth followed and thin carpets of those Algae covered the lagoon bottom, giving origin to the white in organic matter poor laminas.

Conclusions

In the Serbian Cenozoic lacustrine deposits beside other sedimentary rock types the oil shales occur. Organic matter of five randomly selected oil shale samples coming from three depressions: Aleksinac, Valyevo–Mionica and Vranye–Polyanica was characterized using elementary analysis and Rock-Eval pyrolysis. Fossil content and paleoecological conditions were characterized and verified by palynological study. According to results of analyses, the samples from Subotinac, Vranye and Shushevlyanska Bela Stena correspond to aquatic kerogen type I, being rich in organic carbon content (10–30 wt.%), as well as in hydrogen content expressed by hydrogen index (HI = 740–840 mg HC/g TOC). Sample from Mionica represents kerogen type III derived from woody material. According to maximal pyrolytic temperature all investigated samples are in the early mature relict stage. The relatively high maturation of oil shale kerogen indicates the elevated paleoheat flow in Central and Southern Serbia.

Oil shales from Aleksinac and Valyevo–Mionica depressions are Miocene in age and they originated under humid subtropical climate. The oil shales from Vranye–Polyanica Depression are Oligocene in age and originated under tropical to subtropical climate conditions. The oil shales originated in relatively large and deep lakes well supplied by nutritive elements and the water was seasonally eutrophic. The laminated structure of oil shales testifies the annual climatic changes. Small size of *Botryococcus* cells particularly of Aleksinac Depression oil shales indicates the excellent live conditions and high reproduction potential of the algae. The same is testified by the high content of TOC and by the dominant kerogen type I.

Rise of TIC contents in oil shales of Valyevo–Mionica Depression reflects the decrees of TOC contents. The inorganic carbon comes from the authigenic chemogene minerals because the salinity of the lakes was elevated. The pristane/phytane ratio in the oil shales of Aleksinac Depression is generally less than 1, indicating an origin in a saline lake rich in dissolved carbonates.

Comparison with the Cainozoic oil shales of Central Europe indicates the differences in paleolake size, in paleoheat flow intensity and in carbonate lamina origin. Particularly the maar lakes of Slovakia and Hungary were small. The paleoheat flow in surroundings of Drienovec (Slovakia) was significantly lower in comparison with that in Central and Southern Serbia. The Drienovec oil shales differ from those of Shushevlyanska Bela Stena in the origin of organic matter free lamina. Those of Drienovec originated by the activity of calcareous algae, those of Shushevlyanska Bela Stena are of chemogene origin.

D. Vass et al.: Organic matter and fossil content in Serbian...

157

Fig. 13. Sites of Middle Europe oil shales compared with the sampled Serbian oil shales. 1 – Pinciná,2 – Drienovec, 3 – Šiatorská Bukovinka, 4 – Pula, 5 – Gérce, 6 – Sokolov Coal Basin.

References

Bruckner-Wein, A. & Hetényi, M., 1993: Relationship of the organic geochemical features of two maar type Hungarian oil shales. Acta Geologica Hungarica, Vol. 36/2, 223-239.

Capoa, P. de & Radoićić R., 2002: Geological implications of biostratigraphic studies in the external and internal domains of the Central-Southern Dinarides. Mem. soc. geol. Italiana, 57, 185-191.

Cohen, A. S., 2003: Paleolimnology. Oxford University Press, pp. 500.

Ercegovac, M., 1990: Geology of oil shales. Grad. Knjiga, Beograd, pp. 180. (In Serbian.)

Erdtman, G., 1943: An introduction to pollen analysis. Waltham, Mass. USA.

Erdtman, G., 1960: The acetolysis method. Svensk. Botan. Tidskr., 54, 4, 561-564

Espitalié, J., Deroo, G. & Marquis, F., 1986: La pyrolyse Rock Eval et ses application. Partie II. Rev. Inst. Franc. Pétr., 40, 6, 755-784

Dolić, D., 1983: Miocene freshwater molluscs from the Mionica-Valyevo Basin (Serbia). C. rend. seances Soc. Serbe geol. (pour 1982), 117-121, Beograd. (In Serbian with English summary).

Franko, O., Remšík, A., & Fendek, M. (eds.), 1995: Atlas of Geotermal Energy of Slovakia. D. Štúr Geological Institute, Bratislava. (In Slovak with extended English summary).

Gaudant, J., 2002: The Miocene non-marine fish-fauna of central Europe: A review. Bull. Acad Serbe sci. arts CXXV, Cl. sci. math. nat – sci. nat. 41, Belgrad, 65-74.

Jovanović, D., Krstić, N., Crnojević, C. & Popović, Z., 2005: Ribnica: A cut through different depth zones of a Neogene lake. Second conference on geoheritage of Serbia, Spec. ed. Inst. nature protect. Serbia, 20, Beograd, 35-39. (In Serbian with English summary.)

Jovanović, O. & Novković, M., 1988: Tertiary sedimentary complex of Vranye Basin.Vesnik Geol. 44, Beograd, 197-213. (English summary.)

Kaśanin-Grubin, M., 1996: Aleksinac coal formation. Neogene of Central Serbia. IGCP 329. Spec. Publ. Geoinstitute 19, Beograd, 41-43.

Kreutner, H. G. & Krstić B., 2003: Geological map of the Carpatho-Balkanides between Mehadia, Oravitsa, Niš and Sofia, Geoinsitute, Beograd.

Krizak, D., 2003: Geology of the Vranye Depression. In: Paleolimnology of Serbian Neogene. Workshop, July 7.-11. 2003, Serbia. Guide Book. Serbian Geological Society, Beograd.

Krstić, B., Veselinović, M., Divljan, M. & Rakić, M., 1980: Geology of the sheet Aleksinac. Federal geol. Surv. Yugoslavia, Belgrade, 1-55. (In Serbian with English and Russian summaries.)

Krstić, N. 1996: Neogene overstep sequences of the central and western Balkan Penisula. In: Knežević, V. & Krstić, B., eds: Terranes of Serbia. Belgrade, 151-154.

Krstić, N., Savić, Lj., Jovanović, G. & Bodor, E., 2003: Lower Miocene lakes of the Balkan Land. Acta Geol. Hungarica, 46, Budapest, 3, 291-292.

Mihajlović, Dj., 1985: Paleogene fossil flora of Serbia. Ann. geol. penins. Balk., XLIX, Beograd, 299-434. (In Serbian with English summary.)

Milička, J. & Vass, D., 2001: Geochemistry of organic matter of the Šomody Formation; paleogeographic interpretations (Turňa Depression, Eastern Slovakia). Mineralia Slovaca, 33, 45 – 52. (In Slovak with English summary.)

Milivojević, M. & Martinović, M., 2000: Geothermal energy possibilities, exploration and future prospects in Serbia. Proc. World Geothermal Congress, Japan, 319-326.

Müller, P., 1987: Pyrolyse Rock-Eval and TOC/TIC determinations in sediments of Podkrkonose Permian-Carboniferous series and Cypris Formation. Manuscript, Czech Geological Survey, Prague, Brno. (In Czech.)

Novković, M., Jovanović, O. & Grgurević, E., 1987: Geology of the oil shale deposit Goć – Devotin North of town Vranye (Serbia). XIth Congress of geologists of SFR Yugoslavia, vol. 2 – Stratigraphy, Paleontology, Regional Geology, Tara, 457-474.

158

Obradović, J., Djurdjević-Colson, J. &. Vasić, N., 1997: Phytogenic lacustrine sedimentation – oil shales in Neogene from Serbia. Jurnal of Paleolimnology 18, 351-364.

Obradović, J. & Vlasić, N., 2008: Neogene lacustrine basins in Serbia. (In press.)

Pantić, N., Maksimović, B., Gagić, N. & Vujisić, Lj., 1980: The Neogene sediments of one part of the Valyevo-Mionica Basin. Glas CCCXVII, Cl. sci. nat. math. n. ser. 46, Beograd, 23-36. (In Serbian with English summary.)

Petković, K. & Ćićulić, M., 1962: Pojava bituminoznich i ugljonosnich slojeva na zapadnoj strani Juźne Morave. Nefta, Mesećnik Instituta za naftu, 12 Zagreb, 1-2.

Rohrback, B. G., 1983: Crude oil geochemistry of the Golf of Suez. In: M. Bjoroy et al. (ed): Advances in organic geochemistry in 1981. Chichester: Wiley, 39-48.

Stevanović, R. 1964: Stratigraphy of Miocene coal-bearing series in Aleksinac Basin. In: Paleolimnology of Serbian Neogene. Workshop, July 7.-11. 2003, Serbia. Guide Book. Serbian Geological Society. Beograd.

Vass, D., 2001: Oil shales of the world and of Slovakia. Mineralia Slovaca, 33, 147-158.

Vass, D.. Elečko, M., Horská, A., Petrík, F., Barkáč, Z., Mello, J., Vozárová, A., Radóc, Gy. & Dubéci, B., 1994: Basic geological features of Turňa Depression. Geol. Práce, Správy 99, Bratislava, 7-22. (In Slovak with English summary.)

Vass, D., Konečný, V., Elečko, M., Milička, J., Snopková, P., Šucha, V., Kozáč, J. & Škrabana, R., 1997: Alginite: A new resource of the Slovak industrial minerals potential. Mineralia Slovaca, 29, 1-3.

Vukanović, M., Dimitrijević, M. M., Dimitrijević, M. N., Karajčić, Lj. & Rakić, M., 1977: Geology of the sheet Vranye. Federal geol. Surv. Yugoslavia, Belgrade, 1-55. (In Serbian with English and Russian summaries.)

Instructions for authors

Slovak Geological Magazine – periodical of the Geological Survey of Slovak Republic is quarterly presenting the results of investigation and researches in wide range of topics: regional geology and geological maps, lithology and stratigraphy, petrology and mineralogy, paleontology, geochemistry and isotope geology, geophysics and deep structure, geology of deposits and metallogeny, tectonics and structural geology, hydrogeology and geothermal energy, environmental geochemistry, engineering geology and geotechnology, geological factors of the environment, petroarcheology.

The journal is focused on problems of the Alpine-Carpathian-Balkan region

General instructions

The Editorial Board of the Geological Survey of Slovak Republic – Dionýz Štúr Publishers accepts manuscripts in correct English. The papers that do not have sufficient accuracy in language level will be submitted back for language correction.

The manuscript should be addressed to the Chief Editor or the Managing Editor.

Contact address:

State Geological Institute of Dionyz Stur – Dionýz Stur Publishers, Mlynská dolina 1, 817 04 Bratislava, Slovak Republic
e-mail addresses: alena.klukanova@geology.sk
gabriela.siposova@geology.sk
http://www.geology.sk

The Editorial Board accepts or refuses a manuscript with regard to the reviewer's opinion. The author is informed of the refusal within 14 days from the decision of the Editorial Board. Accepted manuscript is prepared for publication in an appropriate issue of the Magazine. The author(s) and the publishers enter a contract establishing the rights and duties of both parties during editorial preparation and printing, until the time of publishing of the paper.

Text layout

The manuscript should be arranged as follows: TITLE OF THE PAPER, FULL NAME OF THE AUTHOR(S); NUMBER OF SUPPLEMENTS (in brackets below the title, e.g. 5 figs., 4 tabs.), ABSTRACT (max. 30 lines presenting principal results) – KEY WORDS – INTRODUCTION – TEXT – CONCLUSION – ACKNOWLEDGEMENTS – APPENDIX – REFERENCES – TABLE AND FIGURE CAPTIONS – TABLES – FIGURES. The editorial board recommends to show a localisation scheme at the beginning of the article.

The title should be as short as possible, but informative, compendious and concise. In a footnote on the first page, name of the author(s), as well as his (their) professional or private address.

The text of the paper should be logically divided. For the purpose of typography, the author may use a hierarchic division of chapters and sub-chapters, using numbers with their titles. The editorial board reserves the right to adjust the type according to generally accepted rules even if the author has not done this.

Names of cited authors in the text are written without first names or initials (e.g. Štúr, 1868), the names of co-authors are divided (e.g. Andrusov & Bystricky, 1973). The name(s) is followed by a comma before the publication year. If there are more authors, the first one, or the first two only are cited, adding et al. and publication year.

Mathematical and physical symbols of units, such as %, ‰, °C should be preceded by a space, e.g. 60 %, 105 °C etc. Abbreviations of the units such as second, litre etc. should be written with a gap. Only SI units are accepted. Points of the compass may be substituted by the abbreviations E, W, NW, SSE etc. Brackets (parentheses) are to be indicated as should be printed, i.e. square brackets, parentheses or compound. Dashes should be typed as double hyphens.

If a manuscript is typed, 2 copies are required, including figures. The author should mark those parts of a text that should be printed in different type with a vertical line on the left side of the manuscript. Paragraphs are marked with 1 tab space from the left margin, or by a typographic symbol. Words to be emphasized, physical symbols and Greek letters to be set in other type (e.g. *italics*) should be marked. Greek letters have to be written in the margin in full (e.g. *sigma*). Hyphens should be carefully distinguished from dashes.

Tables and figures

Tables will be accepted in a size of up to A4, numbered in the same way as in a text.

Tables should be typed on separate sheets of the same size as text, with normal type. The author is asked to mark in the text where the table should be inserted. Short explanations attached to a table should be included on the same sheet. If the text is longer, it should be typed on a separate sheet.

Figures should be presented in black-and-white, in exceptional cases also in colour which must be paid approx. 100 EUR per 1 side A 4. Figures are to be presented by the author simultaneously with the text of the paper, in two copies, or on a diskette + one hard copy. Graphs, sketches, profiles and maps must be always drawn separately. High-quality copies are accepted as well. Captions should be typed outside the figure. The graphic supplements should be numbered on the reverse side, along with the orientation of the figures. Large-size supplements are accepted only exceptionally. Photographs intended for publishing should be sharp, contrast, on shiny paper. High quality colour photographs will only be accepted depending on the judgement of the technical editors.

If a picture is delivered in a digital form, the following formats will be accepted: *.cdr, *.dxf, *.bmp, *.tiff, *.wpg, *.fga., *.jpg *.gif, *.pcx. Other formats are to be consulted with the editors.

References

Should be listed in alphabetical and chronological order **according to annotation in the text** and consist of all references cited.

Standard form is as follows: 1. Family name and initials of author(s), 2. Publication year, 3. Title of paper, 4. Editor(s), 5. Title of proceedings, 6. Publishers or Publishing house and place of publishing, 7. Unpublished report – manuscript should be denoted MS. Unpublished paper can appear as personal communications only. 8. Page range.

Quotations of papers published in non-Latin alphabet or in languages other than English, French, Italian, Spain or German ought to be translated into English with an indication of the original language in parentheses, e.g.: (in Slovak).

Example:

Andrusov, D., Bystrický, J. & Fusán, O., 1973: *Outline of the Structure of the West Carpathians.* Guide-book for geol. exc. of Xth Congr. CBGA. Bratislava: Geol. Úst. D. Štúra, 44 p.

Beránek, B., Leško, B. & Mayerová, M., 1979: Interpretation of seismic measurements along the trans-Carpathian profile K III. In: Babuška, V. & Plančár, J. (Eds.): *Geodynamic investigations in Czecho-Slovakia.* Bratislava: VEDA, p. 201-205.

Lucido, O., 1993: A new theory of the Earth's continental crust: The colloidal origin. *Geol. Carpathica,* vol. 44, no. 2, p. 67-74.

Pitoňák, P. & Spišiak, J., 1989: Mineralogy, petrology and geochemistry of the main rock types of the crystalline complex of the Nízke Tatry Mts. MS – Archiv GS SR, Bratislava, 232 p. (in Slovak).

Proofs

The translator as well as the author(s) are obliged to correct the errors which are due to typing and technical arrangements. The first proofs are sent to author(s) as well as to the translator. The second proof is provided only to the editorial office. It will be sent to authors upon request.

The proofs must be marked clearly and intelligibly, to avoid further errors and doubts. Common typographic symbols are to be used, the list and meaning of which will be provided by the editorial office. Each used symbol must also appear on the margin of the text, if possible on the same line where the error occurred. The deadlines and conditions for proof-reading shall be stated in the contract.

Final remarks

These instructions are obligatory to all authors. Exceptions may be permitted by the Editorial Board or the managing editor. Manuscripts not complying with these instructions shall be returned to the authors.

1. Editorial Board reserves the right to publish preferentially invited manuscript and to assemble thematic volumes,

2. Sessions of Editorial Board – four times a year and closing dates for individual volumes will be on every 31th day of March, June, September and December.

3. To refer to one Magazine please use the following abbreviations: *Slovak Geol. Mag.,* vol. xx, no. xx. Bratislava: D. Štúr. Publ. ISSN 1335-096X.